

**Manufacturing of Sandwich Panels Using Recycled Thermoplastic  
Composites in a Continuous Extrusion Line**

Mohammadreza Azad

A Thesis

In the Department

Of

Mechanical and Industrial Engineering

Presented in Partial Fulfillment of the Requirements

For the Degree of

Master of Applied Sciences (Mechanical Engineering) at

Concordia University

Montreal, Quebec, Canada

Spring 2016

CONCORDIA UNIVERSITY  
School of Graduate Studies

This is to certify that the thesis prepared

By: Mohammadreza Azad

Entitled: Manufacturing of Sandwich Panels Using Recycled Thermoplastic Composites in a Continuous Extrusion Line

and submitted in partial fulfillment of the requirements for the degree of

Master of Applied Sciences (Mechanical Engineering) at Concordia University

complies with the regulations of the University and meets the accepted standards with respect to originality and quality.

Signed by the final examining committee:

Dr. Sivakumar Narayanswamy Chair

Dr. Robin Drew Examiner

Dr. Lan Lin Examiner

Dr. Mehdi Hojjati Supervisor

Approved by \_\_\_\_\_  
Chair of Department or Graduate Program Director

\_\_\_\_\_  
Dean of Faculty

Date May 11, 2016

# ABSTRACT

## **Manufacturing of Sandwich Panels Using Recycled Thermoplastic Composites in a Continuous Extrusion Line**

Mohammadreza Azad

Thermoplastic sandwich panels are attractive for automotive applications since they can be readily formed into the light weight complex structures with good impact resistance and high flexural rigidity. In this experimental study, the extent of enhancement in properties achieved through the use of thermoplastic composite skins combined with a recycled thermoplastic core is demonstrated. The thermal behavior of polypropylene (PP)-based recycled materials and the possibility of turning them into the sandwich panels via a plastic extrusion processing were investigated. A sheet extrudate of recycled thermoplastic composite was sandwiched between two thermoplastic skins on both sides to make the sandwich panels. The core material composed of recycled polypropylene (RPP) and shreds of recycled PP/Fiberglass (e.g. twintex scraps) with the weight ratio of 1:1. A commercial thermoplastic skin, TWINTEX, which is a roving made of commingled E-Glass and polypropylene filaments woven into highly conformable fabrics, is used as the face sheets to bond with the core material.

A good understanding of principles for manufacturing sandwich panels and performing some experimental optimization leads to making high-strength and strongly-bonded sandwich panels. Results of the mechanical tests (3-point bending and peel-off test) show that recycled sandwich panels offer better mechanical performance compared with their honeycomb counterparts in terms of flexural strength and skin-to-core bonding and they are more resistant to delamination. The big issue is that they are high-weight materials compared with honeycomb sandwich panels. So we applied some foaming processes using chemical foaming agents to reduce the density of the core. A significant reduction in sandwich panel's weight and better mechanical performance could be achieved.

## ACKNOWLEDGEMENTS

I express my sincere and deep gratitude to my thesis supervisor, Dr. Mehdi Hojjati, and president of AS Composite Inc., Dr. Hossein Borazghi, for their guidance, encouragement and continued support throughout this work. Their enthusiasm, wide knowledge and motivational ability made this journey easier for me. It's been an honor to work with them and I am truly grateful for giving me this opportunity.

My special thanks goes to my colleagues in Concordia Center for Composites (CONCOM) and AS composite Inc. for providing a friendly and dynamic atmosphere to learn and cooperation in every way.

I sincerely appreciate all the support and assistance I got from AS Composite's engineering team, Ms. Golnaz Shokoohi, Mr. Arash Shahbazian, Mr Ashkan Ahmadi and Mr. Niraj Panthal.

Also, I would like to thank CONCOM research assistants, Mr. Heng Wang and Dr. Daniel Rosca for their time and assistance in experimental works and laboratory procedures.

Last but not least, I am truly grateful to my lovely family for the support that they have provided me through my entire life. Of course, my master studies would not have been possible without their love, encouragement and support.

# Table of Contents

<b>List of Figures</b> .....	<b>VII</b>
<b>List of Tables</b> .....	<b>XI</b>
<b>Chapter 1. Introduction</b> .....	<b>1</b>
1.1 Background.....	1
1.2 Thermoplastic Sandwich Panels .....	2
1.3 Foaming Process .....	4
1.4 Plastic Extrusion.....	5
1.5 Research Motivation .....	7
1.6 Objectives.....	8
<b>Chapter 2. Theory</b> .....	<b>9</b>
2.1 Sandwich Panel Analysis .....	9
2.2 Drag Flow in Extruder .....	14
2.3 Heat Transfer Phenomena .....	17
<b>Chapter 3. Material and Manufacturing</b> .....	<b>21</b>
3.1 Raw Materials Characteristics.....	21
3.1.1 Polypropylene.....	21
3.1.2 Randomly Oriented Chopped Glass Fiber Polypropylene .....	22
3.1.3 Foaming Agents.....	26
3.1.4 Thermoplastic Skins .....	29
3.2 Equipment .....	31
3.2.1 Two-stage Extruder .....	31
3.2.2 Heating Chamber.....	33
3.2.3 Conveyor Double Belt Press .....	33
3.2.4 Pulling System.....	34
3.2.5 Reciprocating Feeding System.....	35
<b>Chapter 4. Results and Discussion</b> .....	<b>36</b>
4.1 Trial Parameters .....	36

4.1.1 Extrusion Process .....	36
4.1.2 Lamination Process .....	40
4.2 Panel Quality Tests.....	48
4.2.1 Visual Test.....	48
4.2.2 Density Test.....	48
4.2.3 3-Point Bending Test.....	49
4.2.4 Peel-off Test .....	50
4.3 Process Optimization.....	51
4.3.1 Skin Thickness.....	51
4.3.2 Lamination Parameters.....	57
<b>Chapter 5. Foam Extrusion.....</b>	<b>67</b>
5.1 Polymer Foam .....	67
5.2 Chemical Foaming Agents [13] .....	68
5.3 RPP Foam Core Extrudate .....	69
5.3.1 Foam Cell Morphology .....	70
5.3.2 Density and Flexural Properties of Foamed PP Extrudate .....	71
5.4 RPP Foam Sandwich Panel.....	74
5.4.1 Foamed-Core Sandwich Panel with Chopped Fiber-Reinforced PP .....	75
5.4.2 Density and Flexural Properties .....	78
5.4.3 Toughness.....	80
5.4.4 Sandwich Effect.....	81
5.4.5 Peel-off .....	84
5.5 Honeycomb vs Recycled PP Foam Sandwich Panels .....	86
5.5.1 Flexural Behavior .....	87
5.5.2 Adhesion Behavior .....	91
5.6 Foaming Challenges.....	93
<b>Chapter 6. Conclusion and Future Works .....</b>	<b>96</b>
6.1 Conclusion.....	96
6.2 Contribution.....	97

6.3 Future Work .....	98
<b>References .....</b>	<b>99</b>

## *List of Figures*

<i>Figure 1.1. Honeycomb and foam sandwich panels .....</i>	<i>3</i>
<i>Figure 1.2. Polymer foam structures .....</i>	<i>4</i>
<i>Figure 1.3. Market share for major thermoplastic processings [14] .....</i>	<i>5</i>
<i>Figure 1.4. Distribution of pressure in the extruder zones [15] .....</i>	<i>7</i>
<i>Figure 2.1. A schematic view of a sandwich panel with rectangular cross section.....</i>	<i>9</i>
<i>Figure 2.2. Cross section of the beam under shear stress .....</i>	<i>12</i>
<i>Figure 2.3. Flexural and shear stress distribution in a sandwich beam; (a) No approximation... 13</i>	
<i>(b) <math>E_c \ll E_f</math>.....</i>	<i>13</i>
<i>Figure 2.4. Effect of core thickness on the weight, bending stiffness and strength of the sandwich panel for <math>\rho_c \ll \rho_f</math> and <math>E_c \ll E_f</math>.....</i>	<i>14</i>
<i>Figure 2.5. Extruder and die characteristic [1] .....</i>	<i>16</i>
<i>Figure 2.6. Flow coefficient as a function of die geometry [15]. .....</i>	<i>17</i>
<i>Figure 2.7. A scheme of thermal diffusion through the thickness of a plate.....</i>	<i>19</i>
<i>Figure 3.1. Methyl group.....</i>	<i>21</i>
<i>Figure 3.2. Short segments of polypropylene; isotactic (above) and syndiotactic(below) tacticity .....</i>	<i>22</i>
<i>Figure 3.3. Basic properties of short glass fiber reinforced thermoplastics .....</i>	<i>23</i>
<i>Figure 3.4 Raw materials for extrusion process; a) PP components, b) PP+RTWT .....</i>	<i>24</i>
<i>Figure 3.5. Heating/cooling/heating cycle for black PP .....</i>	<i>25</i>
<i>Figure 3.6. Heating/cooling/heating cycle for white PP .....</i>	<i>25</i>
<i>Figure 3.7. Heating/cooling/heating cycle for PP pellets.....</i>	<i>26</i>
<i>Figure 3.8. Heating/cooling/heating cycle for RPP extruded plate.....</i>	<i>26</i>
<i>Figure 3.9 TGA thermogram of EV AZ-3.0. ....</i>	<i>28</i>
<i>Figure 3.10. TGA thermogram of EV AZ-3.0; heat/hold process at 200°C for 15 min.....</i>	<i>28</i>
<i>Figure 3.11 TGA thermogram of PN-40E .....</i>	<i>29</i>

<i>Figure 3.12. TGA thermogram of PN-40E; heat/hold process at 200°C for 15 min.....</i>	<i>29</i>
<i>Figure 3.13. Mechanical properties of TWINTEX TPP Fabrics [20] .....</i>	<i>30</i>
<i>Figure 3.14 A schematic view of the experimental setup.....</i>	<i>31</i>
<i>Figure 3.15. A schematic view of a typical extruder machine and a magnified cut-off of the screw ...</i>	<i>32</i>
<i>Figure 3.16. A scheme of the two-stage screw drawing used in our experiment.....</i>	<i>32</i>
<i>Figure 3.17. Conveyor double belt press and skin heating chambers.....</i>	<i>34</i>
<i>Figure 3.18. Pulling machine along the extrusion line.....</i>	<i>34</i>
<i>Figure 3.19. Production line for making thermoplastic sandwich panels via plastic extrusion....</i>	<i>35</i>
<i>Figure 3.20. Reciprocating feeding hopper .....</i>	<i>35</i>
<i>Figure 4.1. Output uniformity for three different compounds; a) 30-70wt% TWT-PP, b) 50-50wt% TWT-PP, c) 70-30wt% TWT-PP; An inconstancy in output flow is evident at TWT ratios higher than 50wt%.....</i>	<i>37</i>
<i>Figure 4.2. Stress-Strain curves for three different PP extrudates.....</i>	<i>39</i>
<i>Figure 4.3. Time-Temperature curve for a 4mm thick plate.....</i>	<i>43</i>
<i>Figure 4.4. Time-Temperature curve at the mid-skin of; a) 0.5mm skin, b) 1mm skin.....</i>	<i>44</i>
<i>Figure 4.5. Time-Temperature curve at the skin surface of; a) 0.5mm skin, b) 1mm skin .....</i>	<i>45</i>
<i>Figure 4.8. Time-Temperature curve at the surface of the core and skin of a sandwich panel with 0.5mm thick skin .....</i>	<i>46</i>
<i>Figure 4.9. Time-Temperature curve at the surface of the core and skin of a sandwich panel with 1mm thick skin .....</i>	<i>46</i>
<i>Figure 4.10. Heat transfer through the core and skin surfaces .....</i>	<i>47</i>
<i>Figure 4.9. A view of 3-point bending fixture .....</i>	<i>50</i>
<i>Figure 4.10. Floating roller peel-off fixture .....</i>	<i>51</i>
<i>Figure 4.11. Small piece of sandwich panel with 0.5 mm skin (S<sub>0.5-2</sub>) .....</i>	<i>53</i>
<i>Figure 4.12. Small piece of sandwich panel with 1 mm skin (S<sub>1-2</sub>) .....</i>	<i>53</i>
<i>Figure 4.13 View of panel specimens subjected to 3-point bending test; .....</i>	<i>54</i>

<i>a)SP<sub>s0.5</sub>-2, b) SP<sub>s1</sub>-1 and c) 3<sup>mm</sup> core material.....</i>	<i>54</i>
<i>Figure 4.14 Force-Displacement curves for different panels.....</i>	<i>55</i>
<i>Figure 4.15 Stress-Strain curves for different sandwich panels.....</i>	<i>55</i>
<i>Figure 4.16. View of broken RPP core and unbroken sandwich panel.....</i>	<i>57</i>
<i>Figure 4.17. Poor surface quality of a sandwich panel with a high preheat temperature.....</i>	<i>57</i>
<i>Figure 4.18. Stress-Strain curves for sample 2; bonding temperature 140°C.....</i>	<i>59</i>
<i>Figure 4.19. Stress-Strain curves for sample 3; bonding temperature 120°C.....</i>	<i>59</i>
<i>Figure 4.20. Stress-Strain curves for sample 6; RPP core plate.....</i>	<i>60</i>
<i>Figure 4.21. Force-Displacement curves for different panels.....</i>	<i>61</i>
<i>Figure 4.22. Stress-Strain curves for different panels.....</i>	<i>61</i>
<i>Figure 4.23. Force applied to peel-off the upper skin of the sandwich panel (SP<sub>2</sub>);.....</i>	<i>63</i>
<i>High lamination pressure, Lamination temperature: 140°C.....</i>	<i>63</i>
<i>Figure 4.24. Force applied to peel-off the upper skin of the solid-core sandwich panel (SP<sub>3</sub>);.....</i>	<i>64</i>
<i>High lamination pressure, Lamination temperature: 120°C.....</i>	<i>64</i>
<i>Figure 4.25. Force applied to peel-off the upper skin of the solid-core sandwich panel (SP<sub>4</sub>);.....</i>	<i>64</i>
<i>Low lamination pressure, Lamination temperature: 140°C.....</i>	<i>64</i>
<i>Figure 4.26. Force applied to peel-off the upper skin of the solid-core sandwich panel (SP<sub>5</sub>);.....</i>	<i>65</i>
<i>Low lamination pressure, Lamination temperature: 120°C.....</i>	<i>65</i>
<i>Figure 4.27. The peeled RPP samples in different lamination conditions; a) SP<sub>2</sub>, b) SP<sub>3</sub>, c) SP<sub>4</sub>, d) SP<sub>5</sub>.....</i>	<i>65</i>
<i>Figure 5.1. Microscopic image of the cross section of the PP foam extrudate with 5wt% PN-40E at a- low melt pressure (200psi) and b- high melt pressure (3000psi).....</i>	<i>71</i>
<i>Figure 5.2. Microscopic image of the cross section of the PP foam extrudate with 5wt% EV AZ-3.0 at a- low melt pressure (200psi) and b- high melt pressure (3000psi).....</i>	<i>71</i>
<i>Figure 5.3. Flexural Stress and stiffness for foamed and solid PP extrudates.....</i>	<i>73</i>

<i>Figure 5.4. Microscopic image of the cross section of the PP foam extrudate with 5wt% EV AZ-3.0; a) GFRPP and b) neat PP .....</i>	<i>76</i>
<i>Figure 5.5. Cross-sectional view of solid (right) and foam (left) neat PP extrudate.....</i>	<i>77</i>
<i>Figure 5.6. Stress-Strain curve for solid and foam PP extrudate with different chopped fiber ratio... </i>	<i>79</i>
<i>Figure 5.7 A view of solid and foam extrudates; 1) core and 2) sandwich panel.....</i>	<i>81</i>
<i>Figure 5.8. Results of 3-point bending test for solid/foam core and sandwich panel.....</i>	<i>82</i>
<i>Figure 5.9. Surface view of the solid (left) and foam (right) core extrudates.....</i>	<i>84</i>
<i>Figure 5.10. Results of the peel-off test for solid and foamed core sandwich panels.....</i>	<i>85</i>
<i>Figure 5.11. Solid-core (left) and foamed-core (right) sandwich panels used for peel-off test.....</i>	<i>85</i>
<i>Figure 5.12. A view of honeycomb and RPP foam sandwich panels under the bending test .....</i>	<i>87</i>
<i>Figure 5.13. Stress-Strain curve for honeycomb and recycled PP foam sandwich .....</i>	<i>88</i>
<i>Figure 5.14. Specific strength of honeycomb and RPP foam sandwich panels .....</i>	<i>89</i>
<i>Figure 5.15. A view of honeycomb and RPP foam sandwich panels after the bending test .....</i>	<i>91</i>
<i>Figure 5.16. Results of the peel-off test for RPP foam and honeycomb sandwich panels.....</i>	<i>91</i>
<i>Figure 5.17. RPP foam extrudate (left) and honeycomb (right) sandwich panels used for peel-off test.....</i>	<i>92</i>
<i>Figure 5.18 Premature foaming due to pressure drop in the extrusion die.....</i>	<i>93</i>
<i>Figure 5.19. A scheme of extrusion gear pump .....</i>	<i>94</i>
<i>Figure 5.20 Diagram of the longitudinal extrusion head with a replaceable forming ring: .....</i>	<i>95</i>
<i>1– screw, 2 – extruder barrel, 3 – extrusion head body, 4 – mandrel, 5– intermediate ring, .....</i>	<i>95</i>
<i>6 – forming ring [51] .....</i>	<i>95</i>
<i>Figure 5.21. Diagram of the longitudinal extrusion head with a diaphragm grid: .....</i>	<i>95</i>
<i>1 –screw, 2 – extrusion head body, 3 – dividing channels in the diaphragm grid, 4 – channel....</i>	<i>95</i>
<i>stoppers, 5 – extruder barrel, 6 – extrusion head adapter [52] .....</i>	<i>95</i>

## *List of Tables*

<i>Table 4.1. Extrusion trial parameters.....</i>	<i>36</i>
<i>Table 4.2. Theoretical values for Young's modulus and density of three different PP extrudate..</i>	<i>39</i>
<i>Table 4.3. Flexural properties and density of three different PP extrudates.....</i>	<i>40</i>
<i>Table 4.4. Practical correlation between the screw rotational speed and pulling speed for 4mm core extrudate .....</i>	<i>41</i>
<i>Table 4.5. Thermal properties of the core and skin and their constitutive components .....</i>	<i>42</i>
<i>Table 4.6. Required time for cooling down an extruded core with water and air .....</i>	<i>42</i>
<i>(Theoretical Results).....</i>	<i>42</i>
<i>Table 4.7. Rate of temperature change with time for the extruded plate.....</i>	<i>43</i>
<i>(Experimental Results).....</i>	<i>43</i>
<i>Table 4.8. Estimated time for cooling down the sandwich panels .....</i>	<i>47</i>
<i>Table 4.10. Skin(0.5 mm) lamination trial parameters.....</i>	<i>52</i>
<i>Table 4.11. Skin(1mm) lamination trial parameters.....</i>	<i>52</i>
<i>Table 4.12 Sample specifications for 3-point bending test .....</i>	<i>54</i>
<i>Table 4.13. Flexural properties and density of RPP core and sandwich panels .....</i>	<i>56</i>
<i>Table 4.14. Sample specifications for 3-point bending test .....</i>	<i>58</i>
<i>Table 4.15. Flexural properties and density of RPP extrudate and sandwich panels according to ASTM D790.....</i>	<i>60</i>
<i>Table 4.16. Sample specifications for peel-off test .....</i>	<i>63</i>
<i>Table 5.1. Density and volume fraction of foamed and solid PP extrudates .....</i>	<i>72</i>
<i>Table 5.2. Theoretical and experimental values of Young's modulus for foamed and solid PP extrudates.....</i>	<i>73</i>
<i>Table 5.3. Sample specification for physical and mechanical tests.....</i>	<i>78</i>
<i>Table 5.4. Flexural properties and density of solid and foam PP extrudates.....</i>	<i>79</i>

*Figure 5.5. Values of fracture strain and toughness of solid and foam PP extrudates ..... 81*

*Table 5.6. Physical and flexural properties of the solid and foam extrudates..... 83*

*Table 5.7. Density and flexural properties of honeycomb and recycled foam sandwich panels ... 88*

*Table 5.8. Effect of skin and core thickness on density and mechanical performance of honeycomb and recycled foam sandwich panels ..... 90*

# Chapter 1. Introduction

## 1.1 Background

It is estimated that since the 1950s, 1 billion tons of plastic have been discarded as garbage. This huge volume of plastic waste could be around for centuries, because the primary bonds of the polymers make them resistant to degradation by the environmental and biological processes of nature [1]. Waste management is one of the major problems facing modern society. The increasing cost of landfill disposal and public interest in support of recycling has forced the industry to look for different innovative ways to reclaim plastic from waste materials [2]. The main challenge is to extract the polymers from material waste and through reprocessing, turning them into a good quality product. It has been common practice to reprocess the waste material arising from normal production.

Plastic recycling is referred to a process in which the scrap or waste plastic materials are recovered and turned into useful products, in some cases products are totally different in form from their initial state like melting plastic bottles and then casting them as plastic plates and sheets<sup>1</sup>. Compared with other materials, such as glass and metal, plastic polymers require more sophisticated processing (heat treating, thermal depolymerization and monomer recycling) to be recycled.

Thermoplastic items can be readily reprocessed into new products by remelting. This is not the case with thermosets and rubbers because of the cross-linking in these polymers. Thus, these materials must be recycled and reprocessed by different means. Plastics are also recycled during the manufacturing process of plastic goods such as polyethylene film and bags. The ultrahigh impact resistance of the thermoplastics structures makes them excellent materials for mass transit systems. Rapid processing cycles, low-cost raw materials, and long shelf life ensure that the thermoplastics offer lower manufacturing cost [3].

---

<sup>1</sup> [https://en.wikipedia.org/wiki/Plastic\\_recycling](https://en.wikipedia.org/wiki/Plastic_recycling)

Plastics extrusion is a high volume manufacturing process in which raw plastic material is melted and formed into a continuous profile [4]. A percentage of the recycled pellets are then re-introduced into the main production operation. Extrusion produces items such as pipe/tubing, weather stripping, fencing, deck railings, window frames, plastic films and sheeting, thermoplastic coatings, and wire insulation.

The first precursors to the modern extruder were developed in the early 19th century. In 1820, Thomas Hancock invented a rubber "masticator" designed to reclaim processed rubber scraps, and in 1836 Edwin Chaffee developed a two-roller machine to mix additives into rubber. The first thermoplastic extrusion was in 1935 by Paul Troester and his wife Ashley Gershoff in Hamburg, Germany. Shortly after, Roberto Colombo of LMP developed the first twin screw extruders in Italy.<sup>1</sup>

## **1.2 Thermoplastic Sandwich Panels**

Sandwich structures typically comprise of skin faces which carry the bending stresses and a low-density core that resists the shear stress. Their superior impact properties and high-energy absorption make these sandwich structures attractive to designers and manufacturers. In transportation, composite sandwich panels have been used in structural roof panels in high-speed trains and in buses structures, front cabins of locomotives, and non-structural interior panels [5]. A proper combination of different core and skin materials allows merging the most advantageous properties of each constituent material, and even eliminating some of their negative properties. The combination of glass fiber reinforced polymers (GFRP) skins (e.g. unidirectional/bidirectional prepreg and twintex) with appropriate cores allows obtaining high stiffness to weight and strength to weight ratios [6]. Thermoplastic sandwich panels provide an effective combination of high flexural properties and good impact strength with a light structural weight. The conventional thermoplastic sandwich panels are made of honeycomb (nomex, polypropylene) or expanded polystyrene (EPS) foam as the core material sandwiched between fiber reinforced thermoplastic skins. Among these core materials, honeycomb is attractive for manufacturing sandwich panels due to its excellent properties, such as light

---

<sup>1</sup> en.wikipedia.org/wiki/Plastics\_extrusion.

weight, rot resistance, impact resistance, recycling ability and thermal insulation. However, honeycombs are quite expensive materials for manufacturing sandwich panels. Moreover, honeycomb sandwich panels are susceptible to delamination under the bending loads because of the lattice structure of hollow cells leads to a poor bonding between skin and honeycomb. Rigid thermoplastic cores could be a good alternative to address this issue since they increase the overall bonding surface and show more resistance to delamination. Furthermore, if the base resin for both the skin and core material is same (e.g. polypropylene in case of PP/GF core and twintex skin), there is a good compatibility between core and skin materials and it creates a strong and well-bonded sandwich panel.

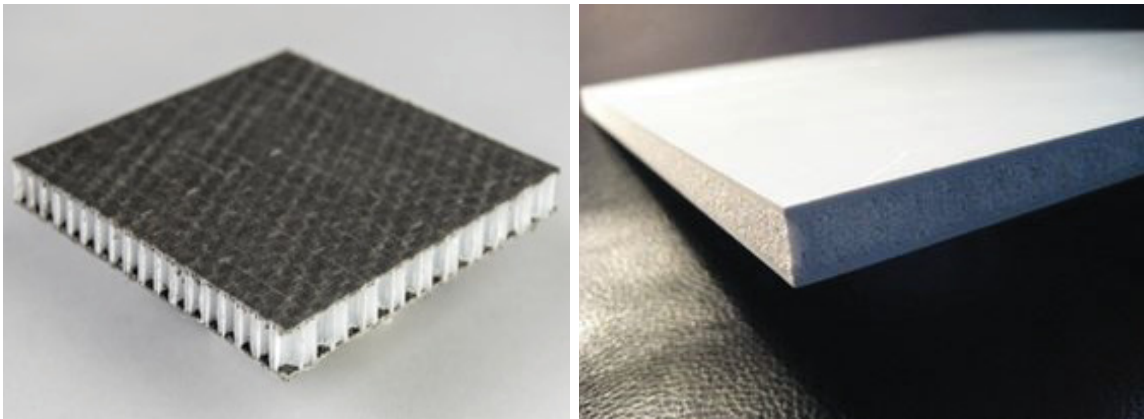


Figure 1.1. Honeycomb and foam sandwich panels

There are several sheet forming processes for manufacturing thermoplastic composites, including match die forming [7], roll forming [8–9], stretch forming [10] and sheet extrusion. Currently, the fabrication of thermoplastic sandwich panels are carried out in multistage manufacturing processes such as diaphragm forming, thermoforming and vacuum bag processing [3], [11-12]. Our present work aims to produce composite sandwich panels using recycled materials in a continuous extrusion processing.

### 1.3 Foaming Process

Polymer foams are widely used in various applications such as disposable packaging of fast food, the cushioning of furniture and insulation material. Using a chemical foaming agent (CFA) along with a thermoplastic polymer in a foam extrusion process has a significant effect on the density and thickness of the final product so that highly light-weight and low-cost structures could be achieved.



Figure 1.2. Polymer foam structures

Foam extrusion is able to produce foam continuously, so it is commercially attractive to use the existing extrusion equipment for foam processing. The basics of foam extrusion consist of mixing a chemical foaming agent (CFA) with the polymer to be extruded. The heat generated to melt the polymer decomposes the chemical foaming agent resulting in gas being liberated. This gas is dispensed in the polymer melt and expands upon exiting the die [13].

There are two different types of foaming agents; one is exothermic foaming agent which generates heat upon decomposition and it results in higher melt temperature than the extruder and die temperature. It's important in terms of melt viscosity, extrusion load and pressure as they are lower in value for high melt temperature. The other type is endothermic blowing agent which absorbs heat to decompose and leads to a melt temperature closely to the die temperature [13].

The extrusion foaming process utilized in this experimental study to manufacture PP foam extrudate and the effective parameters in the foam process will be discussed in chapter 5 of this report.

## 1.4 Plastic Extrusion

One of the most common methods of processing plastics is extrusion in which semi-finished articles such as sheets or rods are forced to flow by compression through the die opening of a smaller cross-sectional area and subsequently fabricated into a desired shape. Among the several plastic processing methods, thermoplastic extrusion has a significant share in industry. Figure 1.3 illustrates the distribution of the thermoplastic processing methods.

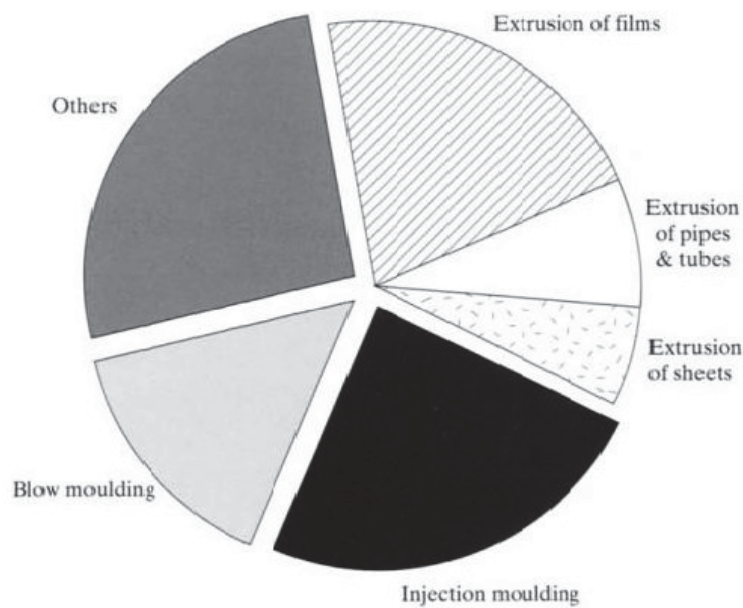


Figure 1.3. Market share for major thermoplastic processings [14]

What happens inside the extruder is first, feeding the barrel through a top-mounted hopper into a rotating screw and then conveying the plastic forward through the heated barrel. As the plastic is conveyed forward along the screw, the channel depth decreases and it forces the plastic into a smaller area. The combination of pressure and screw rotation causes friction which generates heat. This is called shear heating. This heat along with the heat from the barrel heating system melts the plastic. As the molten plastic is moving forward along the barrel, it should be well mixed and flowed under a proper pressure and temperature. A rectangular cross section die has been set at the end of the barrel which produces the thermoplastic sheet with desired width and thickness.

Basically an extruder screw has three different zones.

- **Feed Zone:** The function of this zone is to preheat the plastic and convey it to the subsequent zones. The design of this section is important since the constant screw depth must supply sufficient material to the metering zone so as not to starve it, but on the other hand not supply so much material that the metering zone is overrun. The optimum design is related to the nature and shape of the feedstock, the geometry of the screw and the frictional properties of the screw and barrel in relation to the plastic. The frictional behaviour of the feed-stock material has a considerable influence on the rate of melting which can be achieved.

- **Compression Zone:** In this zone the screw depth gradually decreases so as to compact the plastic. This compaction has the dual role of squeezing any trapped air pockets back into the feed zone and improving the heat transfer through the reduced thickness of material.

- **Metering Zone:** In this section the screw depth is again constant but much less than the feed zone. In the metering zone the melt is homogenised so as to supply at a constant rate, material of uniform temperature and pressure to the die. This zone is the most straight-forward to analyse since it involves a viscous melt flowing along a uniform channel.

The pressure build-up which occurs along a screw is illustrated in Figure 1.4. The lengths of the zones on a particular screw depend on the material to be extruded [15].

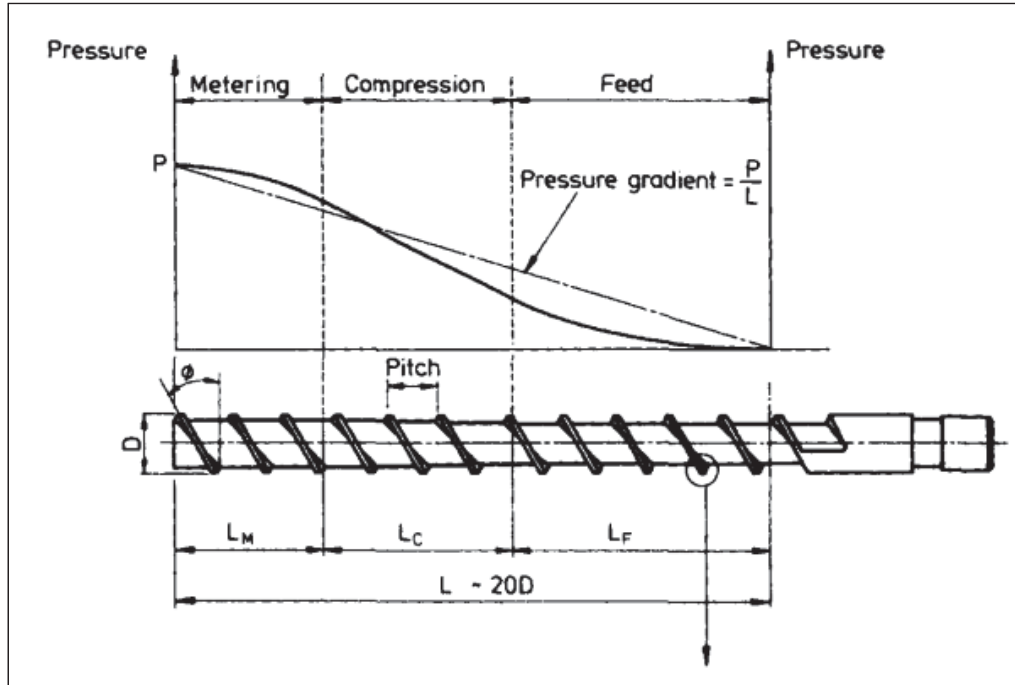


Figure 1.4. Distribution of pressure in the extruder zones [15]

## 1.5 Research Motivation

A better understanding of plastic recycling process will lead to developing new fundamental ways to solve the economic and environmental issues regarding the waste management. Although the plastic recycling technology is well established and utilized in industry to reuse the industrial and domestic scraps, but more investigations are still needed to turn them into the high-performance materials through a low-cost manufacturing procedure. Increasing the production ratio and at the same time reducing the manufacturing cost is a challenging job which needs a precise analysis of the process parameters. More experimental studies are required to replace the existing technology for producing sandwich panels through a high-rate and low-cost manufacturing process.

Plastic extrusion is able to reproduce plastic articles continuously from the starting shredded scraps, so it is commercially attractive to use the existing extrusion equipment for recycling thermoplastic materials. Production of thermoplastic sandwich panels using recycled materials in a continuous extrusion process can speed up the manufacturing process. The big challenge is to create a proper setup of the experimental parameters such

as operating temperature, pressure and take-up speed during the sheet extrusion and skin lamination processes. It is far from being called an easy job and requires a good understanding of theoretical principles for manufacturing thermoplastic sandwich panels and performing some experimental optimization methods such as Taguchi method.

## **1.6 Objectives**

The objective of this experimental research is to study the thermoplastic recycled material behavior under different thermal conditions in a plastic extrusion line and the possibility of turning them into the sandwich panels for different applications including construction and transportation.

The primary goal of this work is to produce a light-weight and high-strength and high-stiffness sandwich panel made of thermoplastic skin and recycled Glass Fiber Reinforced Polypropylene (GFRPP) core material in a continuous plastic extrusion line.

Making a strong and well-bonded sandwich panel needs a precise analysis of thermal behavior of the core and skins during the lamination and consolidation processes. A proper setup of machines (extruder, skin heating chamber, conveyor belt and puller) throughout the production line is also required. When the desired panel is achieved, the effect of operation parameters such as extrusion pressure and temperature and material's characteristics like core and skin thickness on the quality of the final product is investigated.

During our experimental work, in addition to manufacturing thermoplastic sandwich panels, we apply some foaming processes to reduce the density of panels and achieve a light-weight and high-thick core to fabricate foam sandwich panels. Foaming is one of the manufacturing technologies which give plastics a number of unique properties such as reduced density and heat and sound insulating properties. Foam extrusion is able to produce foam continuously, so it is commercially attractive to use the existing extrusion equipment for foam processing.

# Chapter 2. Theory

## 2.1 Sandwich Panel Analysis

Consider a sandwich panel with a rectangular cross section of width (b) and thickness (h) and two identical face sheets of thickness (t) perfectly bonded with a core of thickness (c). This sandwich panel is loaded under a 3-point bending test as shown in Figure 2.1.

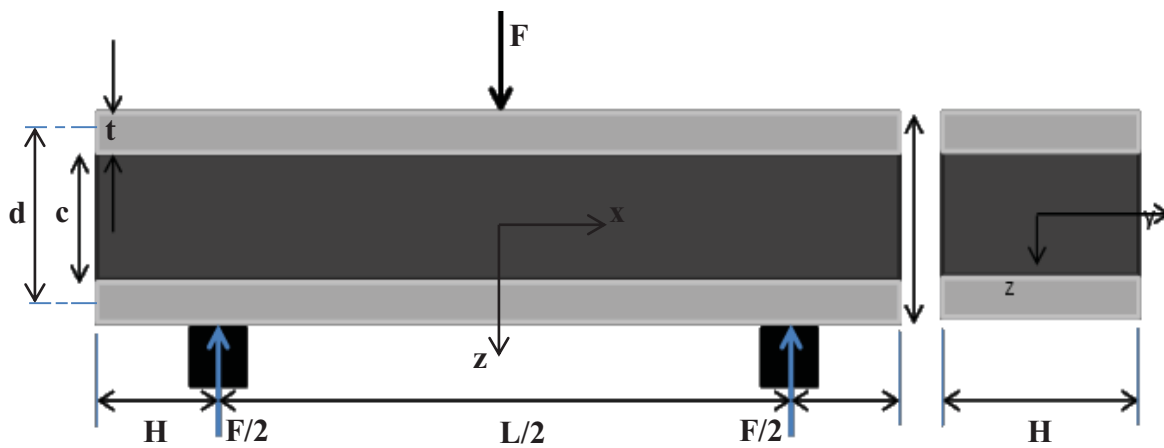


Figure 2.1. A schematic view of a sandwich panel with rectangular cross section

By using the ordinary theory of the bending, the stress distribution in the sandwich panel can be easily calculated. Recall that this theory is based on the assumption that the cross-sections of the beam remain perpendicular to the neutral axis of the beam under the bending load. Then, we have

$$\frac{M}{EI} = \kappa_x = -\frac{1}{R} \quad (2.1)$$

where  $M$  is the bending moment applied on the beam which has a maximum value in the center of the beam equals to

$$M = \frac{PL}{4} \quad (2.2)$$

EI is the flexural rigidity of the beam which is the product of elastic moduli (E) and second moment of area (I) for a homogeneous beam. But, for a sandwich panel consisting of core and face sheets it is a summation of the rigidity of the faces and core measured about the neutral axis of the sandwich panel.

$$(EI)_{eq} = (EI)_f + (EI)_c \quad (2.3)$$

$$(EI)_{eq} = \frac{E_f b t^3}{6} + \frac{E_f b t d^2}{2} + \frac{E_c b c^3}{12} \quad (2.4)$$

where  $E_f$  and  $E_c$  are the elastic modulus of the face sheet and core, respectively and  $d=c+t$  is the distance between the center lines of the upper and lower faces.

The first two terms of the above equation represent the stiffness of the face sheets about the centroidal axis of the entire sandwich. In practical sandwich panels, the ratio of the core to skin thickness is quite large and therefore the first term amounts to less than 1% of the second one when

$$3 \left(\frac{d}{t}\right)^2 > 100 \quad \text{or} \quad \frac{d}{t} > 5.77 \quad (2.5)$$

When the stiffness of the core material is much lower than that of for the face sheets, we can neglect the third term of the equation (2.4) compared to the second one. In other words, the third term in the equation (2.4) is less than 1% of the second if

$$6 \frac{E_f}{E_c} \frac{t}{c} \left(\frac{d}{c}\right)^2 > 100 \quad (2.6)$$

Hence, the dominant term to express the flexural rigidity of a sandwich beam under the bending test is that of the faces bending about the neutral axis of the entire sandwich [16].

For a beam subjected to a bending load, the strain at a point situated in a distance  $z$  from the neutral axis is

$$\epsilon_x = k_x z = \frac{Mz}{EI} \quad (2.7)$$

Multiplying this strain by the modulus of elasticity at the level  $z$  will result to the bending stress within the sandwich panel. For instance, the bending stress in the core and face sheets can be calculated as follows

$$\sigma_c = \frac{Mz}{(EI)_{eq}} E_c \quad (-c/2 \leq z \leq c/2) \quad (2.8a)$$

$$\sigma_f = \frac{Mz}{(EI)_{eq}} E_f \quad (-h/2 \leq z \leq -\frac{c}{2}; \quad c/2 \leq z \leq h/2) \quad (2.8b)$$

Hence the value of bending stress varies linearly within the core and face sheets, but there is a drastic change in the bending stress at the skin/core interface due to the huge difference between the moduli of elasticity of the core and skin materials.

The maximum core and skin stresses occur at the furthest level from the neutral axis for both the core and skin materials. These maximum values are

$$(\sigma_c)_{\max} = \frac{ME_c}{(EI)_{eq}} \frac{c}{2} \quad (2.9)$$

$$(\sigma_f)_{\max} = \frac{ME_f}{(EI)_{eq}} \frac{h}{2} \quad (2.10)$$

The assumptions of the ordinary theory of bending in the same manner as above yield to a general expression for the shear stress at a depth  $z$  below the centroid of the cross-section [17]

$$\tau = \frac{QS}{Ib} \quad (2.11)$$

where  $Q$  is the shear force applied on the section,  $I$  is the second moment of area of the entire section about the centroid,  $b$  is the width at the level  $z$  and  $S$  is the first moment of area of the part of section under the level  $z$ .

In the case of composite beam such as the sandwich panel shown in Figure 2.1 the moduli of elasticity of the different elements must be taken into account and therefore the equation (2.11) can be modified to

$$\tau = \frac{Q}{Db} \sum(SE) \quad (2.12)$$

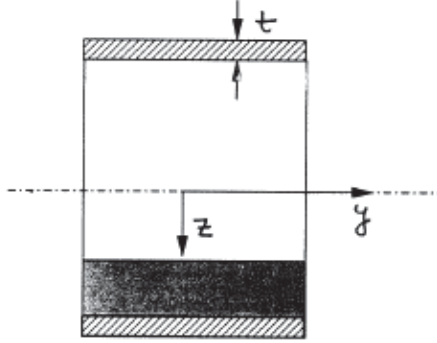


Figure 2.2. Cross section of the beam under shear stress

where  $D=EI$  is the flexural rigidity of the entire section and  $\sum(SE)$  is the sum of the products of  $S$  and  $E$  of all components of the beam under the level  $z$ . For instance, the shear stress at level  $z$  in the core of the sandwich in Figure 2.2 can be calculated as follows

$$\sum(SE) = \frac{E_f b t d}{2} + \frac{E_c b}{2} \left(\frac{c}{2} - z\right) \left(\frac{c}{2} + z\right) \quad (2.13)$$

Combining equations (2.12) and (2.13) will lead to

$$\tau = \frac{Q}{D} \left[ \frac{E_f t d}{2} + \frac{E_c}{2} \left(\frac{c^2}{4} - z^2\right) \right] ; \quad \left(-c/2 \leq z \leq c/2\right) \quad (2.14a)$$

A similar expression can be obtained for shear stress in the faces

$$\tau = \frac{Q}{D} \left[ \frac{E_f}{2} \left(\frac{h^2}{4} - z^2\right) \right] ; \quad \left(-h/2 \leq z \leq -\frac{c}{2}; \quad c/2 \leq z \leq h/2\right) \quad (2.14b)$$

When the core material is too weak ( $E_c \ll E_f$ ), the shear stress may be assumed constant over the depth of the core.

The flexural and shear stress distribution within a sandwich panel has been graphically represented by plotting the equations (2.8) and (2.14) as illustrated in Figure 2.3.

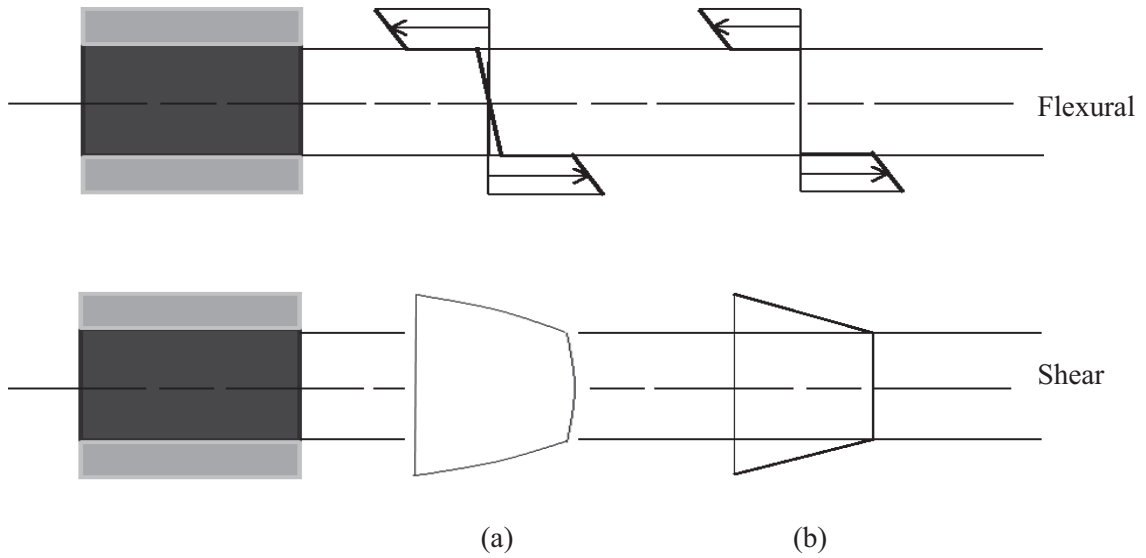


Figure 2.3. Flexural and shear stress distribution in a sandwich beam; (a) No approximation  
 (b)  $E_c \ll E_f$

As a conclusion of the above results, we can now better understand the effect of core thickness on the weight, bending stiffness and strength of the sandwich panel.

The flexural stiffness of the above sandwich panel is given by

$$\frac{F}{\delta} = \frac{48(EI)_{eq}}{L^3} \quad (2.15)$$

Hence, higher the flexural rigidity  $(EI)_{eq}$ , higher the beam stiffness will be. Given the above analysis, we can find out the corresponding stiffness and strength of sandwich panels in terms of core thickness (Figure 2.4).

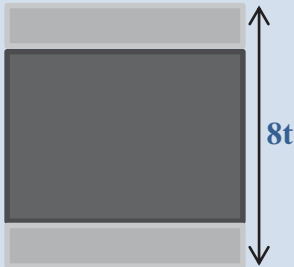
Sandwich Beam	Weight	Flexural Rigidity $(EI)_{eq}$	Bending Strength
	1	1	1
	~1	~12	~6
	1-2	~48	~12

Figure 2.4. Effect of core thickness on the weight, bending stiffness and strength of the sandwich panel for  $\rho_c \ll \rho_f$  and  $E_c \ll E_f$

Thus, the flexural rigidity and stiffness of a beam can be significantly increased by using the sandwich concept in comparison to a homogeneous beam without adding too much weight to the structure.

## 2.2 Drag Flow in Extruder

The principal transport mechanism in the extruder is drag flow, resulting from friction between the viscous liquid and two opposing surfaces moving relative to each other; (1) the stationary barrel and (2) the channel of the turning screw. Also, compressing the polymer melt through the downstream die creates a back pressure in the barrel that reduces the material moved by drag flow. This flow reduction, called the back pressure flow, depends on the screw dimensions, viscosity of the polymer melt, and pressure

gradient along the barrel [1]. Thus, the melt flow in an extruder is the difference between these two opposing flows (drag flow and back pressure flow).

$$Q_m = Q_d - Q_b = 0.5\pi^2 D^2 N d_c \sin A \cos A - \frac{P \pi D d_c^3 \sin^2 A}{12 \eta L} \quad (2.16)$$

where  $Q$  is flowrate  $m^3/s$  ( $in^3/sec$ ) and subscripts  $m$ ,  $d$  and  $b$  refer to melt flow, drag flow and back pressure flow, respectively.  $D$ ,  $d_c$ ,  $A$  and  $L$  are the extruder geometric parameters and depend on the screw configuration and design.  $D$  is screw flight diameter,  $m$  ( $in$ );  $N$  is screw rotational speed,  $rev/sec$ ;  $d_c$  is screw channel depth,  $m$  ( $in$ );  $A$  is flight angle and  $L$  is the barrel length,  $m$  ( $in$ ).  $P$  is the head pressure in the barrel,  $MPa$  ( $lb/in^2$ ) and  $\eta$  is the polymer melt viscosity,  $N.s/m^2$  ( $lb.s/in^2$ ).

As can be seen in equation (2.16), there are two opposing situations happen regarding the extruder's melt flow; one is the case of free discharge when there is no pressure build up at the end of the extruder so the melt flow is exactly same as the drag flow and equals to

$$Q_{max} = 0.5\pi^2 D^2 N d_c \sin A \cos A \quad (2.17)$$

The other case is when the pressure at the end of the extruder is high enough to stop the melt flow. Hence  $Q_m = 0$  and

$$P_{max} = \frac{6 \pi D N \eta L}{12 d_c^2 \tan A} \quad (2.18)$$

The two values  $Q_{max}$  and  $P_{max}$  are the two end points of a diagram known as the extruder characteristic (or screw characteristic) which indicates the relationship between head pressure and flow rate in an extrusion machine with given operating parameters (Figure 2.5).

When a die is coupled to the extruder the situation is quite different than that of an open-end extruder. The extruder has a high output if the back pressure at its outlet is low. However, the outlet of the extruder is the inlet to the die and the output of the die increases with inlet pressure [15]. Flow rate through the die depends on the size and shape of the opening and the pressure applied to force the melt through it. This can be demonstrated as

$$Q_d = K_s P \quad (2.19)$$

where  $Q_d$  is the flow rate,  $m^3/s$  ( $in^3/sec.$ ),  $p$  is the head pressure, Pa ( $lb/in^2$ ) and  $K_s$  is the shape factor depends on the die configuration,  $m^5/Ns$  ( $in^5/lb-sec$ ). For a die with rectangular cross section, it can be shown that

$$K = Fbd^3/12\eta L_d \quad (2.20)$$

where  $b$  is the die width,  $m(in)$  and  $d$  is the die opening size,  $m(in)$ .  $F$  is a non-dimensional factor (Flow coefficient),  $\eta$  is the melt viscosity,  $N-s/m^2$  ( $lb-sec/in^2$ ) and  $L_d$  is the length of the Die,  $m(in)$ .

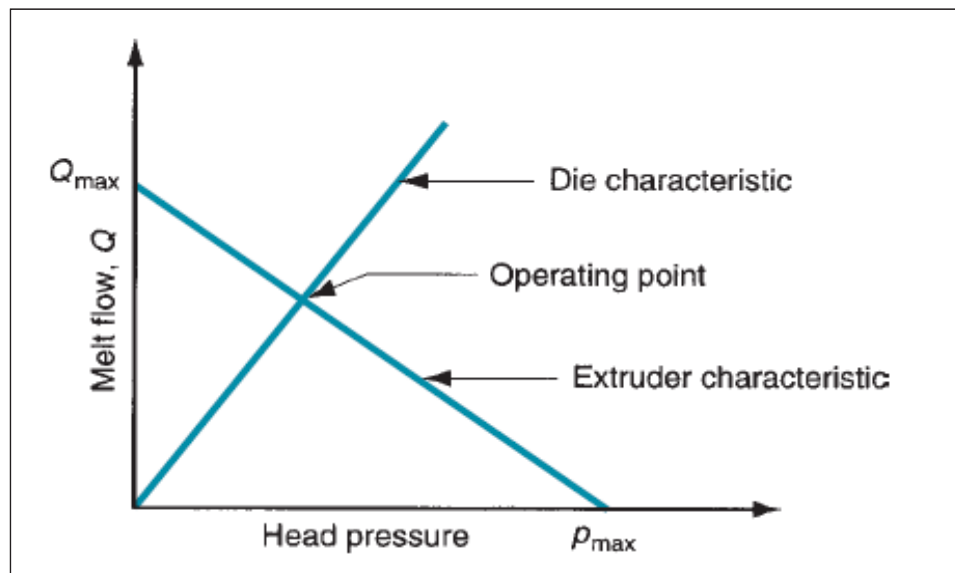


Figure 2.5. Extruder and die characteristic [1]

The flow coefficient can easily be obtained from Figure 2.6.

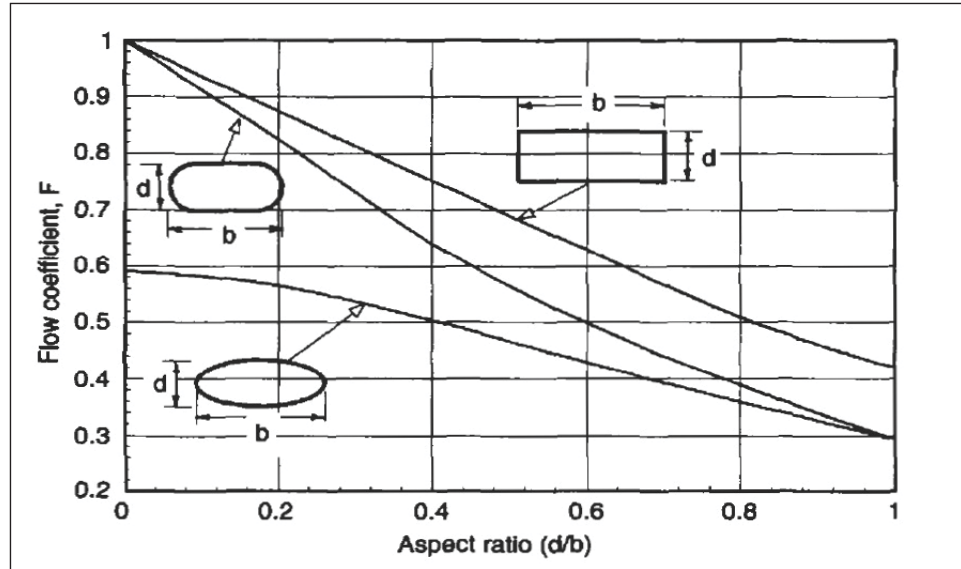


Figure 2.6. Flow coefficient as a function of die geometry [15].

### 2.3 Heat Transfer Phenomena

The main issue in manufacturing thermoplastic sandwich panels through an in-line extrusion procedure is to convey the molten plastic upon exiting from the extruder due to the high temperature of the extruded part. On the other hand, the temperature of the core and skin should be high enough for a proper lamination process. The process parameters optimization could be challenging and needs a careful analysis of thermal properties of the compound materials and also a good understanding of heat transfer phenomena during the extrusion and lamination process.

If we assume that the skins are first preheated and then bonded to the core after it comes out of the extruder, two heat transfer phenomena happen; one is convection heat transfer at the surface of the extruded core before skin lamination and the other one is thermal conduction (or diffusion) through the skin thickness when it starts to get in touch with the hot surface of the core. Thermal convection of the extruded plate is the heat dissipation from the surface by means of the air stream on both sides of the core which cools it down after it comes out of the extruder. Since we desire to follow up the lamination process, the pre-consolidated skins should get in touch with the core material before a drastic reduction in temperature occurs. In Chapters 3 and 4, we will show that the minimum

required temperature for a good bonding between the skins and core material is around 120°C when they are cooled down from their melt temperature (150°C- 160°C).

Heat transfer through the top and bottom surface of the material could be estimated by the Newton's cooling law:

$$\frac{dQ}{dt} = h.A (T_t - T_{env}) \quad (2.21)$$

Q is the thermal energy in joules, h is the heat transfer coefficient (assumed independent of T here) (W/m<sup>2</sup> K), A is the surface area of the extruded material (m<sup>2</sup>), T is the temperature of the object's surface and interior (since these are the same in this approximation), T<sub>env</sub> is the temperature of the environment and t is the time (s).

From the definition of heat capacity, we have:

$$\frac{dQ}{dt} = C \frac{dT}{dt} \quad (2.22)$$

where C is heat capacity (J/°C) of the material defined by mass-specific heat capacity C<sub>p</sub> (J/kg°C) multiplied by its mass (kg):

$$C = m.C_p \quad (2.23)$$

From equations (2.21) and (2.22) we derive:

$$\frac{dT}{dt} = - \frac{hA}{c} (T_t - T_{env}) = -r \Delta T_t \quad (2.24)$$

The solution of this differential equation gives:

$$T_t = T_{env} + (T_0 - T_{env}) e^{-rt} \quad (2.25)$$

where  $r = \frac{hA}{c}$  is a positive constant characteristic of the system (s<sup>-1</sup>) defined by

$$r = \frac{hA}{c} = \frac{hA}{mC_p} = \frac{hA}{\rho C_p (Az)} = \frac{h}{\rho C_p z} \quad (2.26)$$

z is the thickness of the extruded plate which is 4 mm in this work.

Based on the mixing rule, the total  $\rho C_p$  of the material could be calculated by

$$\rho C_p = x_f (\rho c)_f + x_{pp} (\rho c)_{pp} \quad (2.27)$$

where  $x_f$  and  $x_{pp}$  are the FG and PP mass fractions, respectively.

The total  $\rho C_p$  could be predicted by assuming that the core and skins are connected in series and then we have

$$r = \frac{h}{\rho C_p z} = 2 \times h \left[ \left( \frac{1}{\rho C_p z} \right)_{\text{core}} + \left( \frac{1}{\rho C_p z} \right)_{\text{skin}} \right] \quad (2.28)$$

Once the thermoplastic skins touch the extruded core, the heat flux is transferred in the z-direction (through the thickness). So, the thermal diffusivity could be simplified as follows:

$$\frac{dT}{dt} = \alpha \frac{\partial^2 T}{\partial z^2} \quad (2.29)$$

The solution of this differential equation gives:

$$T - T_{\text{sur}} = (T_0 - T) \operatorname{erf} \frac{z}{2\sqrt{\alpha \cdot t}} \quad (2.30)$$

where  $\alpha$  is the thermal diffusivity defined by

$$\alpha = \frac{k}{\rho C_p} \quad (2.31)$$

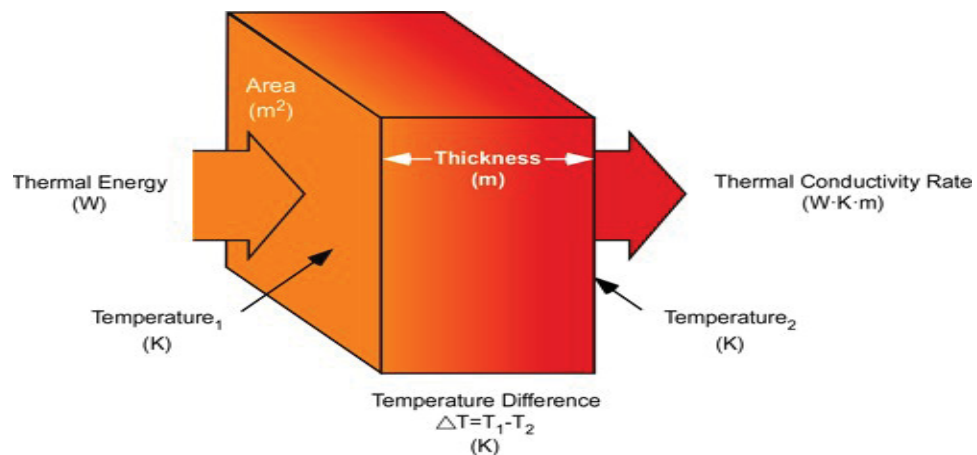


Figure 2.7. A scheme of thermal diffusion through the thickness of a plate<sup>1</sup>

<sup>1</sup> <http://cfbt-us.com/wordpress/?cat=5&paged=2>

The thermal diffusivity of the skin depends upon thermal conductivity  $k$ , density  $\rho$  and  $C_p$  of all components of the thermoplastic skin.

Thermal conductivity could be calculated by rule of mixture in the two principal directions; parallel and normal to the bundle direction. In other words, it is a mixture of parallel and series FG and PP components within the material.

$$k = \frac{k' + k''}{2} \quad (2.32)$$

where  $k'$  and  $k''$  are defined by

$$k' = x_f k_f + x_{pp} k_{pp}, \quad k'' = \frac{1}{\frac{x_f}{k_f} + \frac{x_p}{k_p}} \quad (2.33)$$

where  $x_f$  and  $x_{pp}$  are the mass content of fiberglass and polypropylene, respectively. So, we can easily calculate the amount of  $\rho C_p$ ,  $k$  and  $\alpha$  for the extruded core sheet.

# Chapter 3. Material and Manufacturing

## 3.1 Raw Materials Characteristics

### 3.1.1 Polypropylene

Polypropylene (PP), also known as polypropene, is a thermoplastic polymer used in a wide variety of applications such as packaging, plastic parts and automotive components. A rough estimation of the market share for the major plastic materials shows that PP has got more than 27% of the market share [14]. Most commercial polypropylene is isotactic and has an intermediate level of crystallinity between that of low-density polyethylene (LDPE) and high-density polyethylene (HDPE). PP is normally tough and flexible, especially when copolymerized with ethylene. This allows polypropylene to be used as an engineering plastic, competing with materials such as acrylonitrile butadiene styrene (ABS).

The relative orientation of each methyl group (CH<sub>3</sub> in Figure 3.1) relative to the methyl groups in neighboring monomer units has a strong effect on the polymer ability to form crystals and as well as its physical properties such as melt point and density. The general chemical formula of PP is (C<sub>3</sub>H<sub>6</sub>)<sub>n</sub> and its density varies from 0.855 g/cm<sup>3</sup> to 0.946 g/cm<sup>3</sup>. The melting point of polypropylene occurs at a range, so a melting point is determined by finding the highest temperature of a differential scanning calorimetry (DSC) chart. Perfectly isotactic PP has a melting point of 171 °C (340 °F). Commercial isotactic PP has a melting point that ranges from 160 to 166 °C (320 to 331 °F), depending on tacticity and crystallinity.

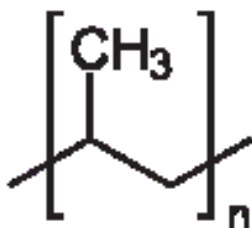


Figure 3.1. Methyl group

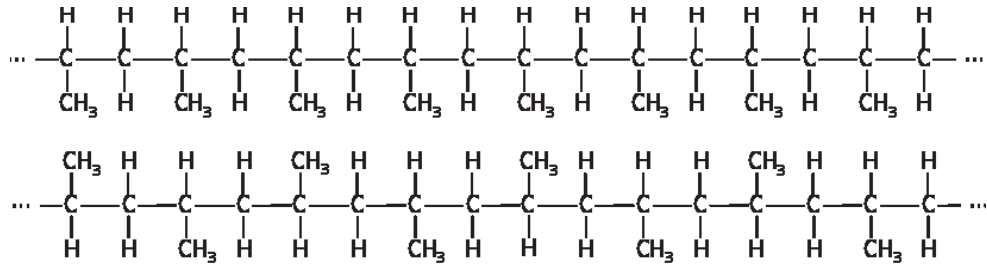


Figure 3.2. Short segments of polypropylene; isotactic (above) and syndiotactic(below) tacticity

Thanks to its straight-chain structure, PP can be readily recycled to produce new items by remelting. Generally, PP can offer better mechanical properties than other common thermoplastics such as polystyrene (PS), polyurethane (PU) and polyethylene (PE). It has higher flexural modulus than PE. Moreover, PP exhibits better impact strength than PS. At room temperature, PP is above its glass transition temperature and below its melting temperature. Hence, it is in a rubbery region and can offer better impact resistance than PS.

### 3.1.2 Randomly Oriented Chopped Glass Fiber Polypropylene

Chopped glass fibers can be added to the resin in a random manner in order to reinforce the polymer and reduce the directionality of the composite structure [18]. The methods for manufacturing these types of composite structures are same as those for neat resins and chopped fibers are added to the raw materials of solid polymer pellets but some points should be taken into account [19];

- Ensure that a homogenous dispersion of the fibers and their random orientation takes place during the whole processing.
- Mixing, machining and manufacturing parts should be designed in a way to avoid the stagnation and accumulation of fibers.
- The manufacturing tools must be sufficiently abrasion resistant to resist the abrasive effect of fibers.

Figure 3.3 shows some basic properties of chopped glass fiber reinforced thermoplastics.

	PP	PA	PBT	POM
Density (g/cm <sup>3</sup> )	1.1–1.2	1.3–1.4	1.5–1.6	1.5–1.6
Tensile or flexural strength (MPa)	40–70	100–160	110–160	130–140
Tensile or flexural modulus (GPa)	4–8	5–9	7–12	9–11
Elongation at break (%)	2–3	4–7	2–7	3–12
Izod notched impact (J/m)	45–160	130–160	50–230	50–100
HDT A (1.8 MPa) (°C)	120–140	230–260	195–240	145–163
Coefficient of thermal expansion (10 <sup>-5</sup> /°C)	2–3	2–3	2–5	2–3
Resistivity (ohm.cm)	10 <sup>16</sup> –10 <sup>17</sup>	10 <sup>12</sup> –10 <sup>13</sup>	10 <sup>15</sup> –10 <sup>16</sup>	10 <sup>15</sup> –10 <sup>16</sup>
	PC	PSU	PPS	PEEK
Density (g/cm <sup>3</sup> )	1.35–1.5	1.4–1.5	1.8–2	1.5
Tensile or flexural strength (MPa)	90–160	100–125	60–150	150–180
Tensile or flexural modulus (GPa)	6–10	7–10	10–17	9–12
Elongation at break (%)	2–4	2–3	1–3	2–3
Izod notched impact (J/m)	90–200	55–80	25–70	95–130
HDT A (1.8 MPa) (°C)	140–150	175–185	170–260	290–315
Coefficient of thermal expansion (10 <sup>-5</sup> /°C)	2–4	2–3	1–2	1.5–2
Resistivity (ohm.cm)	10 <sup>15</sup> –10 <sup>16</sup>	10 <sup>15</sup> –10 <sup>16</sup>	10 <sup>15</sup> –10 <sup>16</sup>	10 <sup>15</sup> –10 <sup>17</sup>

Figure 3.3. Basic properties of short glass fiber reinforced thermoplastics

The recycled polypropylene (RPP) used in this study was a random copolymer grade of industrial recycled scraps. The density and melt index of this PP were 0.82 g/cm<sup>3</sup> and 11 g/10 min at 230 °C (ASTM D 1238), respectively. Chopped glass fibers with the density of 2.5 gr/cm<sup>3</sup> in the form of regrind thermoplastic prepreg (e.g. TWINTEX) were added to the RPP pellets (RTWT/PRP). RTWT is a composition of 60/40 wt% FG/PP. These materials are the scraps of the composite structures which are cut into shreds to be recycled through the plastic extrusion process.

In our extrusion procedure, raw compound materials in form of shred pellets are gravity fed from a top mounted hopper into the barrel of the extruder. RPP is a combination of three different components; black fragments (black PP), white fragments (white PP) and pellet-shape PP. Regrind TWINTEX (RTWT) which is made of commingled E-Glass/Polypropylene in form of chopped fibers added to enhance mechanical properties and reduce the production cost. Figure 3.4 shows the raw materials used to extrude solid PP core.

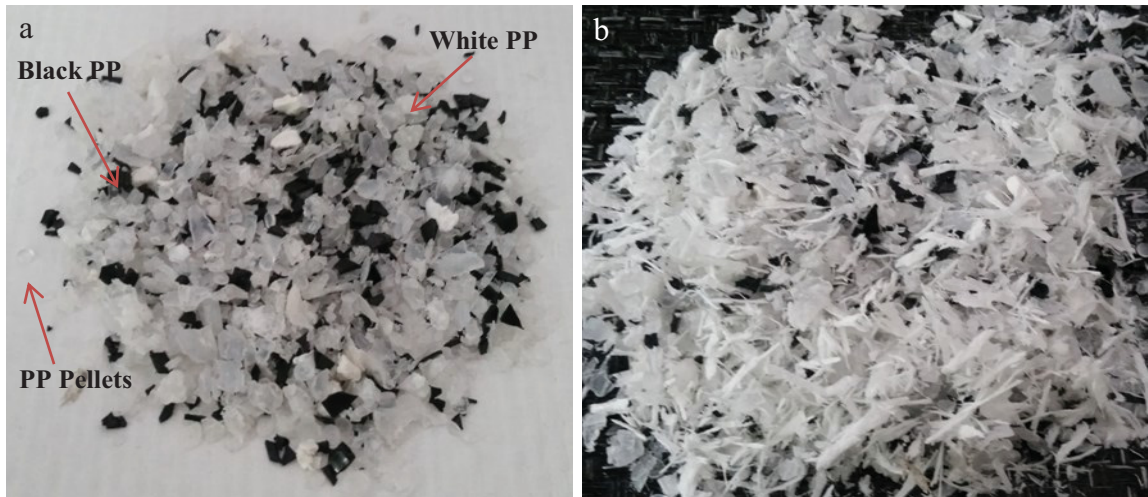


Figure 3.4 Raw materials for extrusion process; a) PP components, b) PP+RTWT

Differential scanning calorimetry DSC and Thermogravimetric Analyzer TGA was used to identify the thermal properties of different components within the recyclate. Melting temperature and decomposition temperature were determined. These are critical parameters for the foaming and lamination processes.

Figures 3.5-3.7 show the heat flow-temperature curve in a heating/cooling/heating cycle of DSC analysis for three different polypropylene components used as raw materials for extruding the core. As seen in these figures, the heat flow pick in the heating cycle for PP occurs slightly above 150°C which shows that the melt temperature for PP is around 150 °C; a close value to our extrusion operating temperature. It can be seen that during the cooling cycle, the heat flow has a maximum value around 120°C which can be interpreted as its recrystallization temperature indicating that PP is still in a molten state when it is cooled down from its melt temperature to 120°C and it would be able to be bonded with the skin upper this value. Since the constitutive components for the both of core and skin materials are PP and Fiber Glass, the same thermal behavior could be expected for them. To be more precise, a small piece of the extruded plate was cut and tested using DSC analysis. The same trend was observed for that in terms of melt temperature and lamination area as illustrated in Figure 3.8.

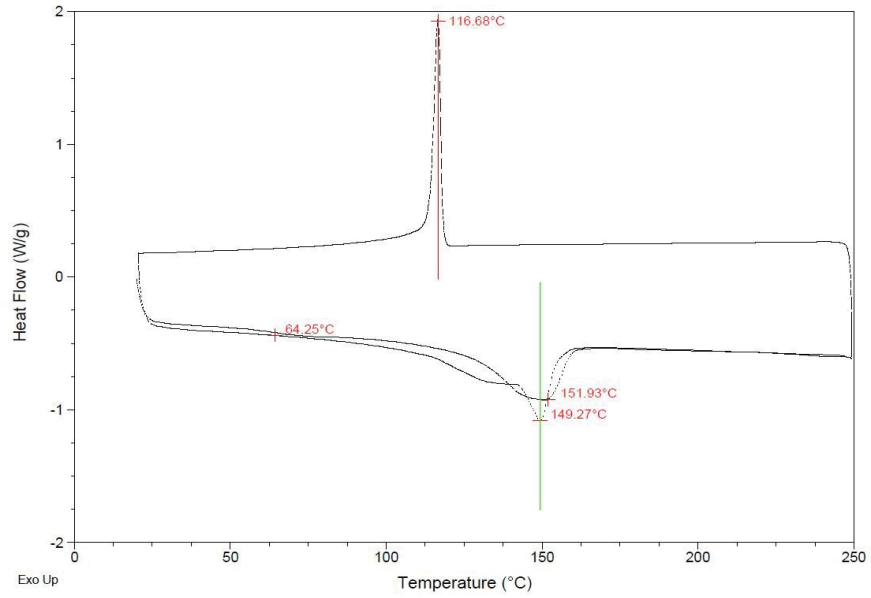


Figure 3.5. Heating/cooling/heating cycle for black PP

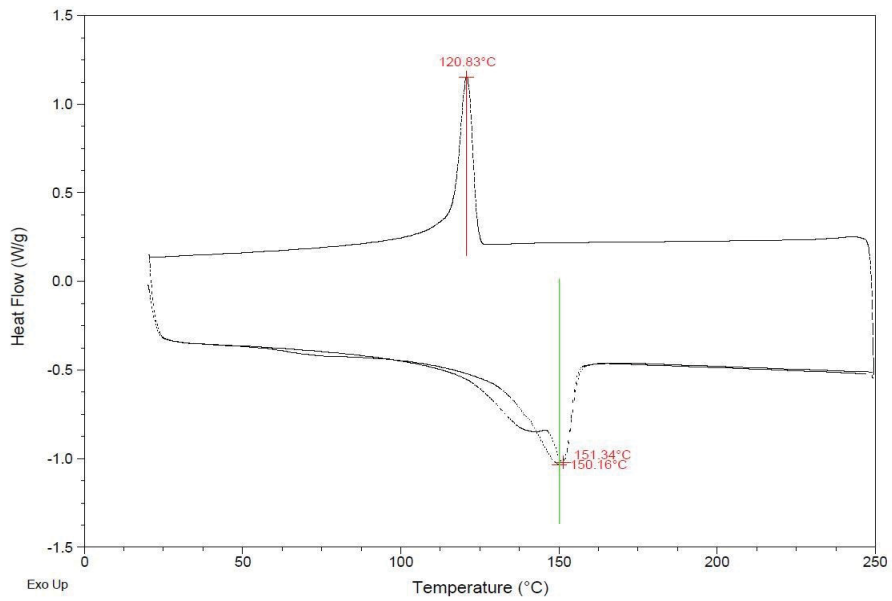


Figure 3.6. Heating/cooling/heating cycle for white PP

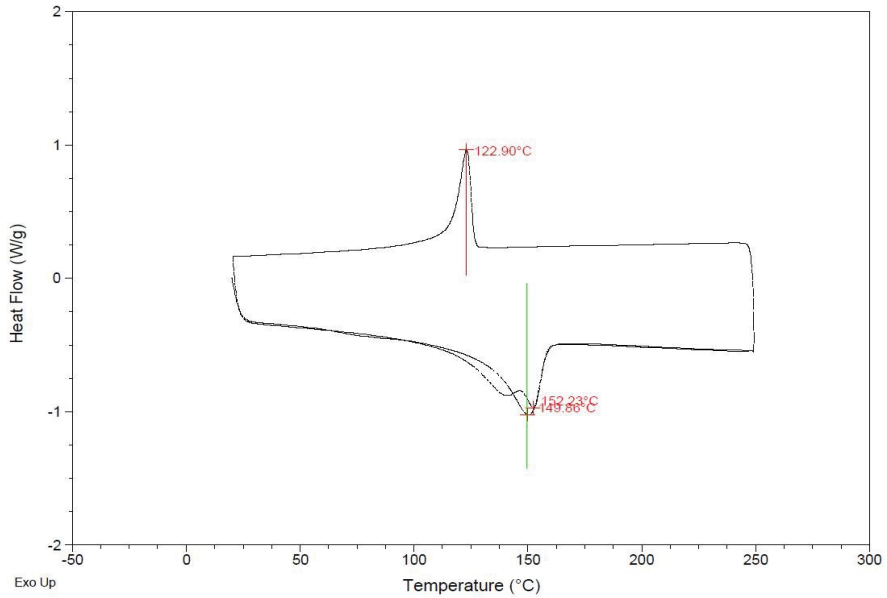


Figure 3.7. Heating/cooling/heating cycle for PP pellets

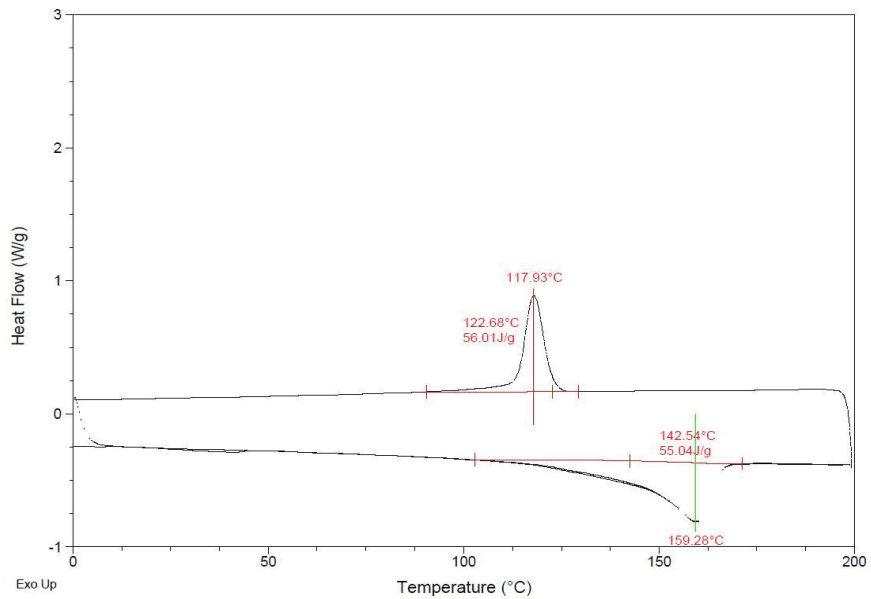


Figure 3.8. Heating/cooling/heating cycle for RPP extruded plate

### 3.1.3 Foaming Agents

The maximum core thickness we can achieve is same with the die opening size which is 4 mm and we can reduce the thickness by squeezing the extrudate between the top and bottom belts of the conveyor double belt press machine. Also, to increase the thickness of

the core and decrease its density, we used a Chemical Foaming Agent (CFA) along with a High Melt Strength PP (HMS-PP). So, the starting materials for manufacturing the foam extruded core are:

- Regrind Twintex (RTWT)
- Recycled PP (RPP)
- High Melt Strength PP (WB 140)
- Endothermic Chemical Foaming Agent (Styrene-Ethylene/Butylene-Styrene “PN-40E”)

or

- Exothermic Chemical Foaming Agent (Azodicarbonamide “EV AZ-3.0”)

The thermal behavior of the exothermic and endothermic CFAs was investigated using thermal gravimetric analysis (TGA) under a simulated heating process as of the extrusion process. First, a small pellet of Azodicarbonamide (EV AZ-3.0) was heated to 800°C at a rate of 20 °C/min to make sure a full decomposition of CFA has occurred. Figure 2.6 gives the heating TGA thermogram of EV AZ-3.0 indicating that there are three distinct weight-loss steps for this foaming agent correspond to its gaseous components; N<sub>2</sub>, CO<sub>2</sub> and CO. The first decomposition step occurs at 200-225°C which is well close to the extrusion operating temperature and results in 56% reduction in sample weight. This means that in our foam extrusion process only 56% of Azodicarbonamide was decomposed to liberate gas which is not so efficient.

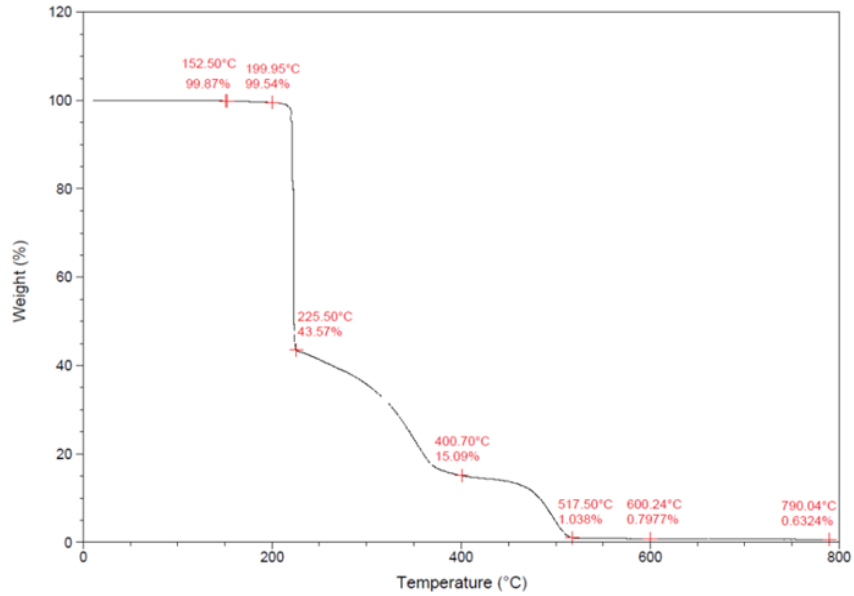


Figure 3.9 TGA thermogram of EV AZ-3.0.

Since Azodicarbonamide is an exothermic foaming agent, it generates some excessive heat during decomposition. Once decomposition is started, it continues spontaneously after the energy supply has been stopped. It means that even if we heat up the starting material in the extruder up to 200 °C and hold at that temperature for few minutes, the exothermic CFA starts gas releasing and the temperature of the polymer melt rises beyond the value of the die temperature and the starting melt temperature. Figure 3.10 illustrates the exothermic behavior of EV AZ-3.0 under a heat/hold process in which the sample loses around 55% of this weight at a constant temperature.

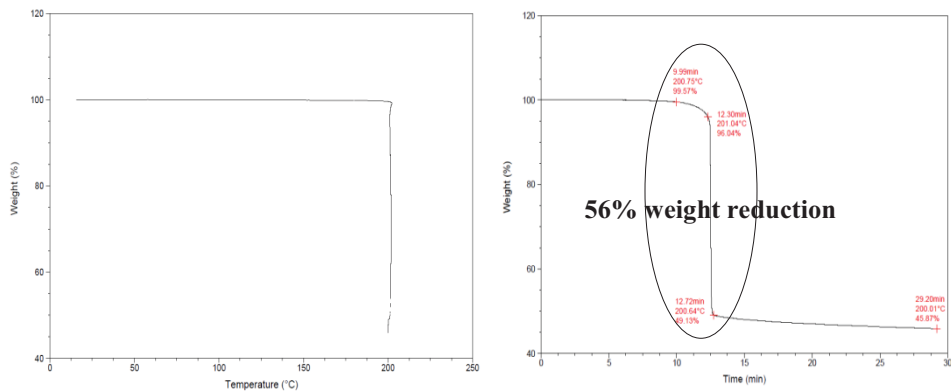


Figure 3.10. TGA thermogram of EV AZ-3.0; heat/hold process at 200°C for 15 min

Same analysis on the endothermic CFA, safoam (PN-40E), shows that the decomposition of this foaming agent is accomplished at very high temperature which is far away from our operating temperature (Figure 3.11). Since PN-40E is an endothermic CFA a same heat/hold cycle as of that in EV AZ-3.0 does not lead to significant gas liberation and just 17% of its weight could be decomposed (Figure 3.12).

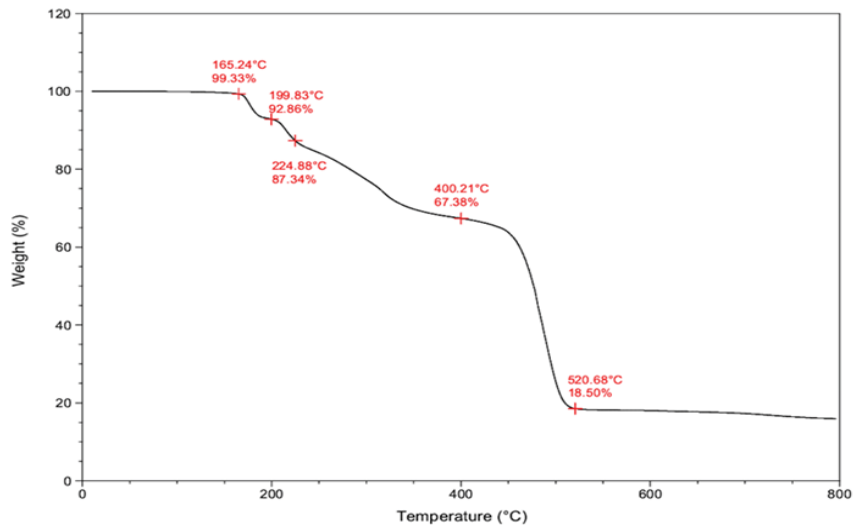


Figure 3.11 TGA thermogram of PN-40E

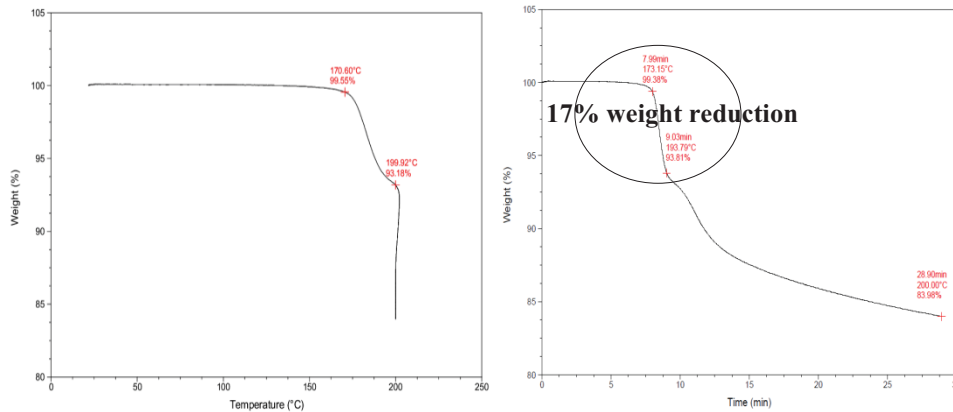


Figure 3.12. TGA thermogram of PN-40E; heat/hold process at 200°C for 15 min

### 3.1.4 Thermoplastic Skins

Fibre reinforced plastics are mainly used in composite structures where weight saving, lower production costs and freedom of design are desired. In these cases, traditionally thermosets or thermoplastics are used reinforced with glass or carbon fibres. Compared to

thermosets, thermoplastic materials often show better impact properties, increased toughness, infinite shelf life and they can be recycled and reused but the creep behavior is not as good as for thermoset composites [15]. In the automotive industry glass mat reinforced thermoplastics (GMTs) are widely used as semi-structural, compression moulded parts.

Thermoplastic roving skins which are woven into 0-90° fabric in different thicknesses used as the face sheets to form the sandwich panels. They provide an excellent stiffness/weight ratio and superior impact properties to the sandwich structure.

After extruding the core material, it is covered with pre-consolidated thermoplastic skins upon exiting from the extruder. The commercial name of the thermoplastic skins we have used is TWINTEX-TPP which is twill weave fabrics (Glass PP Natural, 60%) made of commingled E-glass and polypropylene rovings [20]. It is suitable for filament winding, pultrusion, reinforcement of extruded profiles and weaving. Consolidation is done by heating the roving above the melting temperature of PP matrix (160°C–200°C / 320°F–390°F) and applying a pressure before cooling under pressure. This unique and ready-to-use thermoplastic glass reinforcement has broad applications. Designed with high mechanical properties, it offers an excellent stiffness/weight ratio and superior impact properties over traditional fiberglass. The mechanical characteristic of this type of thermoplastic skin is given in Figure 3.13.

<b>Tensile</b>	<b>Strength</b>	<b>ISO 527</b>	<b>MPa (psi x 10<sup>3</sup>)</b>	<b>300 (43.5)</b>
	<b>Modulus</b>		<b>GPa (psi x 10<sup>6</sup>)</b>	<b>14 (2.0)</b>
<b>Flexural</b>	<b>Strength</b>	<b>ISO 14125</b>	<b>MPa (psi x 10<sup>3</sup>)</b>	<b>280 (40.6)</b>
	<b>Modulus</b>		<b>GPa (psi x 10<sup>6</sup>)</b>	<b>13 (1.9)</b>
<b>Charpy impact unnotched</b>		<b>ISO 179</b>	<b>kJ/m<sup>2</sup></b>	<b>160</b>
<b>Izod impact notched</b>		<b>ISO 180</b>	<b>kJ/m<sup>2</sup></b>	<b>140</b>
<b>Glass content</b>		<b>in weight</b>	<b>%</b>	<b>60</b>
		<b>in volume</b>	<b>%</b>	<b>35</b>

Figure 3.13. Mechanical properties of TWINTEX TPP Fabrics [20]

## 3.2 Equipment

Figure 3.14 shows a schematic of the experimental extrusion and lamination setup used to fabricate recycled sandwich panels. A plastic extrusion machine is used to extrude the core material. In order to pre-heat the thermoplastic skins, they pass through a heating chamber prior to lamination process. There are two heating chambers installed on the bottom and top side of the conveyor double belt machine.

The lamination process is carried out in a conveyor double belt press machine. This machine is specially built for this research work at “AS Composite Inc.”. The vertical distance between the upper and lower rolls can be adjusted based on our desired panel thickness. In order to pull the sandwich panel and take up the extruded part, we used a pulling machine which was synchronized with the extrusion rate.

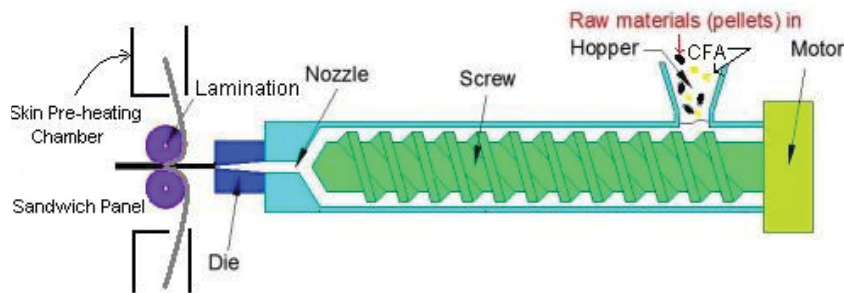


Figure 3.14 A schematic view of the experimental setup

### 3.2.1 Two-stage Extruder

The extruder machine used in this experiment is a standard ultra-extruder (AK 450, 30:1) made by “American Kuhne Co.”. The screw installed in this machine is a two stage screw with a 4.5” pitch. The first stage channel depth starts with 0.825” and decreases to 0.200” and the second stage channel depth starts with 0.800” and ends with 0.350”. The Nominal width is 0.45” on pitch and 0.48” across flight. Also the barrel’s I.D. is 4.50” and the OD is 7.00”.

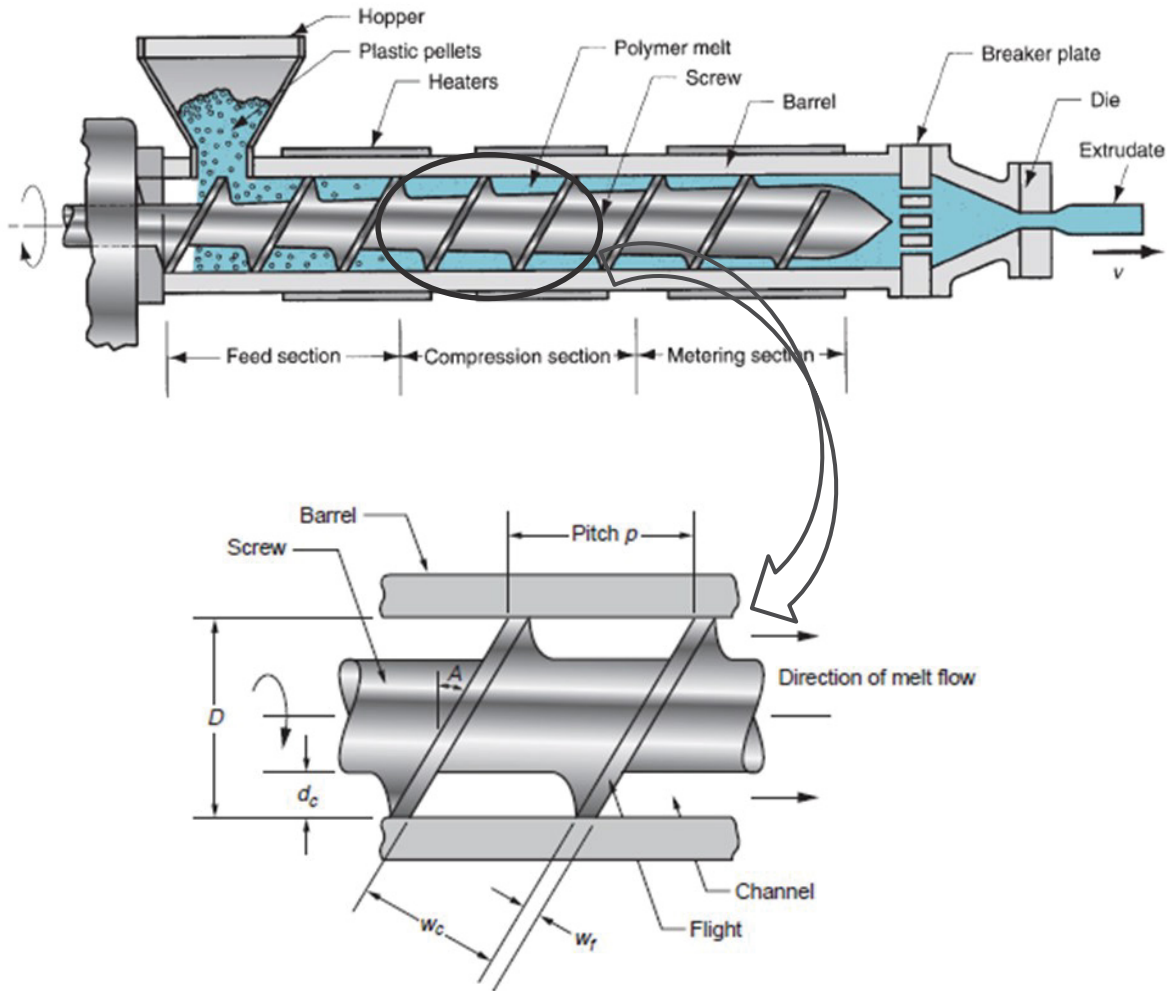


Figure 3.15. A schematic view of a typical extruder machine and a magnified cut-off of the screw

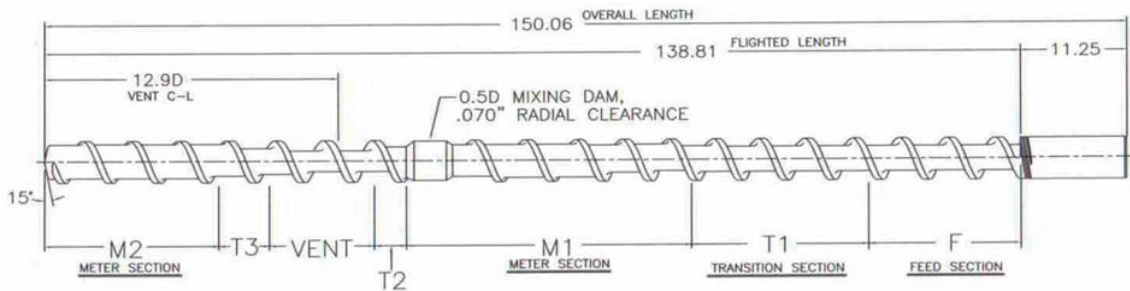


Figure 3.16. A scheme of the two-stage screw drawing used in our experiment

There are six barrel zones installed around the screw to set the temperature profile for the extrusion process. The extruder barrel temperatures can be set for an increasing, flat or reverse profile. Depending upon screw design, the temperature profile will affect the melt

temperature. A reverse profile often reduces the melt temperature. In general, the barrel zones should range from 320 to 465°F (160 to 240°C), but must be optimized for the specific extruder and screw design and based on the polymer thermal properties. Adapter and die temperatures are normally set to maintain the melt temperature exiting the extruder. The melt temperature should be measured with a thermocouple which extends 0.25 to 0.5 channel diameters into the melt stream of the adapter zone. The recommended melt temperature range for polypropylene is 285 to 390°F (140 to 200°C) however, the melt temperatures above 400°F (~210°C) can be used, but generally increase polymer degradation and make use of extruded material more difficult due to the melt softness.

### **3.2.2 Heating Chamber**

In order to pre-heat the consolidated twintex skins, they pass through a heating chamber prior to lamination process. There are two heating chambers installed on the bottom and top side of the conveyor double belt machine. The skins will be heated up to our desired temperature based on the temperature setup of the heating elements. Then, they are bonded to the extruded core material to make the sandwich panel.

### **3.2.3 Conveyor Double Belt Press**

There is also a conveyor double belt press machine right next to the extruder where the lamination process is performed and panel thickness is controlled via sequence of opposing rolls. The vertical distance between the upper and lower belts can be adjusted based on our desired panel thickness. A continuous moving of the extruded material is performed through a rough-top incline conveyor belting with 2ft width and 5ft length. The Conveyor machine is driven by a 1hp AC motor “EMERSON, EM01” and two reducer motors which decrease the rotational speed of driving motor with 40:1 and 5:1 ratios. The final linear speed of conveyor belt can be adjusted up to 14 ft/min.



Figure 3.17. Conveyor double belt press and skin heating chambers

### 3.2.4 Pulling System

Large rigid profiles need large rigid pullers to keep them moving along the extrusion line smoothly. So, we need a continuous pulling machine to pull the sandwich panel and take up the extruded part. A cleat puller (made by CDS company) with a contact length of 12" w × 72" L is run with a 2HP AC motor and is used to pull the extruded sandwich panel.



Figure 3.18. Pulling machine along the extrusion line



Figure 3.19. Production line for making thermoplastic sandwich panels via plastic extrusion

### 3.2.5 Reciprocating Feeding System

In chapter 4, we will see that our gravity fed hopper system is not able to feed the raw materials to the extruder uniformly. In order to make a uniform feeding to the extruder, we designed a special feeding system using a reciprocating mechanism. This mechanism provides a uniform and constant feeding through the hopper and prevents clogging the feeding pathway which is commonplace in gravity fed hopper systems.

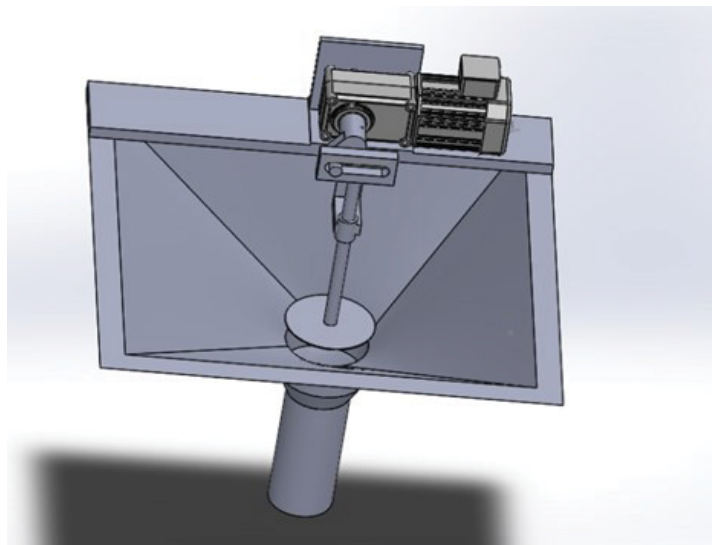


Figure 3.20. Reciprocating feeding hopper

# Chapter 4. Results and Discussion

## 4.1 Trial Parameters

### 4.1.1 Extrusion Process

As discussed in chapter 3, temperature profile for our extrusion process is set based on the results of DSC analysis and industry recommended temperature profile for PP extrusion to provide the proper thermal conditions for skin lamination process. Table 4.1 summarises the trial parameters obtained by thermal analysis and experimental optimization which are fixed throughout the manufacturing process. However, some changes in temperature profile are made in specific cases such as in extrusion foaming.

Table 4.1. Extrusion trial parameters

Die size	Temperature Profile Barrel Zones						Die Temperature		Melt Temp. (In Extruder)	Core Extrudate Temp.
	T <sub>B1</sub> °C	T <sub>B2</sub> °C	T <sub>B3</sub> °C	T <sub>B4</sub> °C	T <sub>B5</sub> °C	T <sub>B6</sub> °C	T <sub>D1</sub> °C	T <sub>D2</sub> °C	T <sub>m</sub> °C	T <sub>c</sub> °C
12"×0.16"	170	175	180	190	195	200	205	210	200-220 (210)	200

The operating parameters which affect the extrusion procedure are the feeding load, rotational speed of the screw, barrel zones' temperature and extrusion die temperature. For manufacturing sandwich panels of uniform thickness, first, we need to produce a uniform extruded core material which depends to the extruder output, and take-up speed. Thus, we need to provide a constant feeding to the extruder and synchronise the extrusion rate with the pulling system.

As mentioned before, in our extrusion process, raw compound materials in the form of shred pellets (Polypropylene and Fiber-Glass) is gravity fed from a top mounted hopper into the barrel of the extruder. Thus, there should be a minimum weight of the material

inside the hopper so it could provide a consistent feeding. The volume content of RTWT in the mixture is another issue as it can easily clog the feeding path in the hopper when the volume fraction of RTWT increased in the mixture.

We extruded the core material of three different compounds including 30, 50 and 70 wt% of RTWT (Figure 4.1). Results show that the maximum amount of RTWT in the compound which allows a consistent feeding and consequently a uniform output is 50 wt%. Upper than this value, we observed some fluctuation in the extrusion flowrate as a result of the inconstant feeding. So, the maximum value of RTWT to obtain a uniform flow in the extruder is 50 wt%.

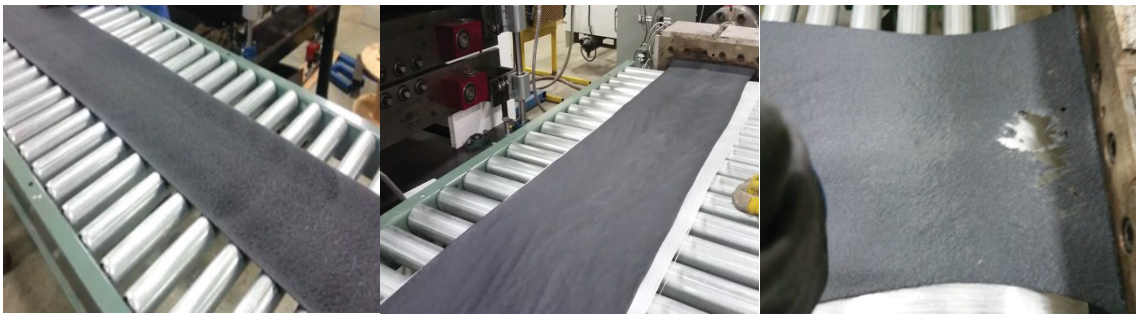


Figure 4.1. Output uniformity for three different compounds; a) 30-70wt% TWT-PP, b) 50-50wt% TWT-PP, c) 70-30wt% TWT-PP; An inconstancy in output flow is evident at TWT ratios higher than 50wt%

To see the effect of fiber volume fraction on the physical and mechanical properties of the extruded core plate, we produced three sets of extrudate with different RPP to regrind TWT ratios as follows;

- 1- 100wt% RPP
- 2- 70wt% RPP and 30wt% RTWT
- 3- 50wt% RPP and 50wt% RTWT

Note that RTWT is composed of 60 wt% FG and 40 wt% PP. So, the weight ratio of fiber for three set of extrudate will be

- 1- 100wt% PP
- 2- 82wt% PP+ 18wt% FG

3- 70wt% PP + 30wt% FG

Since the extruded core plate is a randomly oriented discontinuous fiber lamina, it exhibits planar isotropic behavior. The properties are ideally same in all directions. For this lamina the tensile modulus is calculated from [21].

$$E_{\text{random}} = \frac{3}{8} E_{11} + \frac{5}{8} E_{22} \quad (4.1)$$

where  $E_{11}$  and  $E_{22}$  are the longitudinal and transverse tensile moduli given by

$$E_{11} = \frac{1 + 2\left(\frac{l_f}{d_f}\right)\eta_L V_f}{1 - \eta_L V_f} E_m \quad (4.2)$$

$$E_{22} = \frac{1 + 2\eta_T V_f}{1 - \eta_T V_f} E_m \quad (4.3)$$

where

$$\eta_L = \frac{\left(\frac{E_f}{E_m}\right) - 1}{\left(\frac{E_f}{E_m}\right) + 2\left(\frac{l_f}{d_f}\right)} \quad (4.4)$$

$$\eta_T = \frac{\left(\frac{E_f}{E_m}\right) - 1}{\left(\frac{E_f}{E_m}\right) + 2} \quad (4.5)$$

where  $E_f$  and  $E_m$  are the modulus of GF and PP, respectively (GPa).  $l_f$  is the average length of the chopped fibers (mm) and  $d_f$  is the diameter of fiber (mm).

Also, density of the core depends to the volume fraction of reinforced fiber and can be calculated from

$$\rho_{\text{core}} = V_f \times \rho_{\text{FG}} + (1 - V_f) \times \rho_{\text{PP}} \quad (4.6)$$

We have calculated the modulus and density of the extruded core based on the fiber and matrix properties for three different core materials as shown in Table 4.2.

Table 4.2. Theoretical values for Young's modulus and density of three different PP extrudate

Sample	wt% FG	$v_f$	$E_{11}$ (GPa)	$E_{22}$ (GPa)	$E_{random}$ (GPa)	$\rho$ (kg/m <sup>3</sup> )
C <sub>1</sub>	0	0.0	1.500	1.500	1.500	800
C <sub>2</sub>	18	0.069	5.943	1.814	3.362	910
C <sub>3</sub>	30	0.127	9.670	2.110	4.495	990

A 3-point bending test was also conducted to verify the theoretical results obtained by equation (4.1). This test was carried out based on the standards ASTM D790. The test details will be described later in this chapter. Figure 4.2 shows the results of the 3-point bending test for three different PP extrudates.

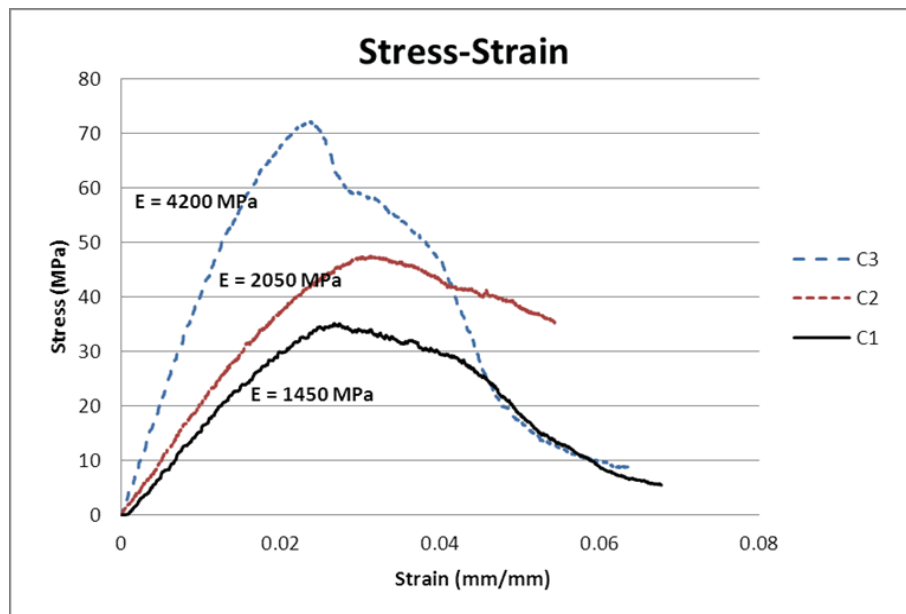


Figure 4.2. Stress-Strain curves for three different PP extrudates

Table 4.3. Flexural properties and density of three different PP extrudates

Sample	Bending Modulus E(GPa)	Bending Strength (MPa)	$\rho(\text{kg/m}^3)$
C <sub>1</sub>	1.450	34	810
C <sub>2</sub>	2.050	47	875
C <sub>3</sub>	4.200	72	970

As can be seen in Tables 4.2 and 4.3, results of the 3-point bending test agree with the theoretical prediction for modulus and density of the fiber reinforced PP extrudate. Also, results of the theoretical and experimental analysis indicate that the bending stiffness of the extrudate could be enhanced by introducing chopped fiber into the polymer. There is just a small difference between the experimental values of modulus and their theoretical counterparts and it might be due the existence of tiny fibers which are smaller than the average fiber length assumed in our analysis (3mm).

#### 4.1.2 Lamination Process

After finding the optimum amount of RTWT in the mixture to produce a uniform and high performance core extrudate, we should set the proper conditions for lamination process. In a continuous lamination procedure, the skins are fed from the top and bottom of the extruded core and move in a same speed with the moving extrudate. The skins are first pre-heated in the heating chambers and then bonded with the extrudate while moving by the pulling system. So, we need to find out the real correlation between the screw rotational speed (or extrusion rate) and the take up speed (pulling speed) to synchronize them together. Trial results of the speed synchronization are tabulated in Table 4.4.

Table 4.4. Practical correlation between the screw rotational speed and pulling speed for 4mm core extrudate

Screw Speed (rpm)	Load (kg/hr)	Pulling Speed (fpm)	Core Thickness (mm)
40	27	1	4
50	30	1.25	4
60	33	1.4	4
70	35	1.5	4

Another parameter which should be taken into account is the temperature of the extruded core and face-sheets for the lamination procedure. As discussed previously, the minimum required temperature for a good bonding between skin and core material is around 120°C when they are cooled down from their melt temperature (150°C- 160°C for skin and core). Thus, the cooling rate of the extruded core material is significant for the lamination process.

Based on the heat transfer relations discussed in chapter 2, the estimated time for cooling down the core surface from the extrusion temperature to a desired pre-lamination temperature (higher than 120 °C) with air has been calculated and results are represented in table 4.6. If we consider a natural cooling process for the extruded core material, we can assume the heat transfer coefficient of air (@ 25 °C) as  $h_{air}=30$  (W/m<sup>2</sup>°C).

Note that all the following results were calculated for a core extrudate composed of 50 wt% shred twintex (60 wt% FG,40 wt% PP) and 50 wt% Recycled polypropylene. So the total mass content of FG and PP is 30 wt% and 70 wt%, respectively. Thermal properties of all components and materials are illustrated in Table 4.5.

Table 4.5. Thermal properties of the core and skin and their constitutive components

	Fiberglass	Polypropylene	Core (30%FG/70%PP)	Skin (60%FG/40%PP)
K(W/°C.m)	0.84	0.16	0.29	0.44
$\rho C_p$ (J/°C.m <sup>3</sup> )	$2.17 \times 10^6$	$1.6 \times 10^6$	$1.77 \times 10^6$	$1.942 \times 10^6$
$\alpha$ (m <sup>2</sup> /s)	$3.8 \times 10^{-7}$	$10^{-7}$	$1.6 \times 10^{-7}$	$2.3 \times 10^{-7}$

Table 4.6. Required time for cooling down an extruded core with water and air  
(Theoretical Results)

T <sub>0</sub> (°C)	T <sub>t</sub> (°C)	Cooling time(air) (s)
	156	19.2
180	132	42.1
	108	70.5
	160	19.4
185	135	42.6
	120	59.0
	178	8.6
190	158	24.6
	136	45.1

We have also conducted a trial experiment to find out the real cooling time of the extrudate at 1.3 fpm (0.4 m/min) (Table 4.7). The experimental and theoretical results of the extrudate's cooling time are illustrated in Figure 4.3.

Table 4.7. Rate of temperature change with time for the extruded plate  
(Experimental Results)

$T_{\text{core}}$ °C	$T_{10\text{s}}$ °C	$T_{30\text{s}}$ °C	$T_{60\text{s}}$ °C
180	170	156	132
185	172	160	135
190	178	163	136

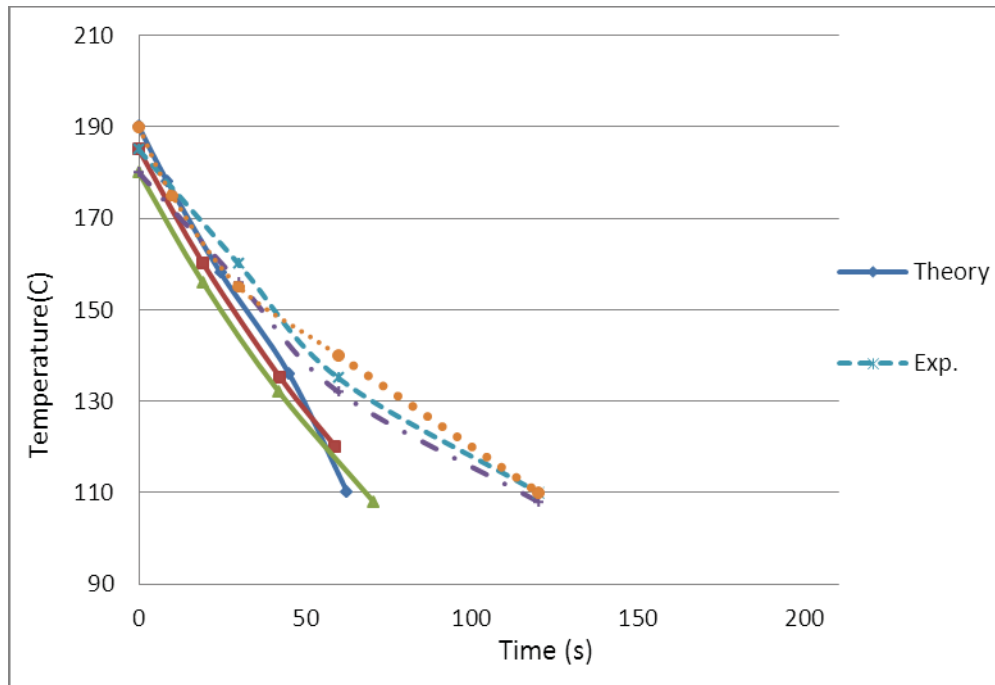


Figure 4.3. Time-Temperature curve for a 4mm thick plate

A good bonding of the skin to core is achieved when the temperature of the skin and core is high enough (around 150 °C). Thus, the skin-to-core lamination process should be carried out within the 30 seconds when the core material comes out of the extruder. The extruded core material is hot so when it contacts with the skin, the temperature increases through the skin thickness due to thermal diffusivity. A comparison between the experimental results and their numerical counterparts explicitly testifies a good and

logical correlation between them in the first 30 seconds of the core extruding process. Since the lamination process is started right after the extrusion process, the theoretical prediction for thermal behavior of the skin and core during the lamination process is valid and the surface of the core material is hot enough to allow a good bonding with the skin.

The thermal diffusivity rate (Time-Temperature curves) based on this heat transfer model is calculated for different skin's thicknesses (at the mid-skin) and different initial temperatures (skins' pre-heating temperature). The results are illustrated in Figure 4.4. The core's surface temperature is supposed to be constant at 180 °C.

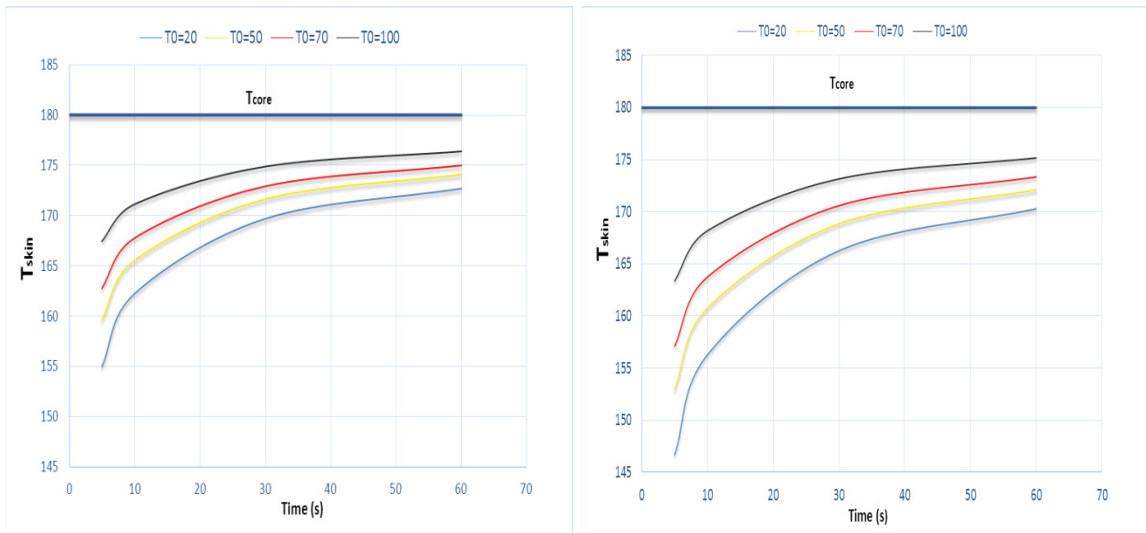


Figure 4.4. Time-Temperature curve at the mid-skin of; a) 0.5mm skin, b) 1mm skin

To compare the theoretical results with their experimental counterparts, we need to monitor the temperature of the skin during the lamination process. Since it is difficult to measure the mid-skin temperature due to their small thickness, we have found out the skins' temperature at the outer surface of them with a thermocouple and compared them with their theoretical counterparts as shown in Figure 4.5.

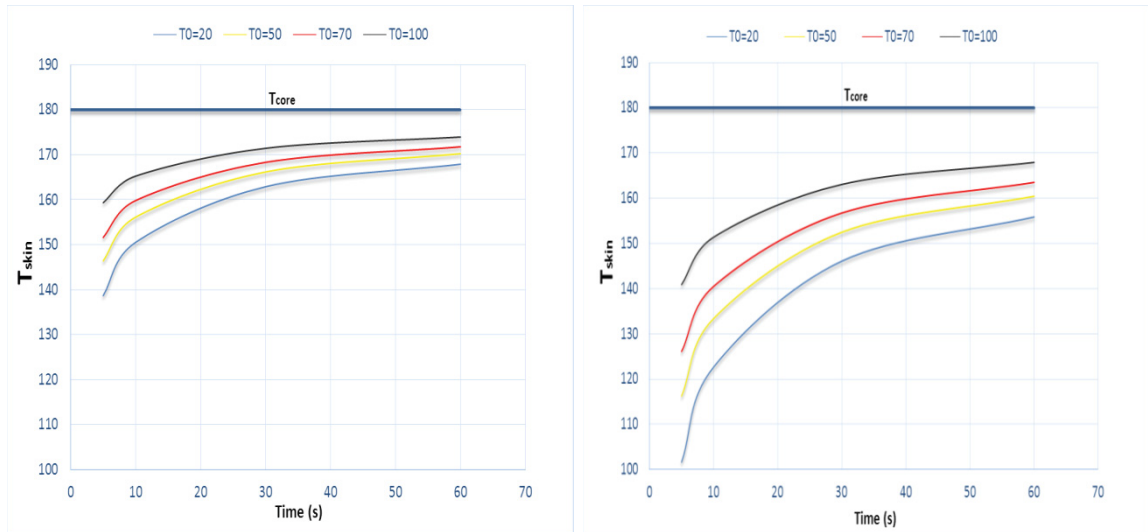


Figure 4.5. Time-Temperature curve at the skin surface of; a) 0.5mm skin, b) 1mm skin

All the above equations and results are only valid in isolated systems where the effect of heat loss through the materials and devices are negligible. Making a close chamber or covering the conveyor belt during the lamination process could be helpful to actualize this condition.

Practically, it is impossible to keep the core temperature at a constant value due to the heat convection at its surfaces. If we consider the effect of heat convection on the surface of the core and skins during the lamination process, results are quite different as illustrated in Figures 4.6 and 4.7. So if we assume that the initial temperature of the extruded core is 180°C, when it touches the consolidated skin with different initial temperatures from 20°C to 150°C, both of them are cooled down due to convection heat transfer by air during the lamination process. Results are shown in Figures 4.8 and 4.9.

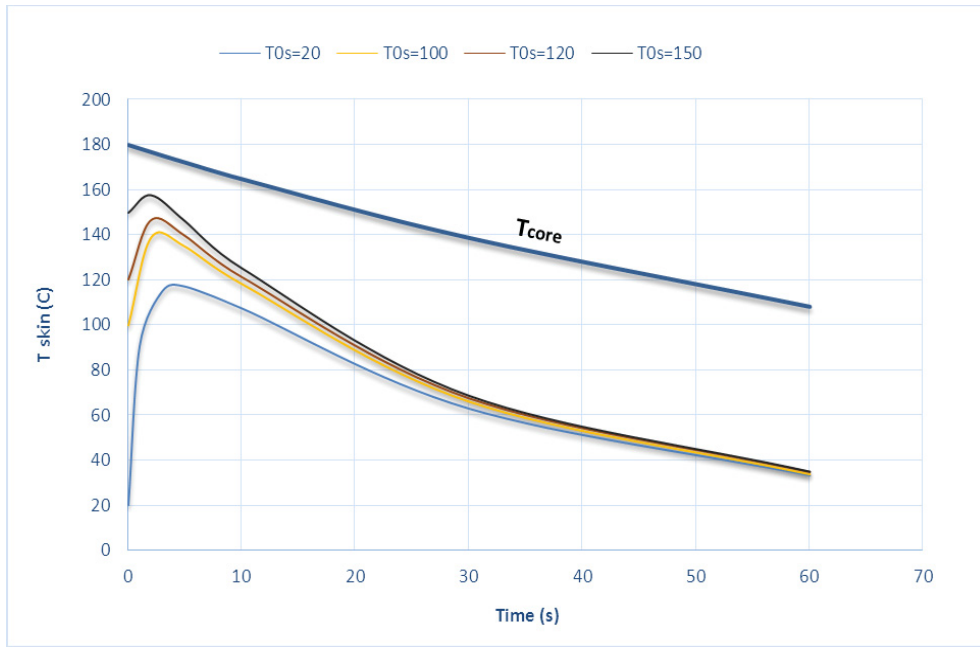


Figure 4.8. Time-Temperature curve at the surface of the core and skin of a sandwich panel with 0.5mm thick skin

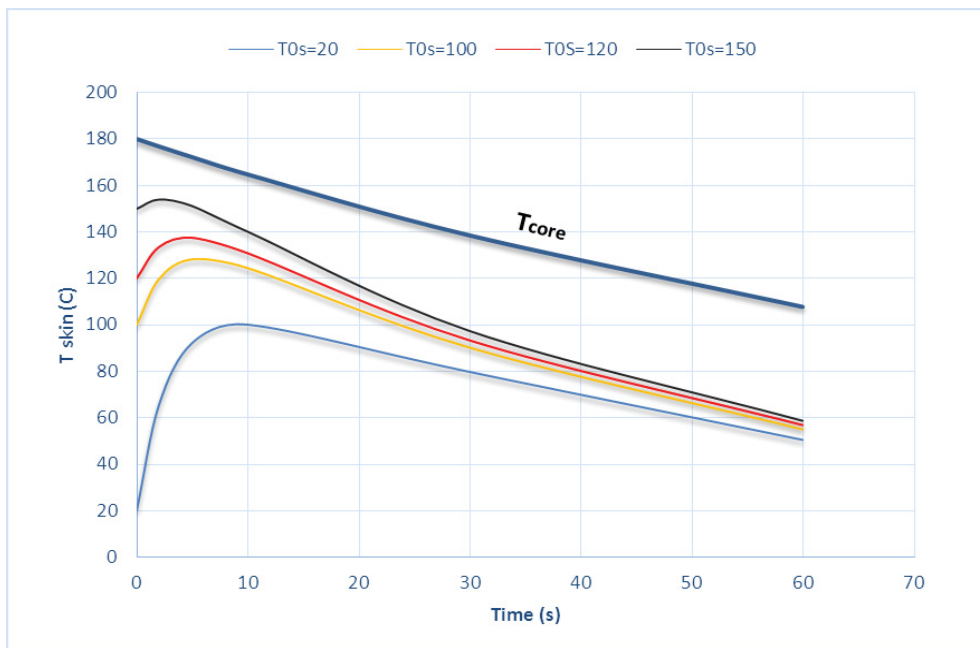


Figure 4.9. Time-Temperature curve at the surface of the core and skin of a sandwich panel with 1mm thick skin

Thus, for a good bonding of the skin to extruded core plate, we need to pre-heat the consolidated skin up to its resin melt point (which is around 150 °C) and skins with lower temperature are not able to be bonded since their surface temperature does not reach the melt point of the PP when they get in touch with the core.

To analyze the cooling process of the sandwich panel after the lamination procedure, again we can assume a one directional convective heat transfer through the core-skin interface as well as the outer surface of the skin. Based on the Equations (2.25) and (2.26) in chapter 2, we can calculate the estimated time for cooling down the panels.



Figure 4.10. Heat transfer through the core and skin surfaces

The estimated time for cooling down the panel based on the values in Table 4.5 and for  $z_{\text{core}}=4$  mm and  $z_{\text{skin}}=1$  mm and  $h_{\text{air}}=30$  (W/m<sup>2</sup>°C, @ 20°C) and  $h_{\text{water}}= 500$  (W/m<sup>2</sup>°C, @ 20°C) has been computed and results are represented in Table 4.8.

Table 4.8. Estimated time for cooling down the sandwich panels

T0 (°C)	Tf (°C)	time(air) (s)	time(water) (s)
180	50	70.0	4.2
180	25	144.9	8.7
170	50	67.3	4.0
170	25	142.2	8.5
160	50	64.4	3.9
160	25	139.3	8.4
150	50	61.3	3.7
150	25	136.2	8.2

## **4.2 Panel Quality Tests**

One of the key parameters to determine the quality of a sandwich panel is the bonding strength between the core and skins during the lamination process. Results of the 3-point bending tests literally show that a sandwich panel can easily fracture under a bending stress much lower than its facesheet yield strength even if a tiny delamination would occur between the core and skin as a result of a weak bonding between them.

There are several parameters playing role in the lamination process and affect the quality of the final product. In order to optimize this process, different sets of sandwich panels were produced in different manufacturing conditions and the effect of skin thickness, lamination temperature and pressure on the physical and mechanical properties of the recycled sandwich panels were investigated.

To determine the quality of the final products, we have conducted bunch of physical and mechanical tests as follows;

### **4.2.1 Visual Test**

Physical quality of the sandwich panels is one of the most important factors that should be taken into account for process optimization. It consists of some apparent parameters such as panel flatness and uniformity of thickness all over the panel, surface finish of the sandwich panel and lack of any crack or defect in the skin-core interphase. A good surface finish could be achieved by setting proper lamination parameters (temperature and pressure) and also a uniform extrusion output.

### **4.2.2 Density Test**

To measure the density of the sandwich panels, a standard test method for apparent density of rigid cellular plastics (ASTM D1622) was performed. Density can be evaluated as the apparent overall density (includes forming skins) or by apparent core density (forming skins removed) and it can be obtained by dividing the total weight of the specimen by its apparent volume [22].

### 4.2.3 3-Point Bending Test

To find the flexural properties of the recycled sandwich panels, a 3-point bending test was carried out based on the standard ASTM D790. This test method determines the flexural properties of unreinforced and reinforced plastics, including high-modulus composites in the form of rectangular bars molded directly or cut from sheets, plates, or molded shapes [23]. This standard is applicable in the case of homogenous solid bars. But it can also be used to find the flexural properties of the sandwich panels when the core stiffness is comparable to the skin stiffness.

The support span to sample thickness ratio is between 12 to 20 and the rate of crosshead motion is calculated as follows

$$R = ZL^2/6d \quad (4.7)$$

where R is the rate of crosshead motion [mm(in)/min], L and d are support span and sample thickness, respectively [mm(in)] and Z is the rate of straining of the outer fiber assumed to be 0.01.

The values of bending stress and strain are calculated based on the equations (2.7) and (2.8) in chapter 2.



Figure 4.9. A view of 3-point bending fixture

#### 4.2.4 Peel-off Test

One of the key parameters to identify the quality of a sandwich panel is the bonding strength between the core and the skins. Results of the 3-point bending test literally show that a sandwich panel can easily fracture under a bending stress much lower than its face-sheet yield strength even if a tiny delamination would occur between the core and skin as a result of a poor bonding between them.

ASTM D3167 is a test method for peel resistance of adhesives which provides determination of metal to metal peel strength of adhesives [24]. Since a sandwich panel is being tested, it also is a measure of how well that facesheet being peeled off is bonded to the core material.

This test method consists of testing the laminated adherends; one of the adherends must be rigid and the other one must be flexible which is peeled-off from the rigid adherend at

a controlled speed and angle of peel using the fixture shown in Figure 4.10. The rate of crosshead motion for this test was picked to be 1 in/min.

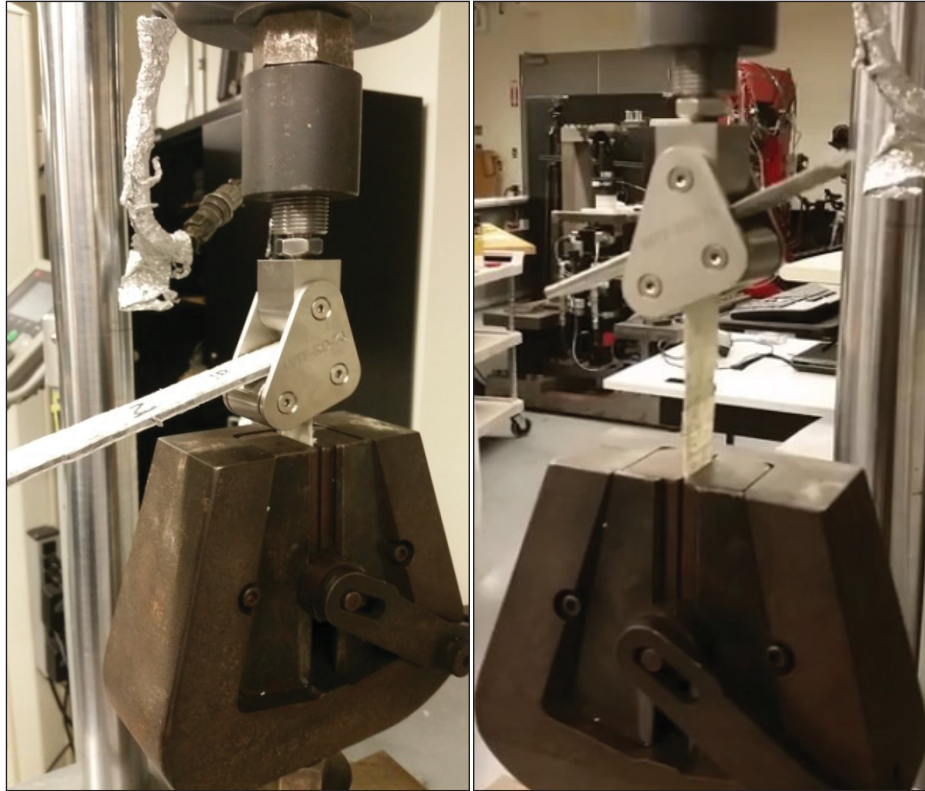


Figure 4.10. Floating roller peel-off fixture

## 4.3 Process Optimization

### 4.3.1 Skin Thickness

To see the effect of skin thickness on the performance of the final product, we produced two sets of sandwich panels using pre-consolidated TWT skins with 0.5mm and 1mm thickness.

- I. 2.5 mm RPP/RTWT core + 2× 22oz (0.5 mm) consolidated twintex

Table 4.10 shows the operating conditions to produce this type of sandwich panel.

Table 4.10. Skin(0.5 mm) lamination trial parameters

Sample No.	Heating Elements		Pulling Speed V <sub>Pull</sub> (ft/min)	Lamination Temperature (°C)		
	T <sub>Top</sub> (°C)	T <sub>Bottom</sub> (°C)		T <sub>core</sub>	T <sub>S.Top</sub>	T <sub>S.Bottom</sub>
SP <sub>s0.5-1</sub>	400	400	1.3	160	100	120
SP <sub>s0.5-2</sub>	400	400	1.7	160	120	125
SP <sub>s0.5-3</sub>	400	400	2	160	130	130

II. 2 mm RPP/RTWT core+ 2×44oz (1mm) consolidated twintex

Same test was conducted for 1 mm skin and the operating conditions are illustrated in Table 4.11.

Table 4.11. Skin(1mm) lamination trial parameters

Sample No.	Heating Elements		Pulling Speed V <sub>Pull</sub> (ft/min)	Lamination Temperature (°C)		
	T <sub>Top</sub> (°C)	T <sub>Bottom</sub> (°C)		T <sub>core</sub>	T <sub>S.Top</sub>	T <sub>S.Bottom</sub>
SP <sub>s1-1</sub>	450	450	1	160	130	130
SP <sub>s1-2</sub>	450	450	1.5	160	135	127

First, a small piece of sandwich panel with uniform thickness is cut in 1'×1' and the quality of panel surface is examined for any visual defect on the surface and also in the skin-core interphase.

By doing a visual inspection on the first sample (SP<sub>s0.5-1</sub>), a skin delamination was evident due to the low lamination temperature but two other samples of different skin thicknesses (SP<sub>s0.5-2</sub>) and (SP<sub>s1-2</sub>) were picked for further physical mechanical tests.

Figures 4.11 and 4.12 show a view of SP<sub>s0.5-2</sub> and SP<sub>s1-1</sub>, respectively.



Figure 4.11. Small piece of sandwich panel with 0.5 mm skin (S<sub>0.5-2</sub>)

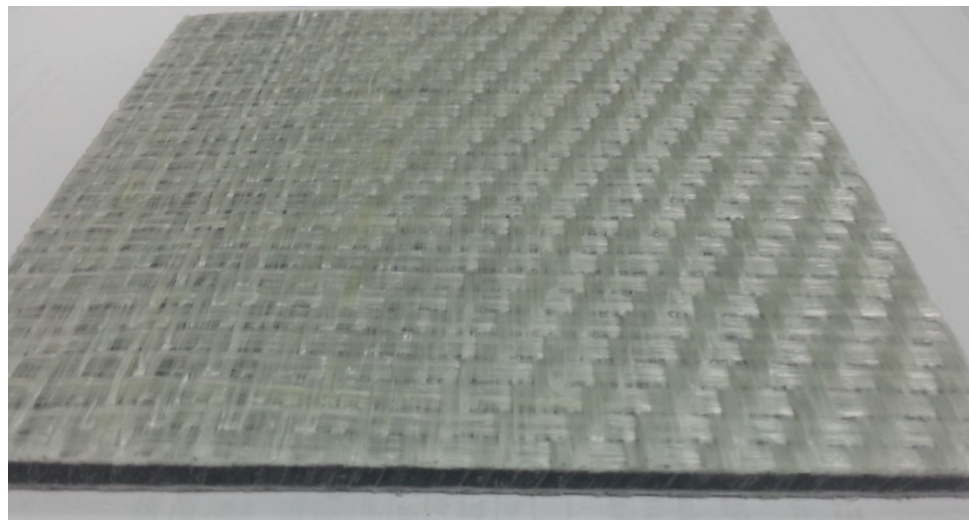


Figure 4.12. Small piece of sandwich panel with 1 mm skin (S<sub>1-2</sub>)

We also conducted a 3-point bending test on the samples above to find the flexural strength and stiffness. This test was carried out based on the standards ASTM D790. Three similar strips were cut out of each sample following the standard rules for test specimen dimensions (Table 4.12). A same bending test was also performed on a 3mm thick core material without any skin to compare its flexural behavior with the sandwich panel samples. Figure 4.13 represents a view of these specimens.

Table 4.12 Sample specifications for 3-point bending test

Sample	Core	Skin	Dimension (mm)
SP <sub>s0.5-2</sub>	Recycled PP+TWT (2.5mm)	Consolidated TWT (2×0.5mm)	3.5×12.5×100
SP <sub>s1-1</sub>	Recycled PP+TWT (2 mm)	Consolidated TWT (2×1mm)	4×16×100
C3	Recycled PP+TWT (3mm)	-	3×12×100

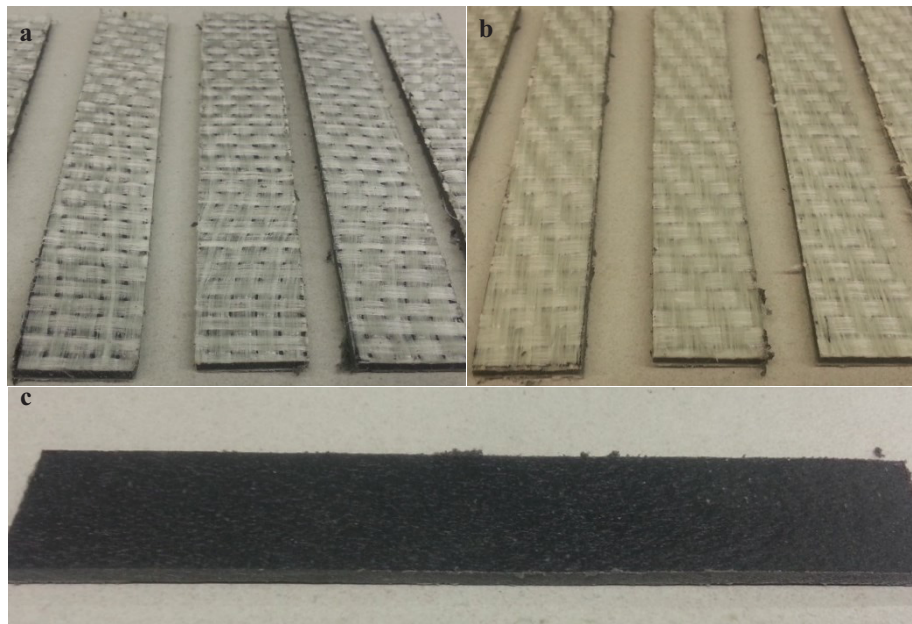


Figure 4.13 View of panel specimens subjected to 3-point bending test;  
a)SP<sub>s0.5-2</sub>, b) SP<sub>s1-1</sub> and c) 3<sup>mm</sup>core material

The Force-Displacement and Stress-Strain diagrams were plotted for each case and their mean values were compared with each other as illustrated in Figures 4.14 and 4.15.

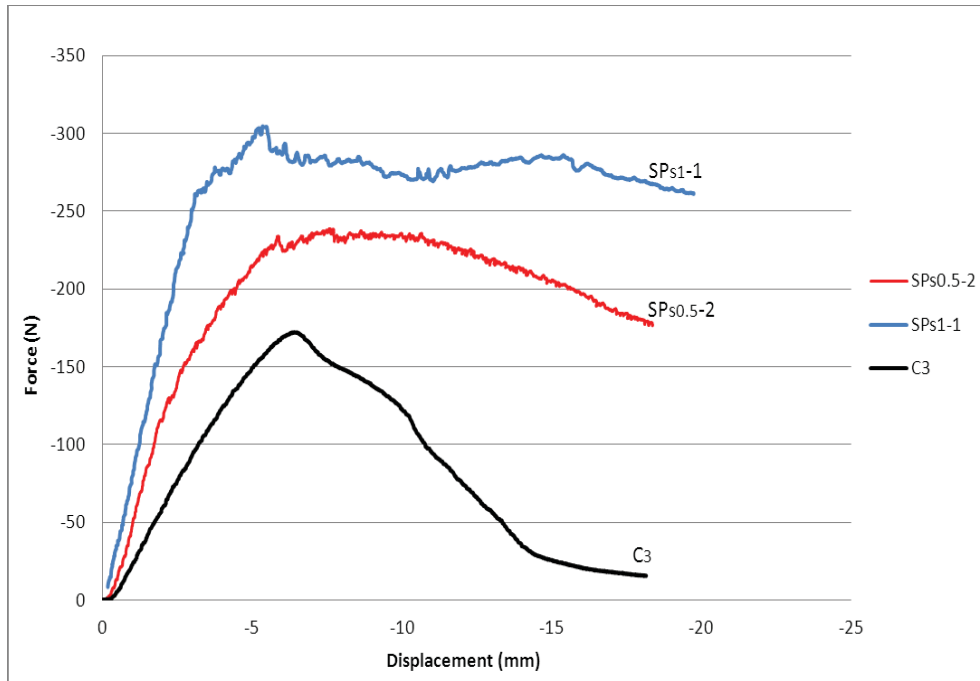


Figure 4.14 Force-Displacement curves for different panels

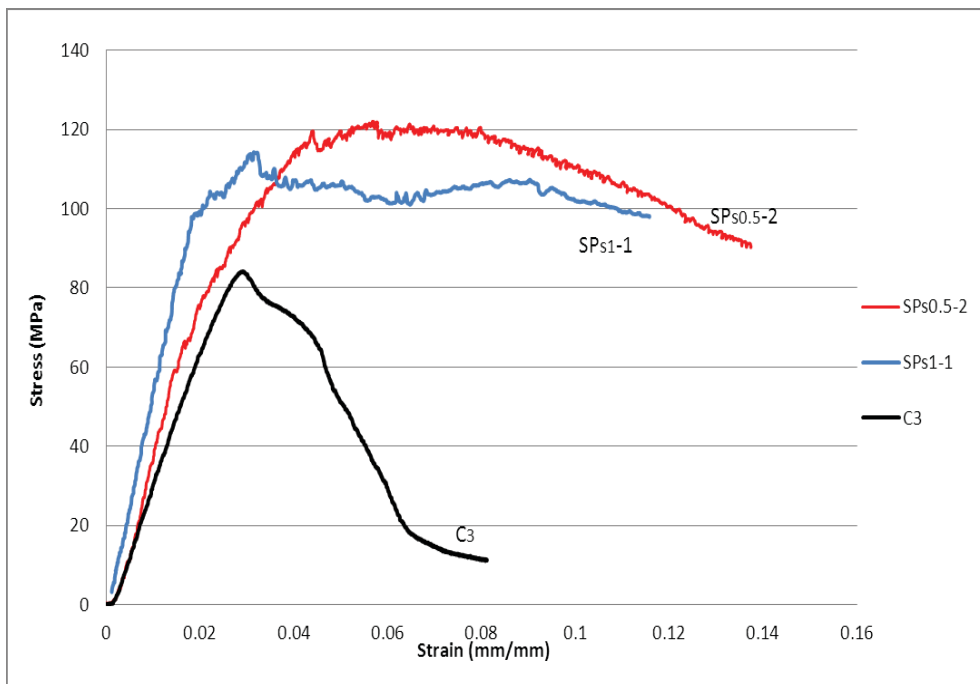


Figure 4.15 Stress-Strain curves for different sandwich panels

Results of the test were tabulated in Table 4.13.

Table 4.13. Flexural properties and density of RPP core and sandwich panels

Material	Flexural Strength (MPa)	Flexural Modulus (Mpa)	Bending Stiffness EI (N.m <sup>2</sup> )	Density (Kg/m <sup>3</sup> )
RPP Core	82	4000	0.2	945
SP <sub>s0.5-2</sub>	120	6000	0.3	1040
SP <sub>s1-1</sub>	115	7300	0.7	1120

As can be seen in Figures 4.14 and 4.15, the mechanical behavior of recycled sandwich panels (SP<sub>s0.5-2</sub> and SP<sub>s1-1</sub>) under 3-point bending test is completely different from RPP core material without any face sheet. Covering the extruded core material with thermoplastic skins provide a high bending stiffness (EI) and high ductility to the material. Our recycled sandwich panels have relatively high ductility and do not fracture at low strains, while the extruded core material which is not covered with the skin undergoes a fracture and finally breaks at a low strain (around 3%) as expected for a non-sandwich structure (Figure 4.16).

Recycled sandwich panel is relatively strong in terms of core-to-skin bonding due to the high compatibility between the RPP core and TWINTEX skin. In fact, the base thermoplastic resin for both of the core and skin materials is polypropylene causes a well bonding between the skin and core. Results of the bending tests also indicate that the flexural strength of sandwich panels with 0.5 mm and 1 mm skins are almost same but there is difference between the value of bending stiffness and consequently the amount of deflection for these two types of sandwich panels based on their skins' thickness. In fact, sandwich panel with 0.5 mm skin has a lower bending stiffness (EI) because of its thinner facesheet and it undergoes a big deflection under a same applying force. Moreover, sandwich panel with 0.5 mm skin has a poor surface quality due to its low weft/wrap density which exposes the core material underneath.



Figure 4.16. View of broken RPP core and unbroken sandwich panel

### 4.3.2 Lamination Parameters

#### a) Lamination Temperature vs Flexural Behavior

As mentioned in chapter 3 and based on the results of DSC analysis for the skin material, the minimum required temperature for a good bonding between skin and core material is around  $120^{\circ}\text{C}$  when they are cooled down from their melt temperature ( $150^{\circ}\text{C}$ -  $160^{\circ}\text{C}$  for skin and core).

To optimize the bonding process of the skin to core, we have produced some sets of sandwich panels with different lamination temperatures.

First, we preheat the skin up to  $180^{\circ}\text{C}$ . The outcome was a panel with poor surface finish. Indeed, a high preheat temperature (higher than  $160^{\circ}\text{C}$ ) burns the skin and causes a dark and rough surface.



Figure 4.17. Poor surface quality of a sandwich panel with a high preheat temperature

The second and third panels were produced by preheating the skins at 155°C in the heating chamber but they were cooled down in different pulling speeds upon exiting from the heating chamber until they reached the core material. Sample No.2 was laminated in a fast pulling speed and its surface temperature was around 140°C when it touched the extruded core but sample No.3 was cooled down in a slow pulling speed and it touched the extruded core with a temperature around 120°C.

To see the effect of lamination temperature on the mechanical properties of the sandwich panel we have performed a 3-point bending test on sample No. 2 and 3. This test was carried out based on the standards ASTM D790. Three similar strips were cut out of each sample following the standard rules for test specimen dimensions (Table 4.14).

Figures (4.18-4.20) show the results of the bending test for these sample specimens.

Table 4.14. Sample specifications for 3-point bending test

Sample	Core	Skin	Dimension (mm)	Result
SP <sub>1</sub>	Recycled PP+ Regrind TWT (2.5mm)	Consolidated TWT (2×1mm)	-	Rejected due to poor surface finish
SP <sub>2</sub>	Recycled PP+ Regrind TWT (2.5mm)	Consolidated TWT (2×1mm)-140°C	4.5×20×120	Figure 4.18
SP <sub>3</sub>	Recycled PP+ Regrind TWT (2.5mm)	Consolidated TWT (2×1mm)-120°C	4.5×20×120	Figure 4.19
C <sub>5</sub>	Recycled PP+ Regrind TWT (3mm)	-	3.25×16×100	Figure 4.20

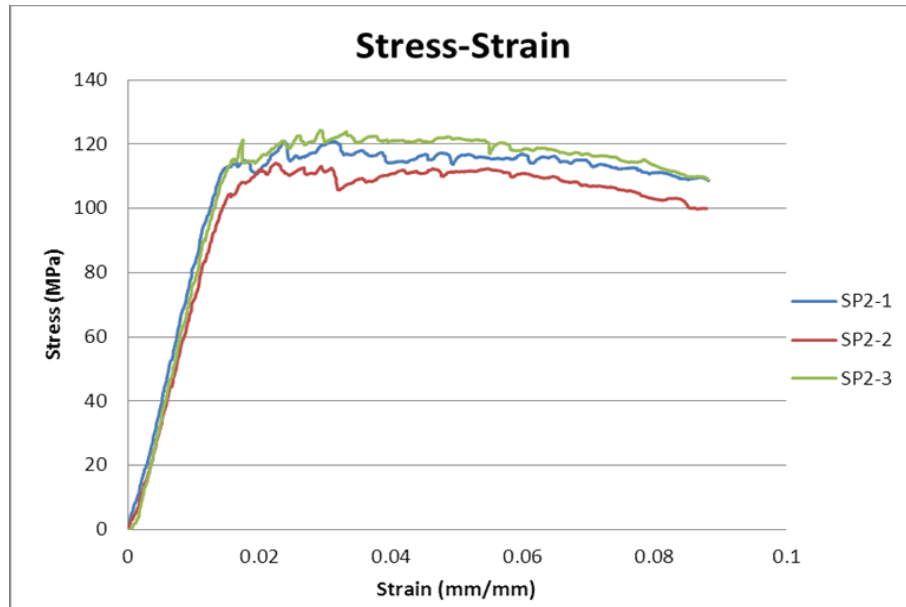


Figure 4.18. Stress-Strain curves for sample 2; bonding temperature 140°C

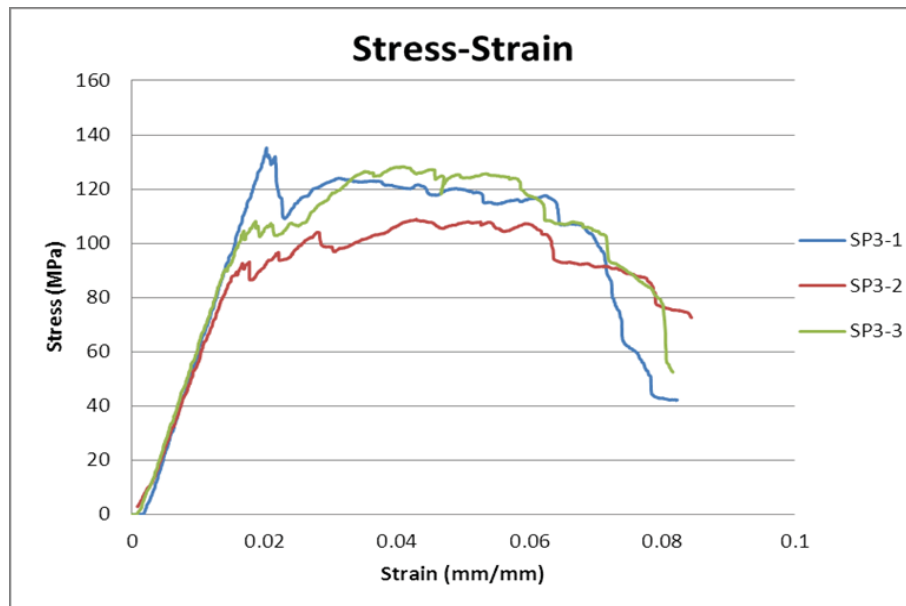


Figure 4.19. Stress-Strain curves for sample 3; bonding temperature 120°C

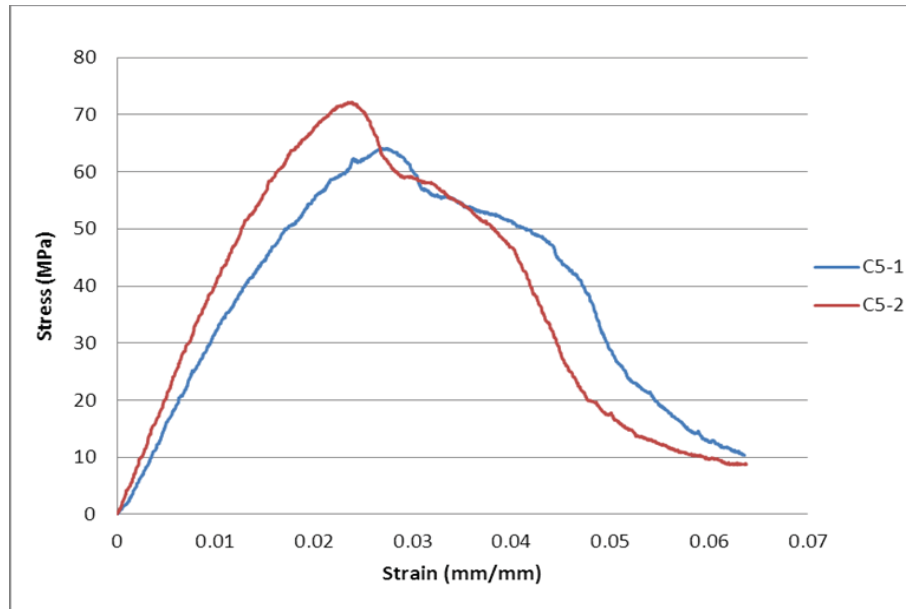


Figure 4.20. Stress-Strain curves for sample 6; RPP core plate

Table 4.15. Flexural properties and density of RPP extrudate and sandwich panels according to ASTM D790

Sample	Bending Modulus $E_{avg}$ (Gpa)	Bending Strength $S_{avg}$ (Mpa)	$\rho$ (kg/m <sup>3</sup> )	Specific Strength (10 <sup>3</sup> m <sup>2</sup> s <sup>-2</sup> )
SP <sub>2</sub>	7.800	125	1150	113.6
SP <sub>3</sub>	7.600	110	1150	100
C <sub>5</sub>	4.100	65	950	68.5

The mean value of force-displacement and stress-strain curves for the above samples were plotted and illustrated in Figures 4.21 and 4.22 which represent a good scale to compare the strength and stiffness of the core extrudate and sandwich panels fabricated in different lamination temperatures.

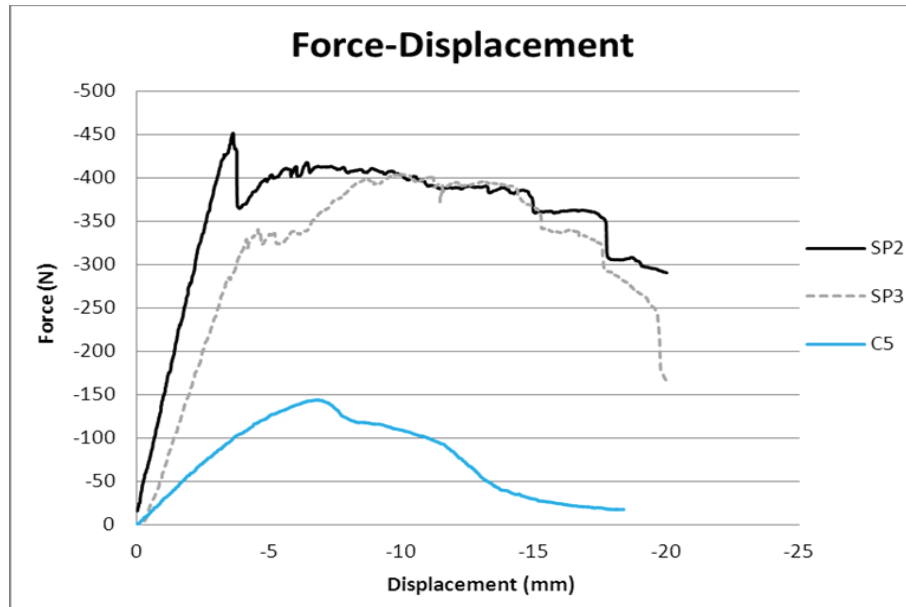


Figure 4.21. Force-Displacement curves for different panels

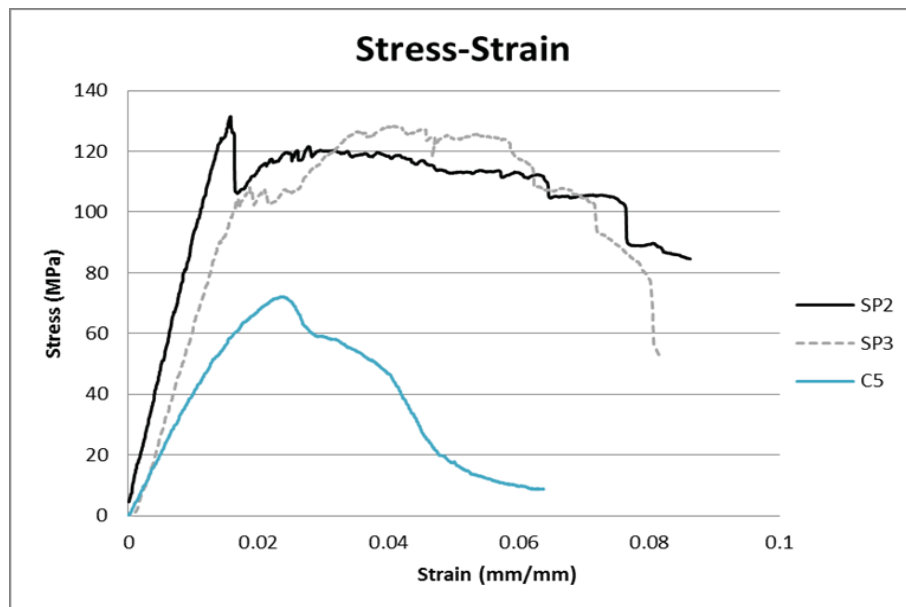


Figure 4.22. Stress-Strain curves for different panels

Among the RPP sandwich panels, the one which is laminated with a higher skin temperature (SP<sub>2</sub>) shows a better performance in terms of strength and stiffness compared to the one which is laminated with a lower skin temperature (SP<sub>3</sub>). By reducing the skin's temperature, the PP resin transforms to its solid state and shows more resistance to bond with the core material. So, the bonding is not as strong as when the lamination is done at

higher temperature and the panel is more potential to be delaminated or failed under the bending load.

#### b) Lamination Temperature/Pressure vs Adhesion Behavior

In order to investigate the effect of lamination temperature and pressure on the bonding strength between the core and facesheets, we have tested different types of sandwich panels in different lamination conditions. As mentioned earlier in this chapter, the lamination temperature can be easily controlled by changing the temperature setup of the skin heating elements. Also, the lamination pressure can be controlled by adjusting the vertical distance between the upper and lower belts of the lamination machine. The maximum allowable distance is equal to the sum of the thicknesses of the core and facesheets. In this case, the lamination pressure is almost zero and it can be increased by reducing the distance between the belts and squeezing the sandwich panel during the lamination process.

To see the effect of lamination temperature/pressure on the peel strength, same specimens as used in the previous bending test (SP<sub>2</sub> and SP<sub>3</sub> in Table 4.14) were tested to determine the adhesive peel strength between the core and skins. These two samples were laminated in the conveyor double belt press with 4.5 mm vertical distance between the upper and lower belts. Two other samples were laminated in the conveyor with 5mm distance between the belts. Hence, there is less pressure on these samples during the lamination process. Table (4.16) shows these samples' specifications for peel-off test.

Figures (4.23-4.26) represent results of the peel-off test for sandwich panels fabricated in different laminating conditions.

Table 4.16. Sample specifications for peel-off test

Sample	Core	Skin	Dimension (mm)	Peel-off Force (N)
SP <sub>2</sub>	Recycled PP+ Regrind TWT (2.5mm)	Consolidated TWT (2×1mm)-140°C	4.5×25×150	160
SP <sub>3</sub>	Recycled PP+ Regrind TWT (2.5mm)	Consolidated TWT (2×1mm)-120°C	4.5×25×150	115
SP <sub>4</sub>	Recycled PP+ Regrind TWT (3mm)	Consolidated TWT (2×1mm)-140°C	5×25×150	125
SP <sub>5</sub>	Recycled PP+ Regrind TWT (3mm)	Consolidated TWT (2×1mm)-120°C	5×25×150	74

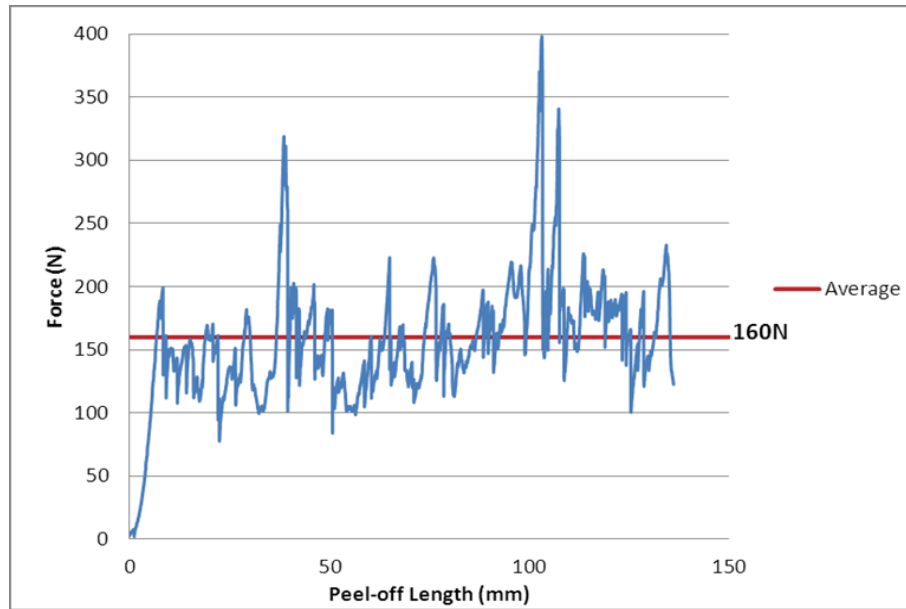


Figure 4.23. Force applied to peel-off the upper skin of the sandwich panel (SP<sub>2</sub>); High lamination pressure, Lamination temperature: 140°C

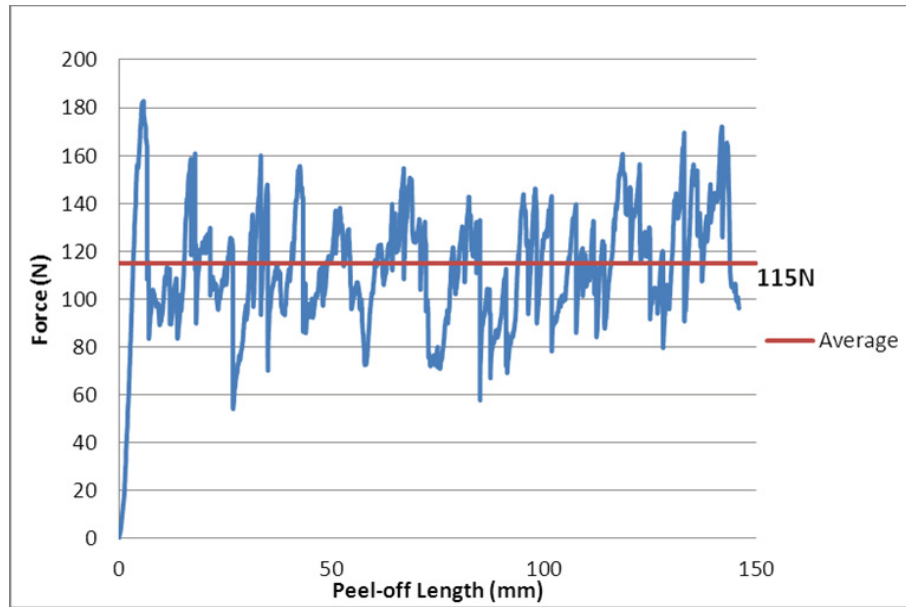


Figure 4.24. Force applied to peel-off the upper skin of the solid-core sandwich panel (SP<sub>3</sub>);  
High lamination pressure, Lamination temperature: 120°C

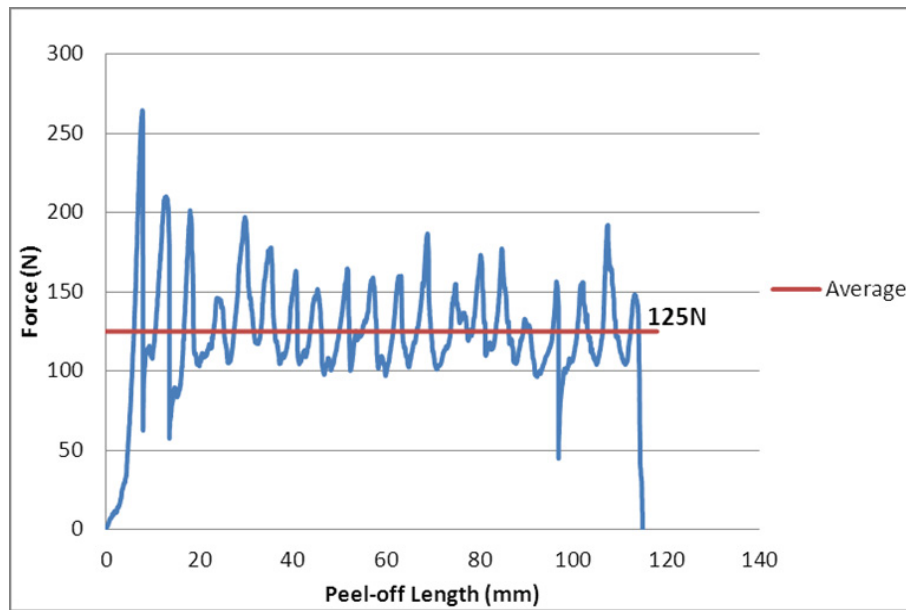


Figure 4.25. Force applied to peel-off the upper skin of the solid-core sandwich panel (SP<sub>4</sub>);  
Low lamination pressure, Lamination temperature: 140°C

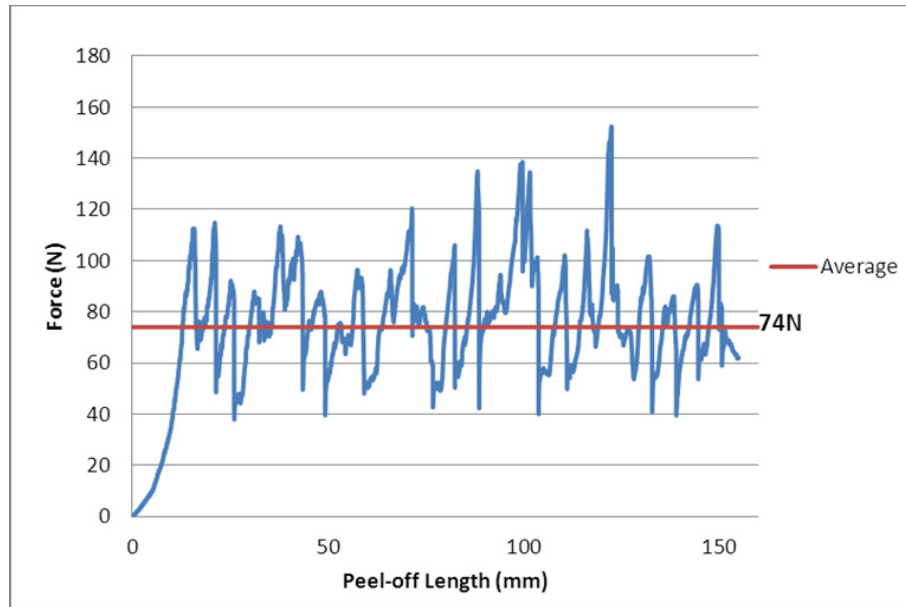


Figure 4.26. Force applied to peel-off the upper skin of the solid-core sandwich panel (SP<sub>5</sub>);  
 Low lamination pressure, Lamination temperature: 120°C

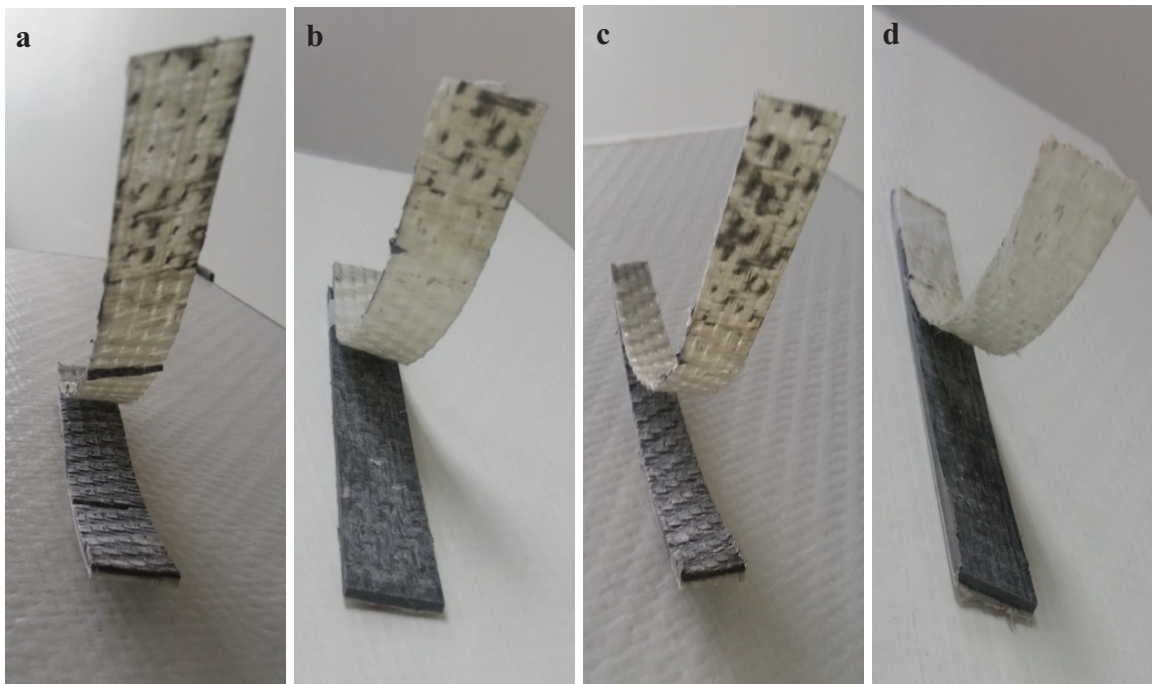


Figure 4.27. The peeled RPP samples in different lamination conditions; a) SP<sub>2</sub>, b) SP<sub>3</sub>, c) SP<sub>4</sub>, d)  
 SP<sub>5</sub>

As anticipated, the higher the lamination pressure and temperature, the higher the force required to peel the skin from the core in RPP sandwich panels. Decreasing the lamination temperature from 150 °C to 120 °C results in poor bonding between the skin and core since PP resin is transforming into its solid state. It can be clearly seen in Figure 4.27-a and 4.27-c that for high lamination temperature (140 °C) the skin has left white marks on the core material which indicate that there is a strong bonding between the core and skins at higher temperatures. Comparing Figures 4.23 and 4.24 with Figures 4.25 and 4.26 reveals the difference in the amount of peeling force for two sets of sandwich panels fabricated in different lamination pressures. At higher lamination pressures, PP resin could more diffuse through the interphase of the extruded core and facesheets which causes a strong bonding between them. It can be seen that the peeling force for the sandwich panel pulses around the average peel-off force with a relatively constant amplitude. The most probable reason for noises seen in peel-off diagram is that the values of peel-off force (100-400 N) are much smaller than the load cell capacity (2 kN) in this test so the applying force for peeling the skin is located in the error range of machine.

# Chapter 5. Foam Extrusion

## 5.1 Polymer Foam

Plastic foaming technology has been developing for many decades; likewise, polymeric foams have evolved from scientific concepts to lab research, pilot line samples, and commercialization, since the 1930s [25]. Cellular plastics or polymeric foams are gaining a high popularity in industrial and consumer applications since they can be easily produced with low material costs to obtain high strength-to-weight ratios and wide range of properties. For any given polymer, the use of different foaming agents and process conditions can yield ‘new materials’ with different densities, structures, and properties [26].

There are various types of polymeric foaming processes, such as foam extrusion, foam injection molding, compression molding, and micro-foaming [27, 28]. Foam extrusion is able to produce foam continuously, so it is commercially attractive to use the existing extrusion equipment for foam processing. In the foam extrusion, the pellets of polymer are mixed with a foaming agent and are melted by heating at high pressure in the extruder which results in gas liberation. The generated gas bubbles are dissolved in the polymer melt under the influence of the pressure inside the extruder. During the foaming procedure, the type of the foaming agent and its weight ratio, the distribution of the pressure and the solubility and diffusivity of the gas in the polymer melt have a direct influence on the nucleation of the foam, the growth of the gas bubbles, and the structure of the cell [29]. The effect of these parameters in foam extrusion and foam injection was researched numerically and experimentally and some theoretical relations and equations for cell formation have been derived in terms of physical and thermal properties of the polymer melt and the foaming agent [30-33]. A large amount of research has been conducted on the production of polyethylene (PE), polystyrene (PS) and polyurethane (PU) foams [34-35], while polypropylene (PP) foams are less favored due to their low melt strength which makes it difficult to be foamed compared to other polymers. However, the use of PP foams has been considered in industrial applications as a

substitute for PS and PE foams because it is an inexpensive material and has a higher flexural modulus than PE. Moreover, PP can offer better impact properties than PS. At room temperature, PP is above its glass transition temperature and below its melting temperature. Hence, it is in a rubbery region and can offer better impact resistance than PS. Finally, PP foams can offer a better performance at high temperatures than PE and PS because of its higher heat deflection temperature [36]. Some investigations have been done to address the issue of PP's low melt strength somehow by manipulating the processing parameters [37].

## **5.2 Chemical Foaming Agents [13]**

The chemical foaming agent (CFA) consisted of chemical compounds which can generate gas molecules such as CO<sub>2</sub>, N<sub>2</sub>, and NH<sub>3</sub> under thermal processing conditions. The CFAs are categorized into two basic groups in terms of chemical decomposition reaction which are: endothermic (absorb heat) and exothermic (release heat) foaming agents [38].

In this chapter we investigate the thermal and chemical behavior of two different types of CFA and their effect on the foam quality and physical/mechanical properties of the final product in an extrusion foaming process. First, a polypropylene-based thermoplastic (PP) sheet was produced via a plastic extrusion machine with 12" width and 4mm thickness. An exothermic foaming agent Azodicarbonamide (EV AZ-3.0) was added into the PP pellets in 5 wt%. They were completely mixed and melted inside the extruder to decompose and liberate gas. The melt temperature and pressure must be high enough to guarantee a total decomposition of the foaming agent and make the generated gas dissolved inside the polymer melt until it exits from the die opening. The same trial was conducted with an endothermic CFA named Styrene-Ethylene/Butylene-Styrene (PN-40E). Our thermal TGA analysis and physical tests demonstrate that each of the foaming agents has its own unique specifications which could be utilized based on the operating temperature and pressure.

The final foam products are light-weight materials usually possess better insulation properties, as well as higher degrees of impact resistance and high specific strength compared with the starting material [39]. The foam density depends on the inherent

properties of the applying CFA, the volume of the liberated gas dissolved into the polymer melt, the fraction lost to the environment and the foam expansion during the cooling step.

### **5.3 RPP Foam Core Extrudate**

The solid extruded core is relatively high-weight and low-thickness material for manufacturing sandwich panels. In order to increase the thickness of the core and reduce its density, two types of foaming agents were added into the starting materials to liberate gas inside the extruder and produce foam.

First, we tried to foam polypropylene extrudate without introducing any fiberglass inside. The polypropylene (PP) used in this experiment was a random copolymer grade of industrial recycled scraps. The density and melt index of this PP were 0.92 g/cm<sup>3</sup> and 11g/10 min at 230°C (ASTM D 1238), respectively. A high melt strength polypropylene (HMS-PP) was added to enhance the stability of PP melt and let the bubbles to grow and form the foam cells. Two different types of chemical foaming agents (CFAs) were utilized for our foaming purpose. An exothermic CFA Azodicarbonamide (EV AZ-3.0) was added into the PP pellets in 5 wt% yielded a blend of N<sub>2</sub>, CO<sub>2</sub> and CO. An endothermic CFA named Styrene-Ethylene/Butylene-Styrene (PN-40E) was also applied to liberate CO<sub>2</sub> into the melt.

A mixture of PP pellets, HMS and CFA with their corresponding weight ratios were fed into a two-stage extrusion machine. Then, they were completely mixed and melted inside the extruder. The operating temperature for the foam extrusion was controlled by the barrel zones and die temperature following the recommended extrusion guideline for PP. The melt temperature and pressure must be high enough to guarantee a total decomposition of the foaming agent and allow the liberated gas to be dissolved inside the polymer melt until it exits from the die opening. Melt temperature was set in the range of 180°C to 200°C (well above the melt point of PP) based on the CFA decomposition temperature. When this mixture is exposed to the atmosphere through the die of the extruder, it reaches the super saturation state, the pressure of the polymer melt decreases, and the dissolved gas is able to form the nucleus. This nucleus grows by the diffusion of

dissolved gas into the polymer melt and builds the foam cells. The final foam extrudates were cooled down in the air and shipped for couple of mechanical and physical tests to measure their density and flexural strength and stiffness.

### **5.3.1 Foam Cell Morphology**

Once the thermal decomposition of CFAs is accomplished, they produce residues which act as effective nucleation sites. Provided that the proper conditions for the growth of these nucleation sites such as high melt strength of the polymer matrix and well distribution of the foaming agent are met, foam cells can be formed and stabilized within the polymer.

A small sample of the extruded PP plate including 30/70 HMS-PP/PP (by weight ratio here and hereinafter), foamed by 5 wt% CFA, was crossly cut and polished for a microscopic observation. Figures 5.1 and 5.2 show foam cell configuration built by two types of CFAs in different melt pressures.

Comparing TGA diagrams of these two types of CFAs in Chapter 3 with Figures 5.1 and 5.2, clearly shows that the thermal properties of the CFA and also the extrusion operating conditions such as temperature and pressure have a significant influence on the cell size and population density of the foam extrudate. Since the melt temperature in our extrusion process (200°C) is not enough for a fully decomposition of PN-40E, a small number of nucleation sites could be created within the polymer melt and a big portion of its weight (around 83%) remained solid inside the polymer melt while more than half of EV AZ-3.0 weight (about 56%) could be decomposed to create foam nuclei. On the other side, increasing the melt pressure of the extruder facilitates the growth of the nuclei and creates larger foam cells. The average cell size for the low pressure PN-40E is 200µm and for the high pressure is 375 µm while for EV AZ-3.0, these values are 400 µm and 600 µm, respectively. Thus, higher population density is expected for EV AZ-3.0 than PN-40E. Also, larger foam cells could be achieved at higher melt pressure as clearly seen in Figures 5.1 and 5.2.

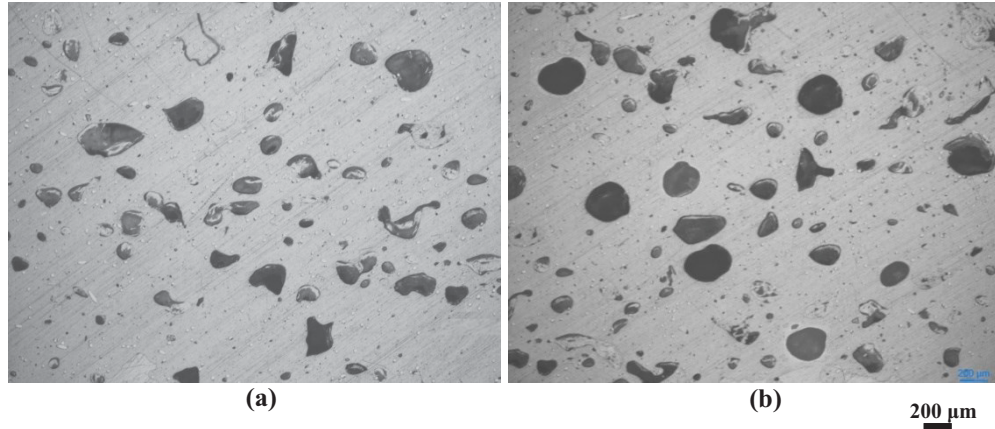


Figure 5.1. Microscopic image of the cross section of the PP foam extrudate with 5wt% PN-40E at a- low melt pressure (200psi) and b- high melt pressure (3000psi)

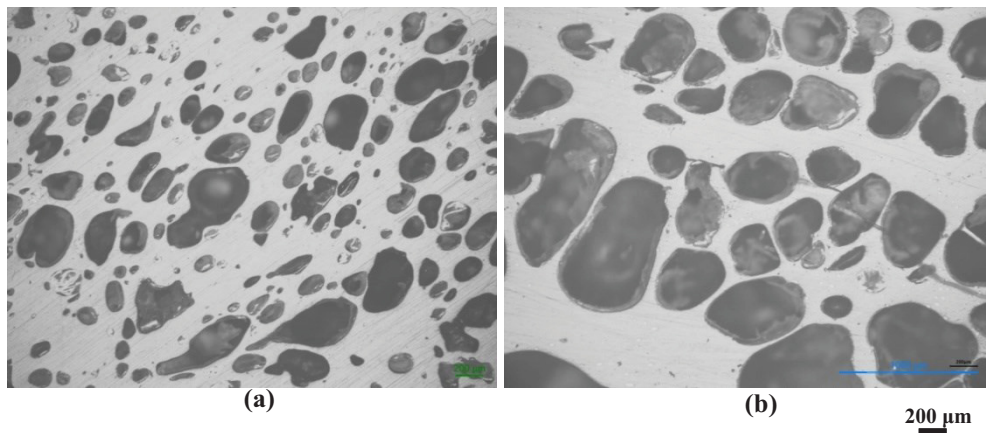


Figure 5.2. Microscopic image of the cross section of the PP foam extrudate with 5wt% EV AZ-3.0 at a- low melt pressure (200psi) and b- high melt pressure (3000psi)

### 5.3.2 Density and Flexural Properties of Foamed PP Extrudate

Since gas has the least mechanical strength, the more gas inside is the less strong the foam will be. Also the lower density foams exhibit the lowest Young's modulus. The volume fraction of foam cells is

$$\phi_g = (\rho_p - \rho_f) / \rho_p = 1 - R \quad (5.1)$$

where  $\rho_p$  is the density of the unexpanded polymer and  $\rho_f$  is the apparent density of the foamed polymer and R is the relative density.

In closed-cell foams, the membranes which form the cell faces, stretch and increase the contribution of the axial cell-wall stiffness to the elastic moduli. If the membranes do not rupture, the compression of the air in the cells also increases their stiffness. So in addition to foam density, melt pressure of the polymer also plays an important role in the stiffness of the product. A simple prediction for the Young's modulus for the closed-cell foam polymer is given by equation (5.2) [40].

$$E_f/E_p = \psi^2 \times R^2 + (1-\psi) \times R + \frac{P_0}{E_p(1-R)} \quad (5.2)$$

where  $E_f$  is the modulus of the foam and  $E_p$  is the modulus of the polymer.  $P_0$  is the air pressure in the cells and  $\psi$  is the fraction of solid contained in the cell edges. Reasonable values for  $\psi$  are 0,6 and 0,8 [40].

Density of foamed and solid PP plates was measured by water displacement and results were tabulated in Table 5.1.

Table 5.1. Density and volume fraction of foamed and solid PP extrudates

Sample	Solid PP (30/70HMS/PP) (S <sub>1</sub> )	PN-40E (200psi) 5wt% (S <sub>2</sub> )	PN-40E (3000psi) 5wt% (S <sub>3</sub> )	EV AZ-3.0 (200psi) 5wt% (S <sub>4</sub> )	EV AZ-3.0 (3000psi) 5wt% (S <sub>5</sub> )
Density (kg/m <sup>3</sup> )	917	812	752	560	438
Volume Fraction $\Phi_g$	-	0.114	0.179	0.389	0.522

Bending stiffness of the foam extrudates was estimated according to equation (5.2). A 3-point bending test was also conducted to verify the theoretical results obtained by equation (5.2). This test was carried out based on the standards ASTM D790. Figure 5.3 shows the results of the 3-point bending test for the foamed and solid specimens.

Table 5.2. Theoretical and experimental values of Young’s modulus for foamed and solid PP extrudates

Sample	Solid PP (30/70 HMS/PP) (S <sub>1</sub> )	PN-40E (200psi) 5wt% (S <sub>2</sub> )	PN-40E (3000psi) 5wt% (S <sub>3</sub> )	EV AZ-3.0 (200psi) 5wt% (S <sub>4</sub> )	EV AZ-3.0 (3000psi) 5wt% (S <sub>5</sub> )
E (MPa) (Eq.2)	1500	958	970	568	449
E (MPa) (3-point bending)	1529	349	415	307	663
Specific Stiffness (10 <sup>6</sup> m <sup>2</sup> s <sup>-2</sup> )	1.67	0.43	0.55	0.55	1.51

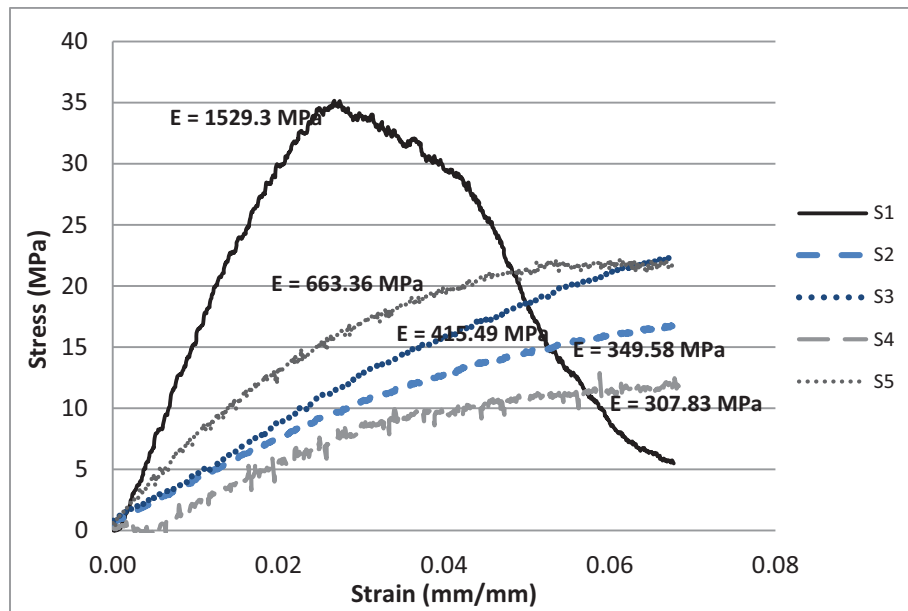


Figure 5.3. Flexural Stress and stiffness for foamed and solid PP extrudates

As seen in Table 5.2, there is a huge difference between the anticipated values for Young’s modulus and results of the 3-point bending test. The most likely reason for this violation is because the equation (5.2) is valid for an ideal closed-cell foam structure in which all the nucleation cites could perfectly grow and turn into the foam cells. When the pressure of the polymer melt is not sufficient, few number of nucleation cites are able to

grow and form the foam cells while a large number of them remain futile. This leads to a drastic reduction in stiffness while the reduction in weight is not considerable. For the high pressure foams, results of the bending test get closer to the theoretical values which indicate that for a same content of CFA, the higher melt pressure and consequently the more compression of the air in the cells yields to higher stiffness and lower density of the foam. Moreover, using our exothermic CFA leads to higher specific stiffness compared with the endothermic one.

On the other hand, adding a foaming agent to the polymer could dramatically increase the ductility and elasticity of the final product regardless of its ability to make the well-distributed and large-size gas bubbles. As illustrated in Figure 5.3, the flexural stress-strain curves reveal a huge difference of the elastic behavior between the solid PP specimen and the foamed ones. The solid PP extrudate is a brittle material which easily breaks under the bending test at 2.5% strain while no sign of fracture or breakage was observed in the foamed specimens at high strain values (up to 7%).

#### **5.4 RPP Foam Sandwich Panel**

After foaming the RPP core extrudate, the effect of using a foamed core on the mechanical and physical properties of composite sandwich panels was investigated. Thus, same as before, solid core material was extruded and a commercial exothermic foaming agent was used to liberate gas inside the extruder and produce foam. Commingled E-Glass/polypropylene woven fabrics are used as the face sheets. Foaming such an extruded PP/GF core leads to an increase in core thickness and decrease in core density. Furthermore, results of the flexural tests (3-point bending) indicate that foamed-core sandwich panels have higher bending stiffness (EI) and lower deformation comparing with the solid-core sandwich panels due to the expansion in their thickness. However, results of the peel-off test show that the bonding strength between the core and face sheets of the foamed-core sandwich panel is slightly lower than that of the solid one due to the spongy surface of the core and less contact area between the core and face sheets.

Typically, sandwich panels consist of two relatively high strength face sheets bonded to a relatively thick, low density, low strength core [41]. Thus, the sandwich structure is

characterized by a high flexural strength with reduced weight. A rigid polypropylene core can provide a high flexural stiffness ( $E_{SP}$ ) to the sandwich structure especially when they are reinforced with high strength fibers. Chopped glass fiber reinforced polypropylene (GFRPP) can be extruded and sandwiched between two composite thermoplastic skins to make the sandwich panels. However, the solid extruded PP core is relatively high-weight material for manufacturing sandwich panels. In order to increase the thickness of the core and reduce its density, an extrusion foaming process can be applied to liberate gas inside the PP melt and produce foam.

The process of foaming PP extrudate is commonly performed in industry and low density PP foams can be easily produced without big challenging issue [42]. However, introducing chopped fiber into the PP melt makes it resistive to be foamed. The existence of fiber inside the polymer creates potential nucleation sites for foam cells but the needle shape of fibers causes the foam cells to be collapsed or pulled along the fiber. It may ruin the spherical shape of the cells and prevent them to further grow.

Foaming the fiber reinforced polymers is becoming a hot topic in composite applications and some experimental studies have been conducted in this area [43,44]. In our previous work [13], we have reported the process of foam extrusion for polypropylene using two types of chemical foaming agents and the effect of melt pressure was investigated. Now, we aim to foam chopped glass fiber reinforced PP using a chemical foaming agent.

#### **5.4.1 Foamed-Core Sandwich Panel with Chopped Fiber-Reinforced PP**

Chopped glass fibers with the density of  $2.5 \text{ gr/cm}^3$  in the form of regrind thermoplastic prepreg (e.g. TWINTEX) were used to reinforce the RPP core extrudate. RTWT is a composition of 60/40 wt% FG/PP. The starting materials to extrude GFRPP solid core are composed of 70/30 wt% RPP/FG. Conventional PP inherently exhibits relatively low melt strength and melt extensibility. This results in processing problems such as uncontrolled bubble growth in PP foam. In case of foam extrusion, a high melt strength polypropylene (HMS-PP) was also added to enhance the stability of polymer melt and let the bubbles to grow and form the foam cells. So, the raw materials to produce neat PP foam extrudate are composed of 80/20 wt% RPP/HMS and to produce GFRPP foam extrudate are 65/15/20 wt% RPP/FG/HMS. These weight ratios were obtained based on

our experimental optimization. An exothermic foaming agent Azodicarbonamide (EV AZ-3.0) was added into the starting materials in 5wt%.

Nucleation of foam cells and growth of bubbles create air voids inside the polymer but there is no control on the size and distribution of the foam cells due to the presence of the fibers and the flow instability in the extrusion process. Figure 5.4 shows foam cell morphology of the neat PP and GFRPP foam extrudate. The operating melt pressure is 6.894 MPa (1000 psi). The operating parameters such as temperature, pressure and melt flow should be precisely monitored and controlled throughout the foaming process. Also, a uniform distribution of fibers and foaming agents is needed in order to achieve a foam extrudate with uniform morphology which is hardly possible in our extrusion process. Moreover, the objective of this experiment is just to reduce the density of the extrudate and study the mechanical performance of the foam extrudate and we do not aim to focus on the size and distribution of the foam cell.

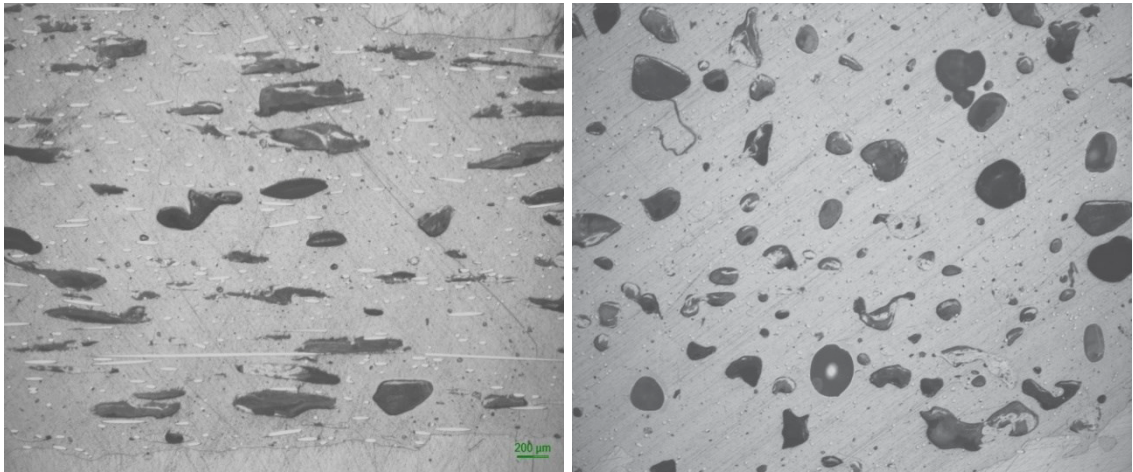


Figure 5.4. Microscopic image of the cross section of the PP foam extrudate with 5wt% EV AZ-3.0; a) GFRPP and b) neat PP

Although the size and shape of foam cells are not perfectly uniform even in the absence of fibers, however they are more spherical in shape when there is no fiber inside the melt. But, adding the chopped fibers into the polymer ruins the spherical shape of the cells and causes them to grow in spontaneous shapes. It may affect the performance of the foam extrudate in both physical and mechanical ways.

In order to investigate the physical and mechanical behavior of the solid and foam core extrudates, we have produced four sets of neat PP and GFRPP core extrudates. Figure 5.5 shows a cross-sectional view of solid and foam neat PP extrudate.



Figure 5.5. Cross-sectional view of solid (right) and foam (left) neat PP extrudate

We have also fabricated two types of sandwich panels using both solid and foam core extrudates reinforced with chopped fiberglass and 1mm TWINTEX skin. Table 5.3 shows these samples' specification. To determine the density of the extruded parts, a standard test method for apparent density of rigid cellular plastics (ASTM D1622) was performed. To find the flexural properties of the extruded core plates and sandwich panels, a 3-point bending test was carried out based on the standard ASTM D790. A peel-off test (ASTM D3167) was also performed to measure the peel resistance of the skins to the extruded core in case of sandwich panels.

Table 5.3. Sample specification for physical and mechanical tests

Sample	Core	Skin	Sample Weight (gr)	Sample Thickness (mm)
S-C1	Solid Core 100% RPP <sup>1</sup>	-	14	3.5
S-C2	Chopped FG <sup>2</sup> Reinforced Solid Core 70/30 wt% RPP/FG	-	18	3.5
F-C1	Foam Core (80/20 wt% PP/HMS <sup>3</sup> ) + 5% FA <sup>4</sup>	-	14	6
F-C2	Chopped FG Reinforced Foam Core (65/15/20 wt% PP/HMS/FG) +5% FA	-	18	6
S-SP	Solid Sandwich Panel S-C2	1mm TWINTEX	21	5.5
F-SP	Foam Sandwich Panel F-C2	1mm TWINTEX	21	8

1. RPP=Recycled Polypropylene 2. FG= Fiber Glass 3. HMS= High Melt Strength 4. FA=Foaming Agent

#### 5.4.2 Density and Flexural Properties

Foaming PP extrudate leads to a significant reduction in weight but it also reduces the flexural modulus ( $E_f$ ) and strength ( $S_f$ ) of the foam product [13]. The presence of chopped fiber glass inside the polymer has a considerable effect on the mechanical performance of both solid and foam PP extrudates as it could enhance the flexural properties of the extrudate. Results of the 3-point bending test for solid and foam neat PP and GFRPP core extrudates were illustrated in Figure 5.6.

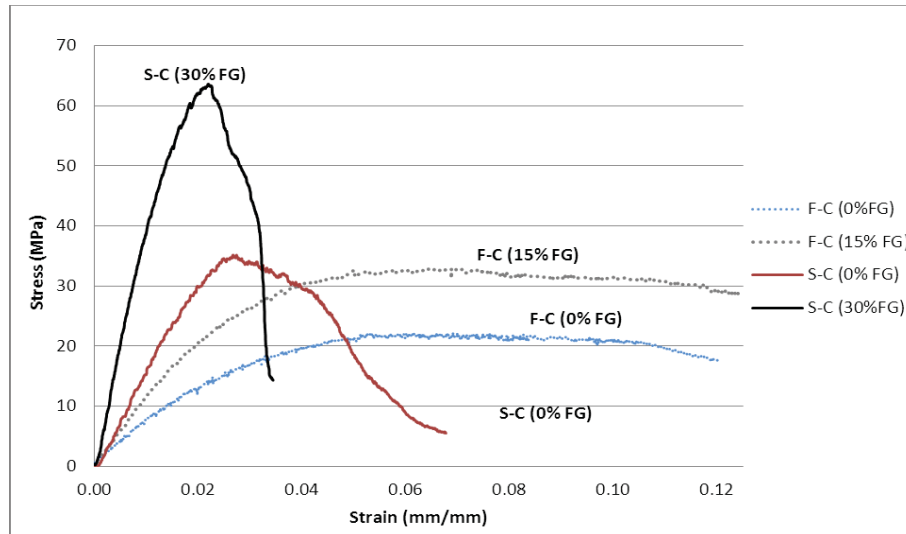


Figure 5.6. Stress-Strain curve for solid and foam PP extrudate with different chopped fiber ratio

As seen in Figure 5.6, a solid GFRPP extrudate has a high flexural strength and stiffness compared with the solid PP extrudate with no fiber inside due to the presence of fibers which fortifies the core extrudate under a bending stress. The same behavior is anticipated for the foam PP extrudate in the presence and absence of fibers.

Table 5.4 summarises the results of the bending and density tests on solid and foam PP extrudates.

Table 5.4. Flexural properties and density of solid and foam PP extrudates

Sample	Flexural Strength (MPa)	Flexural Modulus (MPa)	Density (kg/m <sup>3</sup> )
S-C1	36	1500	800
S-C2	65	4200	1050
F-C1	22	660	510
F-C2	31	1100	650

As seen in Tables 5.3 and 5.4, foaming the PP extrudate expands the product thickness to 1.7 times and reduces the density to about 60% of the solid PP extrudate. It means that a same weight of the foamed core is 1.7 times thicker than the solid core.

Results of the 3-point bending test show that adding 30 wt% chopped fiber glass to the solid PP extrudate results in 80 % increase in flexural strength and about 30 % increase in density of the solid extruded core. The flexural modulus is also increased by 2.8 times. In case of foam PP extrudate, by introducing 15 wt% chopped glass fiber to the PP foam extrudate, flexural modulus will increase about 66 % and flexural strength will increase about 40 %. There is also 27 % increase in density.

### 5.4.3 Toughness

In materials science and metallurgy, toughness is the ability of a material to absorb energy and plastically deform without fracturing [45]. Another definition is the amount of energy per unit volume that a material can absorb before rupturing. It can be calculated by integrating the stress-strain curve up to the fracture point.

$$\text{Toughness} = \frac{\text{Absorbed Energy}}{\text{Volume}} = \int_0^{\epsilon_f} \sigma \, d\epsilon \quad (5.3)$$

The value of toughness has been determined for the above solid and foam core extrudates as illustrated in Table 5.5.

The solid PP extrudate has a brittle structure and it can break at relatively low flexural strain. Adding a foaming agent to the PP could dramatically increase the ductility of the final product and heals up the brittleness of the polymer. As seen in Table 4.5, the amount of toughness for the foam extrudates is about 7 times higher than their solid counterparts. It can also be a sign of impact resistance of the extrudate which indicates that the foam PP extrudates are stronger than the solid ones in this regard. On the other hand, adding chopped fiber glass into the PP melt increases the amount of failure stress ( $\sigma$ ) and consequently the amount of toughness. The amount of toughness for GFRPP extrudate is about 2 times higher than neat PP for both solid and foam extrudates.

Figure 5.5. Values of fracture strain and toughness of solid and foam PP extrudates

Sample	Fracture Strain ( $\epsilon_f$ ) (%)	Toughness (J/m <sup>3</sup> )
S-C1	2.45	0.43
S-C2	2.30	0.85
F-C1	10.8	3.12
F-C2	11.3	5.86

#### 5.4.4 Sandwich Effect

When the extruded core material is sandwiched between two thermoplastic skins, the strength of the sandwich structure is mostly determined by the strength of the skins. Also, the effect of facesheet's stiffness will be dominant and it can compensate the weakness of the core material.

Figure 5.7 shows a view of solid and foam extrudates in shape of core plates and sandwich panels.



Figure 5.7 A view of solid and foam extrudates; 1) core and 2) sandwich panel

A 3-point bending test was performed on the solid and foam core extrudates and sandwich panels to find their flexural strength and stiffness (Figure 5.8).

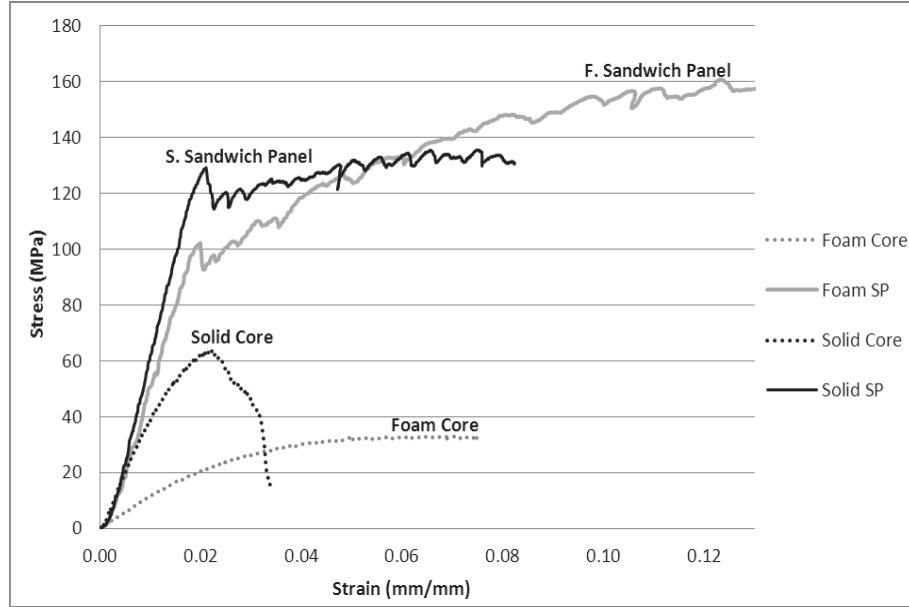


Figure 5.8. Results of 3-point bending test for solid/foam core and sandwich panel

As mentioned before, the foamed extruded core has less density and poor flexural performance compared with the solid extrudate. Results of the flexural tests (3-point bending) also indicate that the foam extrudate has lower bending strength and modulus compared with the solid core. However, when we sandwich these two types of extruded core (foam and solid) with 1mm TWINTEX skin, the effect of facesheets' stiffness will be dominant and it can compensate the weakness of the foamed core.

Flexural rigidity ( $EI$ ) is a product of elastic moduli ( $E$ ) and second moment of area ( $I$ ) for a homogeneous beam. But, for a sandwich panel consisted of the core and face sheets it is a summation of the rigidity of the faces and core measured about the neutral axis of the sandwich panel.

$$(EI)_{eq} = (EI)_f + (EI)_c \quad (5.4)$$

$$(EI)_{eq} = \frac{E_f b t^3}{6} + \frac{E_f b t d^2}{2} + \frac{E_c b c^3}{12} \quad (5.5)$$

where  $E_f$  and  $E_c$  are the elastic modulus of the face sheet and core, respectively,  $b$  is the panel width,  $c$  and  $t$  are the core and skin thicknesses, respectively and  $d=c+t$  is the distance between the center lines of the upper and lower faces.

Increasing the thickness of the core material ( $c$ ) and consequently the total thickness of the sandwich panel ( $d$ ) leads to an increase in the amount of  $(EI)_{eq}$ . Higher the flexural rigidity  $(EI)_{eq}$ , higher the beam stiffness will be.

Therefore, the foamed-core sandwich panels have higher bending stiffness ( $EI$ ) and lower deformation comparing with the solid-core sandwich panels due to the expansion in their thickness.

Results of the physical and flexural properties of the solid and foam samples (core extrudates and sandwich panels) were tabulated in Table 5.6.

Table 5.6. Physical and flexural properties of the solid and foam extrudates

Sample	Density ( $\text{gr}/\text{cm}^3$ )	Bending Strength (MPa)	Bending Modulus (MPa)	Specific Strength ( $10^3 \text{ m}^2\text{s}^{-2}$ )	Specific Modulus ( $10^3 \text{ m}^2\text{s}^{-2}$ )	Bending Stiffness (EI) ( $\text{N.m}^2$ )
S-C2	1050	65	4500	62	4285	0.4
S-SP	1250	130	7500	104	6250	2.7
F-C2	650	35	1100	54	1700	0.5
F-SP	900	105	6300	116	7000	6.1

Results of the bending test literally show that using the foam PP extrudate as the core material in a sandwich structure leads to a significant increase in the amount of bending stiffness ( $EI$ ). Thus, a same weight of foamed core sandwich panel is about 1.5 times thicker and 2.25 times stiffer than the solid core sandwich panel.

### 5.4.5 Peel-off

Decomposition of the foaming agents in the extruder leads to evolving gas inside the melt. A few amount of this gas can escape from the surface and make a rough and spongy surface. This phenomenon reduces the effective contact area between the foam core and facesheets and results in a poor bonding between them. Figure 5.9 shows a surface view of solid and foam PP extrudates. Unlike the solid extrudate, foam core has a rough surface which results in a poor bonding with the facesheets.

Results of the peel-off test on the solid and foam sandwich panels also proves that the force required to peel the skins of a foam core sandwich panel is about half of that for a solid core sandwich panel (Figure 5.10). The peel-off direction is perpendicular to the extrusion direction and from side of the extrudate to the center. As seen in Figure 5.10, the peeling force for the solid core sandwich panel pulses around the average peel-off force with relatively constant amplitude but for the foamed core sandwich panel, the force is gradually increases in the peeling direction which could be due to the non-uniform distribution of pressure applied on the sandwich panel during the lamination process. On the other hand, the distribution of melt pressure in the extrusion die is not perfectly uniform and the foam thickness varies in the widthwise direction of the die. It was observed that the foam thickness increases from sides of the die to the center (in the peel-off direction).

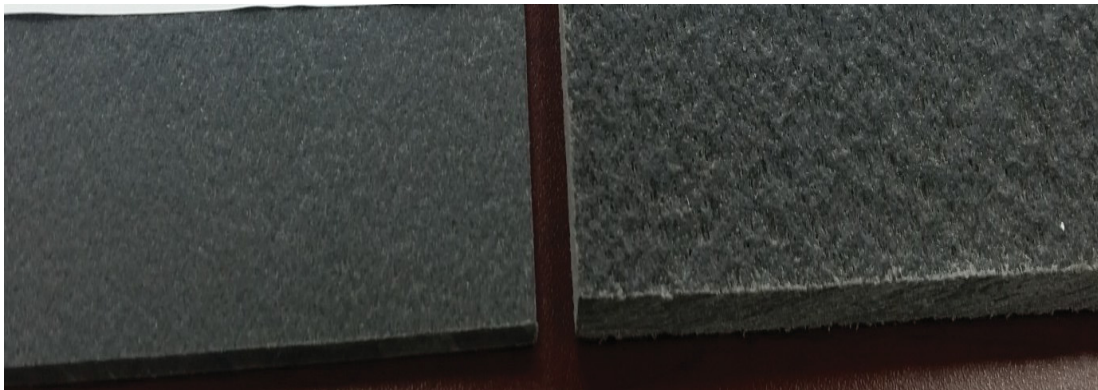


Figure 5.9. Surface view of the solid (left) and foam (right) core extrudates

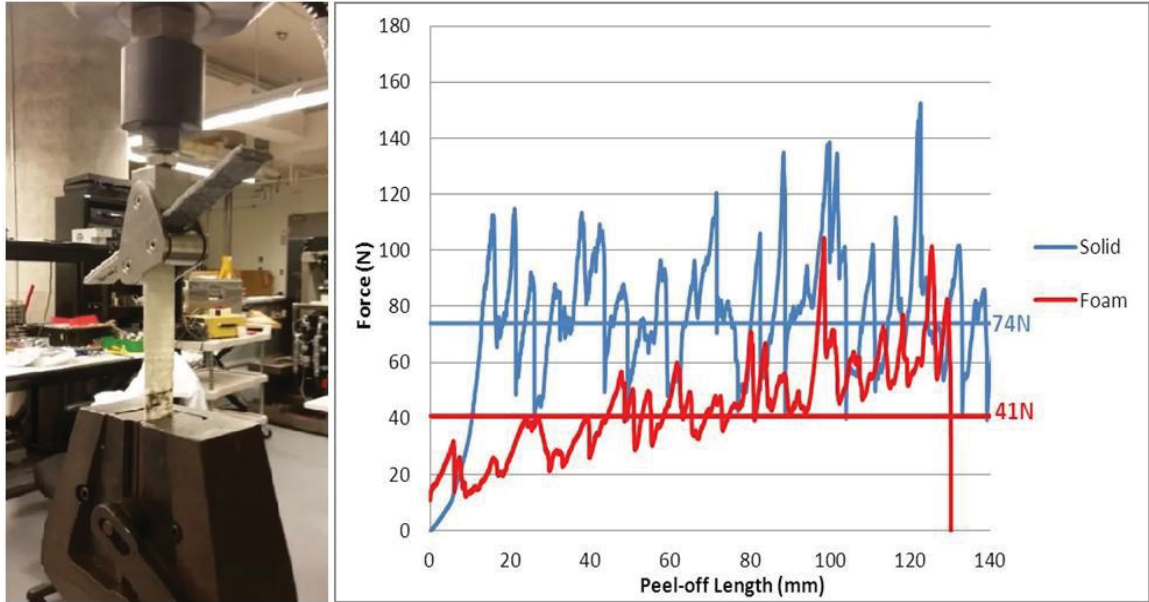


Figure 5.10. Results of the peel-off test for solid and foamed core sandwich panels

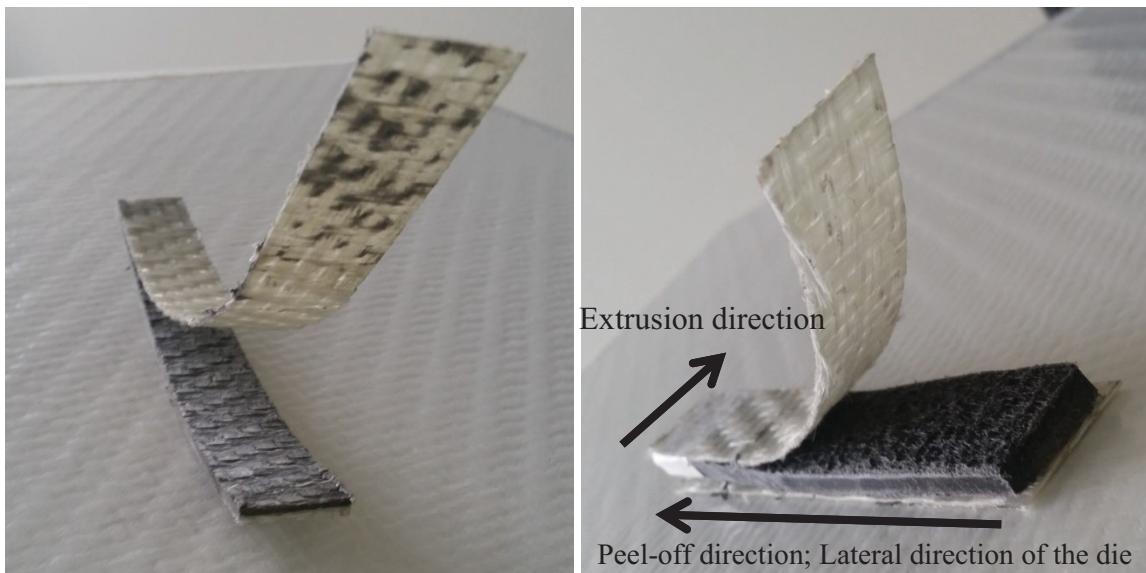


Figure 5.11. Solid-core (left) and foamed-core (right) sandwich panels used for peel-off test

As illustrated in Figure 5.11, in solid core sandwich panel, the skin has left white marks on the core material after it was removed. Also, a few amount of core material has been stuck to the skin which indicates that there is a strong bonding between the core and skins for this type of sandwich panel while this phenomenon is not observed in foamed-core sandwich panels.

## 5.5 Honeycomb vs Recycled PP Foam Sandwich Panels

Among the thermoplastic core materials for manufacturing sandwich panels, honeycombs are so popular due to their superior properties, such as light weight, rot resistance, recycling ability and thermal insulation. However, honeycombs are expensive materials requiring a sophisticated fabrication process. Moreover, honeycomb sandwich panels are more susceptible to delamination under the bending loads compared with the rigid core sandwich panels. Considered in most of experimental and numerical studies, debonding and delamination are the most important failure modes in composite sandwich panels [46-47]. The load carried by sandwich structures continues to increase after core yielding. Knowing that the core could not carry additional load after yield, this increasing load carrying capacity of post yield sandwich structure initiates the postulation that the additional shear load was transferred to the face sheets [48]. If the applied shear stress on the core material exceeds its ultimate shear strength, the sandwich structure will fail and is not able to carry the higher load. This is the case which commonly occurs in honeycomb sandwich panels since they are not strong materials under the shear stress. Solid-surface polymeric foams could be a good alternative since they have higher shear strength. Also, increasing the effective contact area to bond with thermoplastic skins makes this type of sandwich panels more resistant to delamination and provides higher adhesion strength [49-50]. In this section, the flexural and adhesion behavior of RPP foam sandwich panels was compared with a typical polypropylene honeycomb sandwich panel based on the classical theory of sandwich panels [51-53] and the criteria for choosing a proper core material based on the application and panel thickness is represented.

In order to compare the mechanical performance of this type of sandwich panels with our recycled foam sandwich panels, a 3-point bending test was performed on two similar samples made of our recycled foam sandwich panel and a typical honeycomb sandwich panel with same thickness of the core and facesheets. A honeycomb sandwich panel with the core thickness of 6mm and skin thickness of 1 mm was produced using the innovated and fully automated machine in “AS Composite Inc.”. A recycled foam sandwich panel

made of neat PP foamed core (70/30 wt% PP/HMS and 5% CFA) and 1mm TWINTEX skin was tested under the 3-point bending load.

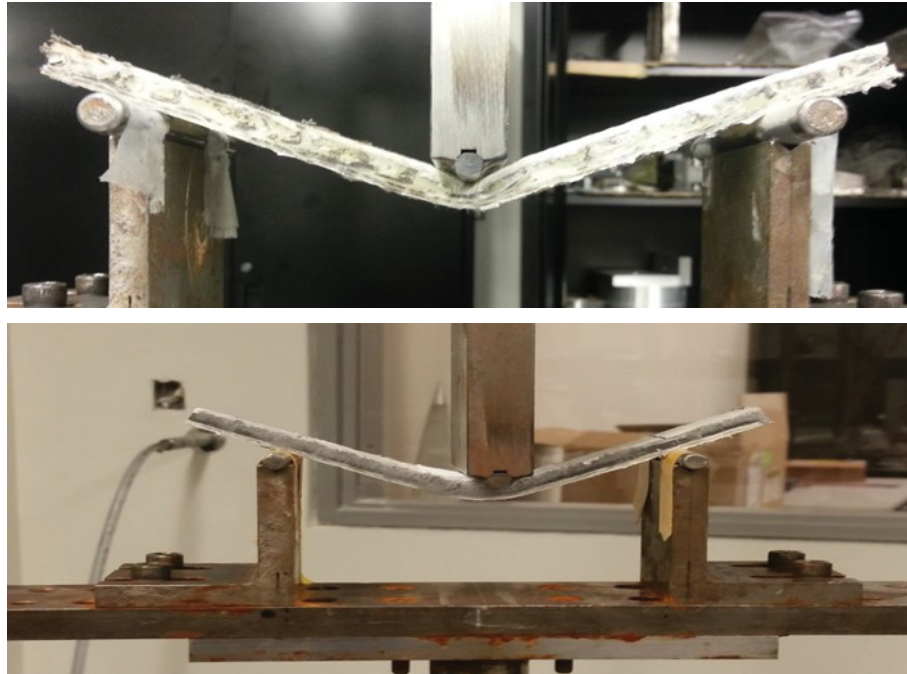


Figure 5.12. A view of honeycomb and RPP foam sandwich panels under the bending test

### 5.5.1 Flexural Behavior

As illustrated in Figure 5.13, the mechanical behavior of recycled sandwich panel under 3-point bending test is completely different from the honeycomb sandwich panel. A drastic reduction in the applied force (stress) is evident in case of honeycomb while there is no such thing in case of recycled sandwich panels. It could be due to the skin delamination in honeycomb panel while there is no sign of fracture or delamination in our recycled sandwich panels. In other words, honeycomb sandwich panel is more potential to be delaminated under the 3-point bending because of its lattice structure of hollow cells results in a poor bonding between skin and honeycomb. Unlike the honeycomb panels, the RPP foam sandwich panel is relatively strong in terms of core-skin bonding due to the high effective contact area between the core and skins. The most probable reason for flexural failure in RPP sandwich panels (if occurs) is due to the fracture in the core material not the skin delamination.

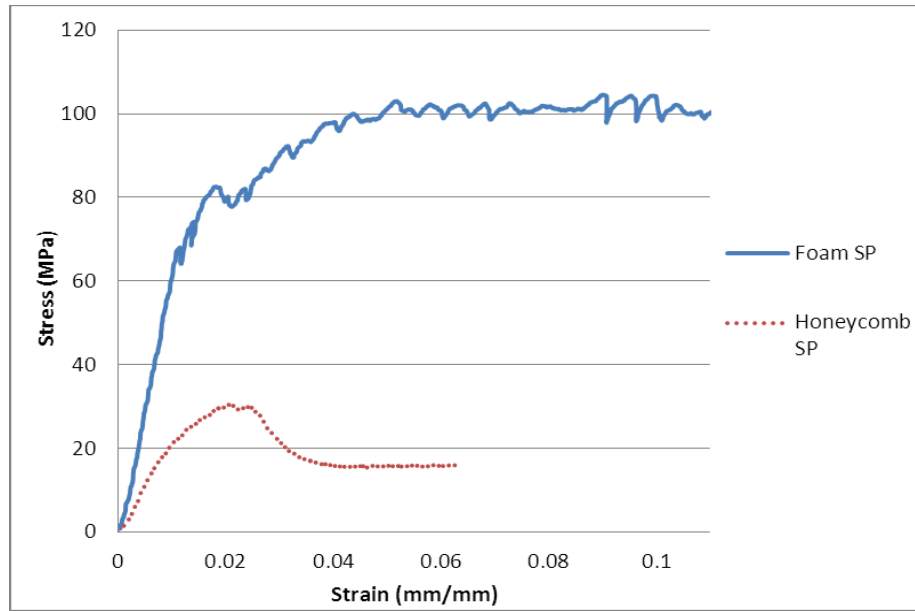


Figure 5.13. Stress-Strain curve for honeycomb and recycled PP foam sandwich

Table 5.7. Density and flexural properties of honeycomb and recycled foam sandwich panels

Sample	Bending Modulus $E_{avg}$ (Gpa)	Bending Strength $S_{avg}$ (Mpa)	Core Density (kg/m <sup>3</sup> )	Panel Density (kg/m <sup>3</sup> )	Specific Strength (10 <sup>3</sup> m <sup>2</sup> s <sup>-2</sup> )
Foam SP (8mm thick)	3.200	100	450	700	143
Honeycomb SP (8mm thick)	2.350	30	90	430	69

Results of the density and bending tests show that the flexural strength of RPP foam sandwich panels are about 3 times stronger than the honeycomb sandwich panel with the same dimensions but they are higher in weight compared to the honeycomb. The RPP foam core extrudate is about 5 times heavier than honeycomb but for high skin-to-core thickness ratios ( $t/c > 1/5$ ), the skins' weight has a considerable effect on the total weight

of the sandwich panel. Therefore, the RPP foam sandwich panel is just 1.7 times heavier than the honeycomb sandwich panel. Altogether, the specific strength of RPP foam sandwich panel is about 2 times higher than that one for the honeycomb sandwich panel.

However, for low-weight and high-thick sandwich panel applications, there is a remarkable difference between the weight of honeycomb and RPP foam sandwich panels and using honeycomb core is more recommended for  $t/c < 1/10$ .

We have also calculated the maximum values of flexural and shear stress in the core and facesheet of honeycomb and RPP foam sandwich panels based on the theory of sandwich panels discussed in chapter 1. The amount of applied force and sample dimensions are obtained from the 3-point bending test. Figure 5.14 shows the specific strength of honeycomb and RPP foam sandwich panels for different skin to core thickness ratios. Also the results of stress distribution and panel density are represented for these two types of sandwich panels (Table 5.8).

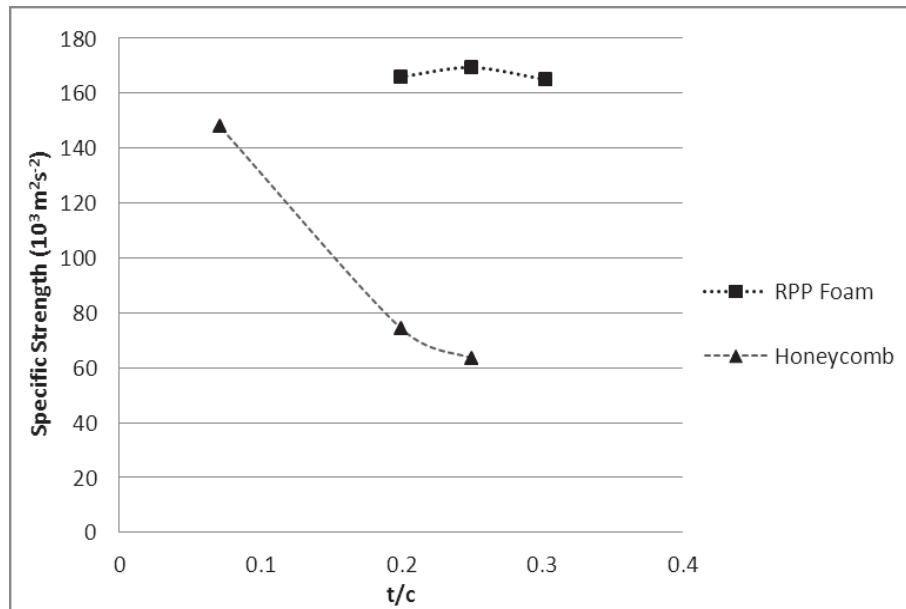


Figure 5.14. Specific strength of honeycomb and RPP foam sandwich panels

Table 5.8. Effect of skin and core thickness on density and mechanical performance of honeycomb and recycled foam sandwich panels

Sample	Core (c) (mm)	Skin (t) (mm)	t/c	Density (kg/m <sup>3</sup> )	( $\sigma_c$ ) <sub>max</sub> (MPa)	( $\sigma_f$ ) <sub>max</sub> (MPa)	( $\tau_c$ ) <sub>max</sub> (MPa)	Specific Strength (10 <sup>3</sup> m <sup>2</sup> s <sup>-2</sup> )
Honeycomb Sandwich panel	5	1	1/5	500	0	37.2	0.5	74.4
	6	1.5	1/4	550	0	34.9	1	63.5
	28	2	1/14	280	0	41.4	0.1	147.8
RPP Foam Sandwich Panel	5	1.5	1/3.3	825	6.2	136.0	3.5	165.0
	6	1	1/6	700	6.4	118.6	2.2	169.4
	7	1	1/7	670	5.9	109.2	2.0	163.0

The flexural modulus of honeycomb is assumed to be zero which is practically true compared to the skin material and the ultimate shear strength of the honeycomb we used is 0.5 MPa while this value is about 25 MPa for PP. Thus, as seen in Table 5.8, for low-thick sandwich panels, honeycomb will fail due to the exceeding shear stress in the core, so it is not able to undertake higher bending load. A failure in honeycomb core is evident in Figure 5.15 while there is no sign of fracture in RPP foam core. Moreover, the low-thick honeycomb panels are relatively high-density products since the skin effect will be dominant which results in low specific strength of the structure. For low-thick sandwich panel applications, RPP foam sandwich panels offer better mechanical performance with a specific strength of about 2.5 times more than honeycomb sandwich panels.

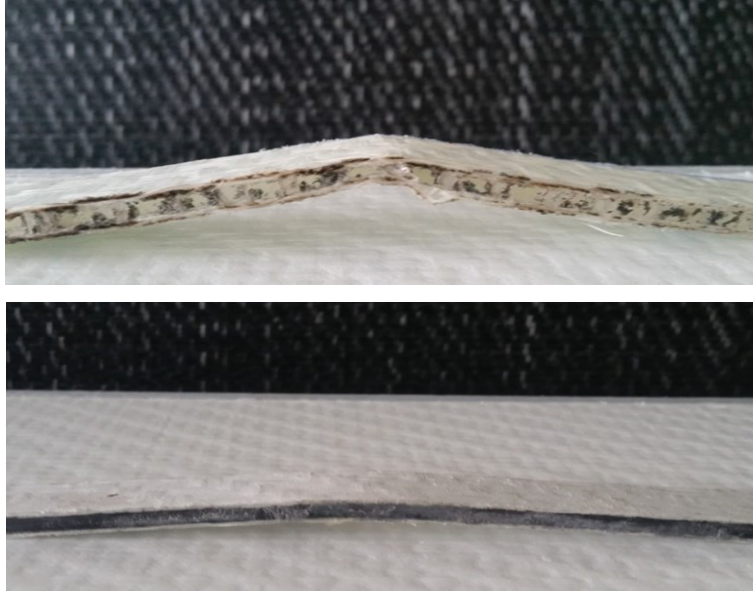


Figure 5.15. A view of honeycomb and RPP foam sandwich panels after the bending test

### 5.5.2 Adhesion Behavior

A roll peel-off test (ASTM D3167) was carried out to compare the bonding strength of skin-to-core for both the honeycomb and RPP foam sandwich panels and results are represented in Figures 5.16.

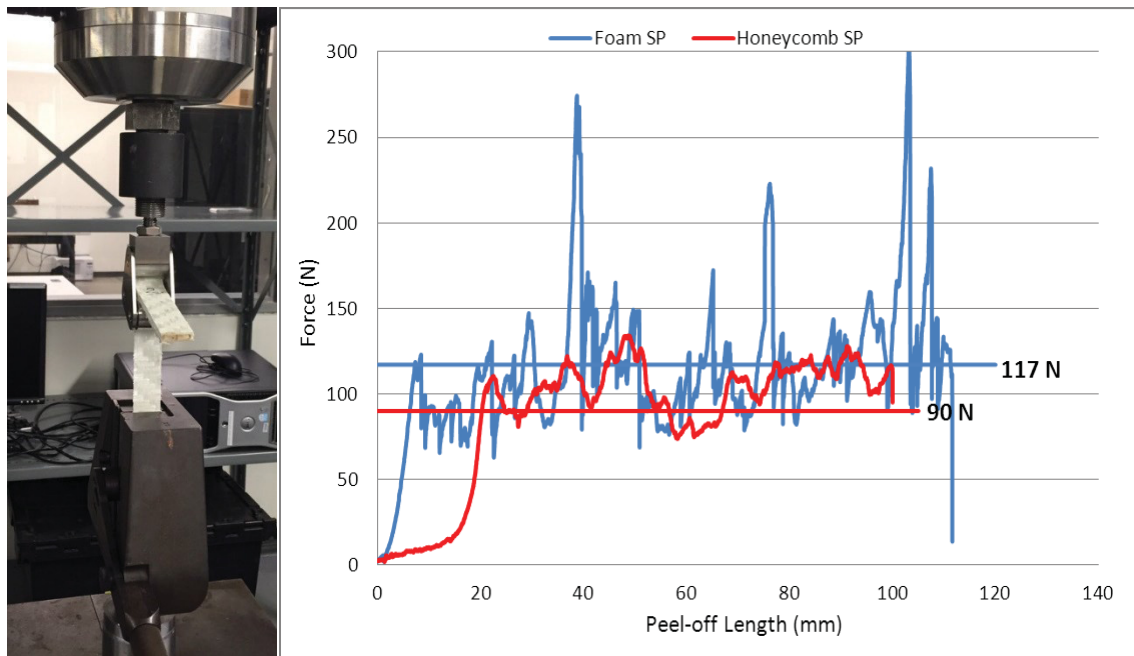


Figure 5.16. Results of the peel-off test for RPP foam and honeycomb sandwich panels

Both honeycomb and RPP foam sandwich panels are fabricated under the same lamination temperature and pressure. The lamination process is done under relatively high pressure applied by the squeezing rollers of the conveyor double belt press machine (Figure 3.17 in chapter 3). The vertical distance between the rollers is set 1 mm less than the total thickness of the core and skins so that it could squeeze the sandwich panel and apply enough pressure to bond the skin to core. The lamination temperature is around 150 °C for both of the above samples.

As seen in Figure 5.16, the applied force for peeling the skin of a honeycomb sandwich panel is less than that one for RPP foam sandwich panel. The average peeling force for honeycomb sandwich panel is about 77% of RPP foam sandwich panel. The reason is due to the lattice structure of honeycomb which creates a small contact area to bond with the skin. Figure 5.17 shows the honeycomb and RPP foam sandwich panels after the roll peel-off test. As illustrated in Figure 5.17, the effective contact area between the core and skin of honeycomb sandwich panel is much smaller than a solid-surface core material like our RPP foam extrudate.

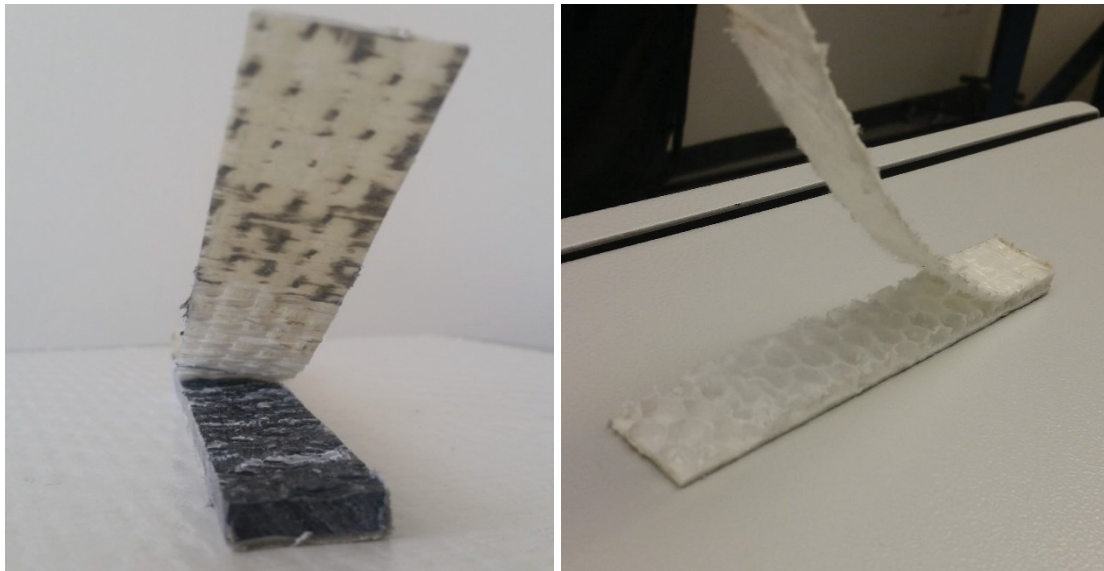


Figure 5.17. RPP foam extrudate (left) and honeycomb (right) sandwich panels used for peel-off test

## 5.6 Foaming Challenges

As mentioned earlier in this chapter, the melt pressure of the polymer must be high enough to let the nucleated agents grow inside the polymer melt and create high density foam. Unfortunately, we were not able to reach the required back pressure at the extruder with our existing extruder and die. The issue is that the die we used in this experiment is a sheet die with a simple rectangular profile and constant cross section. This type of extrusion die is unable to maintain the back pressure built by the screw at the end of the extruder. The result is premature foaming in the extruded product (Figure 5.18). There are some ways to prevent the pressure drop in the die. One is placing wire mesh plates such as screen filters which increase the back pressure in the extruder but they can get easily clogged by the chopped fibers within the melt passing through them. The other way is using a gear pump (melt pump) between the extruder and die. In order to obtain an extruded profile of consistent quality, it is necessary to keep both the extruder output and melt viscosity constant. Extruder screws efficiently melt, mix and convey polymer, but are not as efficient at providing a consistent pressure and volume to the die. A melt pump, while not a mixing or melting device, is extremely efficient at building pressure and metering the polymer output.



Figure 5.18 Premature foaming due to pressure drop in the extrusion die

The use of melt pumps can improve the extrusion process in the following ways:

- The mass flow is stabilized
- The pressure in the barrel can be increased
- Less work-intensive material must be transported in the barrel

Figure 5.19 represents a schematic view of a conventional gear pump structure.

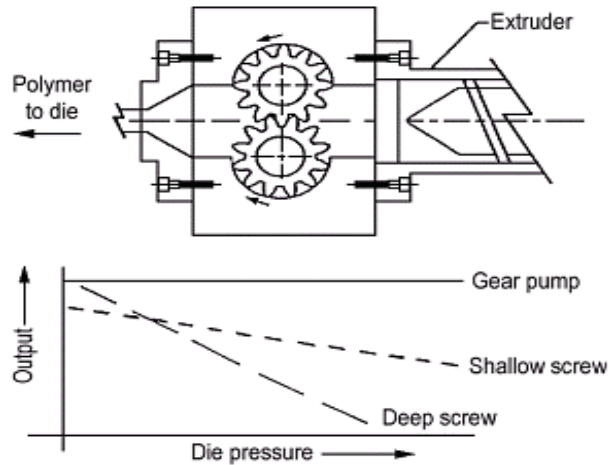


Figure 5.19. A scheme of extrusion gear pump

One of the key parameters to make a uniform and high density foam extrudate is using an extrusion die specially designed for foam process. High density foam extrusion die has bigger design challenges than regular extrusion die.

There are some common designs for foam extrusion die. Longitudinal extrusion die with a mandrel is mainly used in the foam extrusion process. The standard longitudinal extrusion heads for solid polymers are mainly used for extruding foam extrudates that have small cross-sections and thin walls. Required shape and dimensions of the foam extrudate can be obtained by using a replaceable forming ring with a die. The conical mandrel facilitates achieving adequate pressure of polymer in the extrusion head flow channels. Figure 5.20 shows a diagram of the longitudinal extrusion head with a replaceable forming ring.

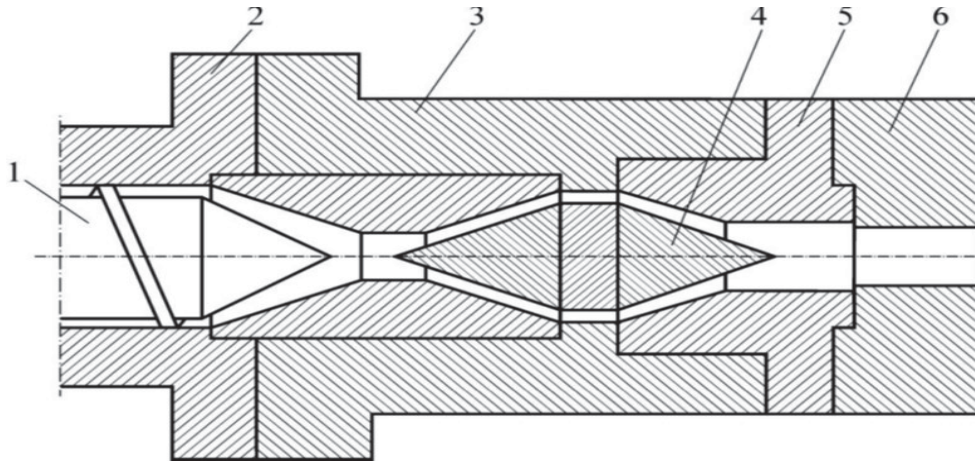


Figure 5.20 Diagram of the longitudinal extrusion head with a replaceable forming ring:  
 1– screw, 2 – extruder barrel, 3 – extrusion head body, 4 – mandrel, 5– intermediate ring,  
 6 – forming ring [51]

A longitudinal extrusion head with a thin-wall diaphragm grid can also be used to obtain foam extrudates of a considerable cross-section area and a very low density (Figure 5.21). The use of a thin-wall diaphragm grid in the extrusion head flow channels in combination with a possibly low reduction of the polymer stream cross-section area enables simultaneous flow resistance adjustment and polymer pressure increase.

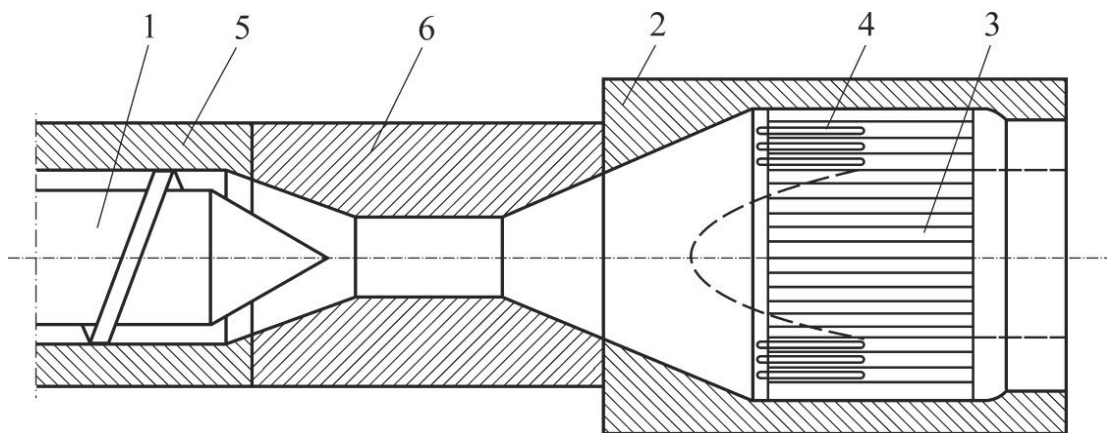


Figure 5.21. Diagram of the longitudinal extrusion head with a diaphragm grid:  
 1 – screw, 2 – extrusion head body, 3 – dividing channels in the diaphragm grid, 4 – channel  
 stoppers, 5 – extruder barrel, 6 – extrusion head adapter [52]

# Chapter 6. Conclusion and Future Works

## 6.1 Conclusion

The most important advantage of manufacturing recycled sandwich panels in a continuous extrusion line is the high-speed and low-cost manufacturing process it can provide. The production of recycled sandwich panels is done in a single-stage process by extruding very low-cost raw materials composed of recycled thermoplastic scraps /recycled polypropylene and laminating with high-strength glass fiber reinforced thermoplastic skins. During this experimental study, we tried to optimize the extrusion process to extrude a uniform and high performance core material. We found that increasing the amount of chopped fiber glass inside the extruded core will increase the stiffness and strength of the extrudate, however, a large amount of regrind twintex (RTWT) in the mixture (higher than 50wt %) will clog the feeding path in the hopper. So the optimum amount of RTWT in the mixture is 50wt%. After finding the optimum amount of RTWT in the mixture, we attempted to set the proper conditions for skin lamination process. Covering RPP core extrudate with high strength thermoplastic skins will enhance the stiffness and ductility of the product. Results of the 3-point bending tests on our recycled sandwich panels show that they are relatively strong structures under the bending load. There is no sign of fracture or delamination in our recycled sandwich panels provided that the proper conditions for lamination process are met. A higher lamination temperature (in the range of 120-160 °C) creates a stronger bonding and results in better performance of the panel in terms of strength and stiffness. So the skin lamination should be done before a drastic reduction in temperature occurs when the skin exits the heating chamber. Also a higher lamination pressure causes a strong bonding between the core extrudate and face sheets.

The big issue in the solid-core recycled sandwich panels is that they are relatively high-weight materials compared with honeycomb and foam-core sandwich panels. Hence, we applied a foaming process using chemical foaming agents to reduce the density of the

extruded core. Adding a foaming agent to the polymer could also increase the ductility and elasticity of the final product and heals up the brittleness of the polymer.

The decomposition temperature of the applied foaming agent should be well close to the extrusion operating temperature in order to liberate sufficient volume of gas. Using an exothermic CFA is recommended when the operating temperature is limited and cannot be further increased.

Foaming the core extrudate leads to the expansion in its thickness upon exiting from the extrusion die. Therefore, a foamed-core sandwich panel has higher bending stiffness (EI) and lower deformation comparing with the solid-core sandwich panel of the same weight due to the expansion in the thickness. However, the bonding strength between the core and face sheets of the foamed-core sandwich panel is lower than that of the solid one due to the spongy surface of the core which results in less contact area between the core and face sheets.

Comparing our low-density foam sandwich panel with a honeycomb sandwich panel of same thickness reveals that the RPP foam sandwich panels offer better flexural performance (higher specific strength). However, for low-weight and high-thick applications, there is a remarkable difference between the weight of honeycomb and RPP foam sandwich panels and using honeycomb core is more recommended for  $t/c < 1/10$ .

## **6.2 Contribution**

- A novel method for fabrication of high-strength and low-cost sandwich panels using recycled thermoplastic composites in a single-stage manufacturing procedure was developed.
- An extrusion foaming process was applied to reduce the density of the extruded core and increase the core thickness in order to enhance the physical and mechanical performance of recycled sandwich panels.

### **6.3 Future Work**

Although a huge effort has been done in developing the manufacturing process of recycled sandwich panels, but more investigations are still needed to turn them into the high-performance materials through a low-cost manufacturing procedure. Thus, further work should be carried out to

- Optimize the process parameters to obtain the characterization of a high performance sandwich panel based on the physical and mechanical properties.
- Address the current foaming challenges in the extrusion process in order to produce low-density and uniform foam extrudate.
- Modeling of the manufacturing process to apply for other thermoplastic materials like PET, PEEK etc.

## References

1. Mikell P. Groover, "Fundamentals of Modern Manufacturing", 4<sup>th</sup> ed., John Wiley & Sons, Inc.
2. Vanessa Goodship, "Introduction to Plastics Recycling", 2nd ed., iSmithers Rapra Publishing, Page 6.
3. Haibin Ning et al., "Thermoplastic sandwich structure design and manufacturing for the body panel of mass transit vehicle", *Composite Structures*, Vol. 80: 82-91 (2007).
4. Serope Kalpakjian, "e-Study Guide for: Manufacturing Processes for Engineering Materials", Cram 101 Publishing (2012).
5. Potluri P, Kusak E, Reddy TY, "Novel stitch-bonded sandwich composite structure", *Composite Structures*, Vol. 59:251-9 (2003).
6. Alampalli, S., "Field performance of an FRP slab bridge", *Composite Structures*, Vol. 72: 494-502 (2005).
7. Krebs J, Friedrich K, Bhattacharyya D., "A direct comparison of matched-die versus diaphragm forming. *Composites: Part A*", 29A:183-8 (1998).
8. Henninger F, Friedrich K., "Production of textile reinforced thermoplastics profiles by roll forming *Composites: Part A*", 35:573-83 (2004).
9. Dykes RJ, Mander SJ, Bhattacharyya D., "Roll forming continuous fibre-reinforced thermoplastic sheets: experimental analysis. *Composites: Part A*", 31:1395-407 (2000)
10. Lim TC, Ramakrishna S, Shang HM., "Axisymmetric sheet forming of knitted fabric composite by combined stretch forming and deep drawing. *Composites: Part B*", 30:495-502 (1999)
11. O Rozant et al., "Manufacturing of three dimensional sandwich parts by direct thermoforming", *Composites Part A Applied Science and Manufacturing*, Vol. 32, 1593-1601, (2001)
12. J. Kratz, P. Hubert, "Out-of-Autoclave Manufacturing of Composite Aircraft Sandwich Structures", 17<sup>th</sup> International Conference on Composite Materials (ICCM 17), Edinburgh, Scotland (2009)

13. M. R. Azad, M. Hojjati, H. Borazghi, "Influence of Exothermic and Endothermic Chemical Foaming Agents on the Physical and Mechanical Properties of the Polypropylene-Based Thermoplastic Structures", American Society for Composites, 30th Technical Conference, Michigan, US (2015)
14. M. Biron, "Thermosets and Composites-Technical Information for Plastic Users", 1<sup>st</sup> edition, 2004, ch. 1,5,6
15. R.J. Crawford, "Plastics Engineering", 3<sup>rd</sup> edition, 1998, pp 254-342.
16. D. Zenkert, "An Introduction to Sandwich Construction", 1<sup>st</sup> edition, 1997, pp 39-48
17. H. G. Allen, "Analysis and Design of Structural Sandwich Panels", 1<sup>st</sup> edition, 1969, pp 8-18
18. F. C. Campbell, "Structural Composite Materials", 1<sup>st</sup> edition, 2010, ch. 14
19. M. Biron, "Thermoplastics and Thermoplastic Composites: Technical Information for Plastic Users", 1<sup>st</sup> edition, 2007, ch. 5,6
20. <http://www.fiberglassindustries.com/twintex.htm>
21. P.K. Mallick, "Fiber-Reinforced Composites; Materials, Manufacturing and Design", 2<sup>nd</sup> edition, 1993, pp 121-132
22. ASTM Standard D1622, "Standard Test Method for Apparent Density of Rigid Cellular Plastics", West Conshohocken, PA, 2008, DOI: 10.1520/D1622\_D1622M-14
23. ASTM Standard D790, "Standard Test Methods for Flexural Properties of Unreinforced and Reinforced Plastics and Electrical Insulating Materials", West Conshohocken, PA, 2009, DOI: 10.1520/D0790-15E01
24. ASTM Standard D3167, "Standard Test Method for Floating Roller Peel Resistance of Adhesives", West Conshohocken, PA, 2010, DOI: DOI: 10.1520/D3167-10
25. S.T. Lee, C.B. Park, and N.S. Ramesh," Polymeric Foams", Taylor & Francis (2007)
26. I. Coccorullo, L. Di Maio, S. Montesano, L. Incarnato, "Theoretical and experimental study of foaming process with chain extended recycled PET", eXPRESS Polymer Letters Vol.3, No.2, 84–96 (2009)

27. Kumar V., Suh N. P.” Process for making microcellular thermoplastic parts”, *Polymer Engineering and Science*, 30, 1323–1329 (1990)
28. Baldwin D. F., Suh N. P., Park C. B., Cha S. W, ” Supermicrocellular foamed materials”, U.S. Patent 5334356, USA (1994)
29. Jae Gyoung Gwon et. al. “Effects of Sizes and Contents of Exothermic Foaming Agent on Physical Properties of Injection Foamed Wood Fiber/HDPE Composites”, *Int. J. of Precision Engineering and Manufacturing*, Vol. 13, No. 6, 1003-1007
30. Han, C. D.; Villamizar, C. A., “Studies on structural foam processing: The rheology of foam extrusion”, *Polymer and Engineering Science* 18, 687 (1978)
31. Han, C. D. and Ma, C. Y. ” Foam Extrusion Characteristics of Thermoplastic Resins.I. Low Density Polyethylene”, *J. Applied Polymer. Science*, 28, 2961 (1983)
32. James J. Feng, Christopher A. Bertelo, “Prediction of bubble growth and size distribution in polymer foaming based on a new heterogeneous nucleation model”, *The Society of Rheology; J. Rheology*. 48, 439-462 (2004)
33. Vipin Kumar et al. “Extrusion of Microcellular Foams Using Pre-Saturated Pellets and Solid-State Nucleation”, *Cellular Polymers*, Vol. 23, No. 6, 369 (2004)
34. J.H. Saunders “Handbook of Polymeric Foam and Foam Technology”, Hanser Publishers, 5 (1991)
35. Nigel Mills, “Polymer Foams Handbook: Engineering and Biomechanics Applications and Design Guide”, 1st ed. (2007)
36. Chul B. Park, Lewis K. Cheung, “A study of cell nucleation in the extrusion of polypropylene foams”, *Polymer Engineering & Science*, Vol. 37, 1–10 ( 1997)
37. Naguib, Hani E et al. “Strategies for achieving ultra low-density polypropylene foams”, *Polymer Engineering & Science*, Vol. 42, 1481-1492 ( 2002)
38. Li, Q. and Matuana, L. M., “Foam Extrusion of High Density Polypropylene/Wood Flour composites Using Chemical Foaming Agents”, *J. Appl. Polym. Sci.*,Vol. 88, pp. 3139-3150 (2003)

39. Lee C. H., Lee K.-J., Jeong H. G., Kim S. W. "Growth of gas bubbles in the foam extrusion process", *Advances in Polymer Technology*, 19, 97–112 (2000)
40. Katrine Sivertsen, "POLYMER FOAMS", 3.063 Polymer Physics, Spring 2007
41. William L. Ko, "Elastic Constant for Superplastically Formed/Diffusion-Bonded Corrugated Sandwich Core", NASA technical paper 1562, 1980
42. Altepping J., Nebe J., "Production of Low Density Polypropylene Foam", European Patent 0 359517 A2, 1990
43. Laurent M. Matuana, et al., "Processing and cell morphology relationships for microcellular foamed PVC/wood-fiber composites", *Polymer Engineering & Science*, Vol. 37, pp 1137-1147 , 1997
44. Chul B. Park, et al., "Plastic wood fiber foam structure and method of producing same", US Patent US6936200 B2, Filed Dec. 2001, and published Aug. 2005
45. Brian Larson, "Toughness", NDT Education Resource Center, 2001-2011, The Collaboration for NDT Education, Iowa State University
46. G.S. Langdon, et al., "The response of sandwich structures with composite face sheets and polymer foam cores to air-blast loading: Preliminary experiments", *Engineering Structures*, 36, 104 (2012).
47. D. Feng and F. Aymerich, "Damage prediction in composite sandwich panels subjected to low-velocity impact", *Composites A*, 52, 12 (2013).
48. L. L. Mercado, et al., "Higher order theory for sandwich beams with yielded core", *Proceedings of ICSS-5 Conference*, Zurich, September 2000.
49. I. Coccorullo, et al., "Theoretical and experimental study of foaming process with chain extended recycled PET", *eXPRESS Polymer Letters* Vol.3, No.2, 84–96 (2009).
50. M. Azad, et al., "Mechanical Performance of Composite Sandwich Panels Made of Recycled Foamed Polypropylene Core and Glass/PP Skins", *Society for the Advancement of Material and Process Engineering (SAMPE)*, California, US, May 2016.

51. D. Zenkert, "An Introduction to Sandwich Construction", 1st edition, pp 39-48 (1997).
52. F. J. Plantema, Sandwich Construction, John Wiley and Sons, New York, 1966.
53. H. G. Allen, Analysis and Design of Structural Sandwich Panels, Pergamon Press, Oxford, 1969.
54. Janusz Sikora, "Design of Extrusion Heads", Department of Polymer Processing, Lublin University of Technology
55. Michaeli W., "Extrusion Dies for Plastics and Rubber", Hanser Publishers, Munich 1992.